M-PM-Sy1 ACTIN STRUCTURE AND REGULATION OF ITS POLYMERIZATION. T.D. Pollard, Dept. of Cell Biology and Anatomy, Johns Hopkins University School of Medicine, Baltimore, MD. 21205.

We have used computer image reconstruction of electron micrographs of negatively stained 2-dimensional Acanthamoeba actin crystals to determine the structure of the actin molecule (Fowler, Smith, Pollard & Aebi). A projection model at 1.1 nm resolution and a 3-D model at 1.5 nm resolution show that actin is an asymmetric bilobed molecule with dimensions of 5.5 x 4.0 x 3.3 nm. Fowler and Aebi are now attempting to orient the 3-D model in the actin filament. We have studied actin polymerization by measuring the rates of the nucleation and elongation steps. The initial rate of polymerization depends on the actin concentration to a power of 1.2 to 2 (so the nucleus probably consists of 2 molecules). Mg^{++} in the range of 1 μM to 10 mM increases the bulk rate of polymerization without changing the elongation rate, so it must promote nucleation (Cooper and Pollard). The elongation rate constants differ at the 2 ends of the filament: at the barbed end $k_+ \sim 10^7 M^{-1}s^{-1}$, $k_- \sim 2s^{-1}$; at the pointed end $k_+ \sim 2x10^6 M^{-1}s^{-1}$, $k_- \sim 1s^{-1}$ (Pollard & Mooseker). These assembly reactions can be regulated by proteins. Acanthamoeba profilin binds weakly ($K_d = 10^{-5}$ M) to actin monomers and reduces the nucleation rate without inhibiting elongation. It may serve as an actin monomer buffer in the cell (Runge, Tseng, Cooper and Pollard). Acanthamoeba capping protein blocks monomer addition at the barbed end of the filament, but increases the initial rate of polymerization by promoting nucleation. High concentrations of capping protein reduce polymer length by increasing the number of filaments. Acanthamoeba has an 180,000 MW (subunit 90,000), rod-shaped (3x55 nm) gelation protein which can cross-link actin filaments into a gel. These proteins are thought to constitute part of the system which regulates the consistency of the cytoplasm.

M-PM-Sy2 MOLECULAR DYNAMICS OF ACTIN IN VITRO AND IN VIVO: A FLUORESCENCE APPROACH
D. Lansing Taylor, The Biological Laboratories, Harvard University, Cambridge, Mass.

Fluorescence techniques have been used to characterize the structure and the state of assembly of actin both in vitro and in vivo. Resonance energy transfer has been used to characterize the rates of actin assembly and disassembly as well as to define the kinetics of steady state subunit exchange in solutions of actin. The distribution and organization of actin in living cells has been defined by the use of fluorescence analog cytochemistry. This latter method involves the labelling of actin with a fluorescent probe, the incorporation of the labelled actin into living cells and the analysis of the fluoresecent analog in vivo with microspectrofluorimetry and image intensification methods. Fluorescence approaches have permitted the same molecular questions to be addressed under standard solution conditions and in living cells

M-PM-Sy3 STRUCTURE OF CORTICAL CYTOPLASM. T.P. Stossel, J.H. Hartwig, K.S. Zaner, Massachusetts General Hospital, Boston, MA.

The cell cortex is composed primarily of actin filaments. Actin-binding protein (ABP), a cortical protein of vertebrate cells, is a potent actin crosslinking factor. ABP molecules are large flexible dimers able specifically to bind adjacent actin helices into an isotropic lattice with a minimum of redundant crosslinks. This efficient crosslinking has been documented by means of gel point measurements and by estimating the dynamic rigidity modulus of actin-ABP. Each added ABP molecule crosslinks a new actin filament. The dynamic rigidity modulus and the pseudoequilibrium compliance values of ABP-actin are equivalent and of a magnitude predicted from rubber elasticity theory at low ABP:actin ratios, with upward deviation at higher ratios. This deviation can be explained by the relative stiffness of actin fibers compared with Gaussian chains. The isotropy of this stiff chain network is the result of perpendicular branching of actin by ABP. Striking perpendicular branching is observed in electron micrographs of actin fragments fixed shortly after the onset of assembly in the presence of ABP. Critical point dried replicas of ABP-actin matrices reveal three dimensional actin networks with perpendicular branches. The structure is similar to that of cortices of Triton-extracted cells. The compliance of ABP-actin is low but finite, consistent with the existence of an extensively branched, stiff, entangled but not necessarily "infinite" network. This structure provides for maximum extension with minimal mass and a rigid matrix able to flow in response to forces acting within or upon it. Directionality and rate of flow can be controlled by local changes in average filament length in different matrix domains (Biochem Biophys Res Commun 92:675, 1980). Filament length can be regulated by gelsolin, a Ca^{2+}-modulated protein of the cortex of many vertebrate cells that shortens actin filaments in a Ca^{2+}-dependent manner.

M-PM-Sy4 MORPHOLOGY OF CYTOPLASMIC FILAMENTS IN THICK SECTIONS AND CRITICAL POINT DRIED WHOLE MOUNTS. H. Ris, Dept. of Zoology, University of Wisconsin, Madison, WI.

High voltage electron microscopy of intact cells prepared with the critical point drying procedure is a promising method to study three-dimensional relationships between various cytoplasmic organelles. It has been claimed that critical point dried specimens reveal a structure that is not visible in sections of plastic embedded material and which in association with known cytoplasmic filaments forms a meshwork of tapering threads (microtrabecular lattice), e.g. Wolosewick and Porter, J. Cell Biol. 82, 144). Alternatively the trabecular structure might be a surface tension artifact produced during critical point drying. I have previously shown that residual water in the CO_2 produces trabecular structures with pure suspensions of chromatin, collagen and actin (Ris, 38th Ann.Proc. EMSA 1980, 812). BS-C-1 and BHK-21 cells grown on gold grids, fixed in 2% glutaraldehyde in 0.1 M Hepes buffer (7.0), followed by 0.1% OsO_4, stained with 1% uranyl acetate were dehydrated in ethanol (100% containing molecular sieve) and critical point dried with CO_2 (dried with molecular sieve). During exchange of ethanol with CO_2 the chamber was agitated to remove all ethanol from the grid holder. Stereo micrographs were obtained with the 1 MeV microscope at the Madison HVEM facility and compared with micrographs of 0.25-0.5 µm thick sections of plastic embedded cells. The cytoplasmic filament systems were very similar in both preparations consisting of predominantly uniformly thick filaments, probably actin, which are associated with particles 5-10 nm in diameter. In the cortex these filaments form networks with particles at nodal points. After critical point drying identical structures were seen in the thin edge of spreading coelomocytes from sea urchins which are known to contain a network of actin filaments.

M-PM-Min1 QUATERNARY STRUCTURE-DEPENDENT PROTEIN/HEME INTERACTIONS IN HEMOGLOBIN.
D. L. Rousseau, M. R. Ondrias, S.-L. Tan, Bell Laboratories, Murray Hill, NJ 07974, S. R. Simon, State University of New York at Stony Brook, Stony Brook, NY 11790

To determine if the free energy of cooperativity in hemoglobin is localized in any interactions at the heme, we have examined the quaternary structure dependence of heme and ligand vibrational modes by infrared absorption and resonance Raman difference spectroscopies. We have detected systematic quaternary structure-dependent changes in porphyrin skeletal modes in deoxy, carbonmonoxy, and met hemoglobins and changes in the iron-histidine stretching mode in deoxyhemoglobins. In solutions of native, mutant, chemically modified and hybrid deoxyhemoglobins, quaternary structure-dependent changes in the electron density sensitive porphyrin modes correlate with the changes in the iron-histidine stretching mode, suggesting a single parameter response. However there are conditions under which this correlation is disrupted. In studies of human and carp methemoglobins and Kansas and carp carbonmonoxyhemoglobins, no significant quaternary structure dependence in the ligand-iron modes or in the internal ligand modes were detected. These data bear on models of cooperatively in several ways: First, distal interactions with bound ligands do not contribute to cooperatively; second, significant chain heterogeneity exists in deoxyhemoglobins; third, the iron histidine bond does not store significant energy in deoxyhemoglobins; fourth, the quaternary structure change affects the heme electron denisty in all forms of hemoglobins. The various models for cooperativity will be discussed in view of these findings.

M-PM-Min2 EXAFS STUDIES OF Hb AND HbNO. R.G. Shulman[a], P. Eisenberger[b], S. Simon[c], S. Ogawa[d] and A. Mayer[e]. a) Yale University, b) Exxon Research Labs, c) SUNY, Stony Brook, d) Bell Labs and e) Bremen University, Germany.

We have used dedicated beam time at the Stanford Synchrotron Radiation Laboratory to measure the EXAFS spectra of Hb and HbNO. Both states of ligation were switched between R and T and differences in the EXAFS spectra were sought. None were observed, nor were any significant differences detected between low temperature (approaching 77°K) and 300°K. Radiation damage was shown to be negligible. The Hb samples were Hb des Arg at pH9 and pH7 reflecting R and T respectively, and Hb NES des Arg which was switched from R to T with IHP. The HbNO samples, at pH7, were also switched from R → T with IHP, following earlier procedures (1), and the switch was monitored at 77°K by ESR. Our earlier EXAFS comparisons (2) showing no differences between Hb Kempsey (in R) and Hb (in T) are supported by these more extensive results. The present spectra gave good signal-to-noise ratios out to $k = 13\text{Å}^{-1}$. There is no indication, in these results, that an iron-imidazole bond breaks upon switching HbNO to the T state. We have also taken EXAFS spectra of single crystals of Met Mb and Met MbCN which show anisotropy in the EXAFS spectra as a result of using the polarized x-rays.

[1]Salhany, J.M., Ogawa, S. and Shulman, R.G. (1974) Proc. Natl. Acad. Sci. USA 71: 3359.

[2]Eisenberger, P., Shulman, R.G., Brown, G.S. and Ogawa, S. (1976) Proc. Natl. Acad. Sci USA 73:491

M-PM-Min3 THE TRIGGER MECHANISM FOR QUATERNARY STRUCTURE CHANGE IN HEMOGLOBIN: A TRANSIENT RAMAN STUDY. J. M. Friedman and R. A. Stepnoski, Bell Laboratories, Murray Hill, New Jersey 07974

An essential but still undetermined element in the analysis of Hb cooperativity is an understanding of those features associated with the heme-hemepocket configuration in liganded Hb's which upon deligation result in the structural instability that brings about a change in quaternary structure. Using time resolved resonance Raman scattering, we have probed the non-equilibrium configurations associated with both photolyzed Hb's (R and T) and Mb's. By focussing on a variety of Raman lines, we have been able to characterize the temporal evolution of manifestations of the response of the heme and the heme environment to ligation and deligation as a function of quaternary structure. From the time evolution studies as well as comparisons of transients to the corresponding stable species, we find[1] that the configuration about the heme is comparably responsive to ligation and quaternary structure. Our findings with regard to the iron proximal histidine linkage indicates that even within the T structure there may well be sufficient flexibility in the protein to accommodate a liganded porphyrin without a major increase in strain energy.[2] Instead our findings are more consistent with a trigger mechanism for quaternary structure change that originates from the electronic redistributions associated with the deligation.

[1]J. M. Friedman, R. A. Stepnoski, M. Stavola, M. Ondrias and R. L. Cone, Biochemistry, in press.

[2]J. M. Friedman, D. L. Rousseau, M. Ondrias and R. A. Stepnoski, submitted for publication.

M-PM-Min4 PICOSECOND TIME-RESOLVED RESONANCE RAMAN SPECTROSCOPY OF THE PHOTOLYSIS OF OXY-HEMOGLOBIN. James Terner, David F. Voss, Carolyn Paddock, Richard B. Miles, and Thomas G. Spiro, Depts. of Chemistry, and Mechanical and Aerospace Engineering, Princeton University, Princeton, NJ 08544.

The resonance Raman spectrum of the picosecond transient produced upon photolysis of oxyhemoglobin has been obtained with the 30 picosecond, 0.1 mj pulses from the doubled output (532 nm) of a mode-locked Nd:YAG laser with double pass amplification. Our spectra show bands at 1538 (dp), 1550 (ap), and 1590 (dp) cm^{-1}. These results are appreciably different from what has been previously reported for the picosecond resonance Raman spectra of photolysis of CO-hemoglobin (1), and oxyhemoglobin (2) using longer pulse duration and lower pulse energy. The previously reported spectra showed bands at 1543 (dp), 1552 (ap), and 1603 (dp); slightly downshifted from the corresponding bands of deoxyhemoglobin at 1549 (dp), 1556 (ap), and 1605 (dp).

It is possible that we have observed the rapidly relaxing spectral intermediate observed for HbO_2 by Chernoff et al (3), that appeared during 6 picoseconds but decayed within 90 picoseconds. This short lived transient is most likely an electronically excited deoxyhemoglobin, and a precursor of the photoproduct observed by Nagumo et al (2).

1. J. Terner, J.D. Stong, M. Nagumo, M. Nicol, and M.A. El-Sayed J. Amer. Chem. Soc., 102, 3238 (1980).
2. M. Nagumo, M. Nicol, and M.A. El-Sayed J. Phys. Chem., 85, 2435 (1981).
3. D.A. Chernoff, R.M. Hochstrasser, and A.W. Steele Proc. Nat. Acad. Sci. USA, 77, 5606 (1980).

M-PM-Min5 METALLOPORPHYRIN π-π CHARGE-TRANSFER COMPLEXES AS MODELS OF THE PROTEIN-HEME INTERACTION IN HEMOGLOBIN.* J. A. Shelnutt, Sandia National Laboratories,† Albuquerque, New Mexico 87185

The control of axial ligand affinity and reactivity by formation of π-π charge-transfer complexes between the porphyrin moiety and aromatic residues of the protein is being examined. The similarities between the shifts of the heme Raman lines that are markers of Hb quaternary structure and those shifts that occur on formation of metalloporphyrin π-π charge-transfer complexes have been determined. Previous studies of metalloporphyrin complexes have focussed on the copper (II) uroporphyrin aqueous system for two reasons. (1) The highly ionic uroporphyrin is not aggregated at the concentrations used for Raman difference spectroscopy (RDS), and (2) copper (II) is normally four-coordinate, and therefore axial ligation is weak. This latter property was chosen so that direct interaction with the porphyrin moiety could be studied. For the phenanthroline-CuURO complexes, the magnitudes of the Raman frequency shifts in a group of lines, including the oxidation state marker lines, indicate that the π-electron density in the porphyrin ring decreases with increasing acceptor ability of the phenanthrolines. A planar π-π complex was indicated. Recent studies indicate that the phenanthrolines also form π-π donor-acceptor complexes with Fe(III) uroporphyrin (FeURO) in structured solvents. The correlation between the acceptor properties of the phen derivatives and the Raman frequency shifts has also been observed for the iron (III) porphyrin complexes. Furthermore, interaction at the metal site has been ruled out since a hindered phen derivative gives the Raman shifts expected on the basis of the effect of induction by substituents on its acceptor ability. Also, the change of metals does not affect the affinity of the porphyrin for phen. *Supported by U.S. Dept. of Energy under Contract DE-AC04-76-DP00789. †U.S. DOE facility.

M-PM-Min6 RESONANCE RAMAN STUDIES OF GAS PHASE METALLOPORPHINS AND HEME COMPLEXES. Sanford A. Asher and James Murtaugh, Department of Chemistry, University of Pittsburgh, Pittsburgh, PA 15260

Resonance Raman and absorption spectra have been obtained for a series of metallooctaethylporphin complexes (MOEP) in the gas phase at ca. 400°C. The Raman data are qualitatively similar to that observed from MOEP complexes in organic solution. However, differences are observed for the Raman frequencies and excitation profiles which are interpreted to result from the absence of intermolecular interactions in the gas phase. These are the first resonance Raman spectra obtained for "isolated" hemes. Since the gas phase data are not complicated by intermolecular interactions they can be used as a basis for quantifying the heme structural changes induced by protein-heme interactions in hemoglobin and other heme proteins.

M-PM-A1 OPTIMAL DESIGN OF IMMOBILE AND SEMI-MOBILE NUCLEIC ACID JUNCTIONS. Nadrian C. Seeman and Neville R. Kallenbach, Center for Biological Macromolecules, SUNY/Albany, Albany, NY 12222, Department of Biochemistry, Stanford University School of Medicine, Palo Alto, CA 94305.

Nucleic acid junctions are formed by the confluence of three or more double helices about a single point. Forked replicative intermediates and four-stranded Holliday recombination intermediates are examples of naturally occurring nucleic acid junctions. Because of their internal sequence symmetries, these forms are capable of resolution to double helical structures via the process of branch point migration. Since this is a very rapid process, these forms have not been tractable to physical characterization at the oligonucleotide level. We have recently indicated[1] that the migratory range of these structures may be reduced (to form semi-mobile junctions) or eliminated (to form immobile junctions). Rules have been formulated which must be obeyed by oligonucleotide sequences if they are to form junction structures[1]. These conditions must be supplemented by thermodynamic criteria in optimizing the sequence of a given designed junction. A rapid algorithm has been generated which tests all possible sequences for fulfillment of the conditions (typically about 1% of sequences pass this test). Successful sequences must then be tested for competing pairing interactions as well as for the predominance of the complete junction as the major molecular species in solution. A sorted list of the best sequences can be generated from this algorithm, to aid in oligonucleotide synthetic decisions.

[1]N.C. Seeman, in BIOMOLECULAR STEREODYNAMICS, ed by R.H. Sarma, Adenine Press, New York (1981), pp. 269-278.

This work has been supported by a Basil O'Connor grant from the March of Dimes Birth Defects foundation and by grant GM-26467 from the NIH.

M-PM-A2 MOST PROBABLE LOCATIONS OF REGULAR SECONDARY CONFORMATIONAL REGIONS IN PROTEINS R. L. Jernigan and S. Miyazawa, Laboratory of Mathematical Biology, DCBD, NCI, NIH, Bethesda, MD 20205

To avoid dependences on statistics derived from X-ray crystallographic data, we have devised a non-empirical method for calculating approximate conformational energies of regions of regular secondary conformation. All atoms are taken as hard spheres with excluded volume. For fixed backbone conformations and representative samples of all side chain conformations, numerous conformations are examined for atomic overlaps. Backbone-side chain electrostatic energies are calculated explicitly for the permitted conformations, in the point charge approximation with Debye-Huckel shielding. The energies of backbone-backbone and backbone-C^{β} atom interactions are approximated by means of parameters; these parameters, one for each standard backbone conformation, are identical for all amino acids except glycine and proline. Results indicate the importance of position within regular helices. The energies of all possible helices and beta strands are calculated for every location within a protein. The total energy, as the sum of those for independent regions, of all combinations of these regular secondary conformations is minimized. Results favor placement of polar side chains near the ends of the regular regions so that they interact favorably with helix and beta strand backbone dipole moments. By default such locations near the ends of regular regions will often permit the polar residues to interact with solvent. The results for a group of globular proteins are correct for about 60% of all residues. Similar qualities of results for most empirical secondary structure prediction methods may imply that inadequacies originate less from limitations in the data than from conformational perturbations, over local preferences, as required to achieve stable globular forms. The present description may correspond to an early stage of folding in which there are few persistent long range interactions.

M-PM-A3 CALCULATION OF PARTITION ENERGIES OF AMINO ACID RESIDUES FROM WATER TO APOLAR SOLVENTS AND THE USE OF THESE ENERGIES TO PREDICT THE STRUCTURE OF APOLIPOPROTEINS. H. Robert Guy, Lab Biophysics, NINCDS, NIH, Bethesda, Md. 20205.

Several studies of the partitioning of amino acids and their analogs into various solvents and of the distribution of amino acid residues in proteins of known structure were analyzed to predict the partition energy of each amino acid residue as a function of its distance from a water-protein and a protein-oil interface. The analysis indicates that the interior of proteins has a polarity similar to that of ethanol, that oil is substantially more apolar than the interior of proteins, and that side chains with well differentiated apolar and polar moieties concentrate at the interfaces. The analysis was used to develop a program to predict the most stable conformation of a lipid-associated protein from its sequence, assuming that amphipathic α helices stack side by side to form a barrier between water and the apolar phase of lipids. Molecular models of the ApoA-I phospholipid disc structure and the high density lipoprotein particle (HDL) were developed using the program and other theoretical and experimental constraints. For both models ApoA-I has nine amphipathic α helices that stack side by side in the order they occur in its sequence. The helices are held together in part by a series of salt bridges. In the disc model, three ApoA-I molecules form the perimeter around a circular phospholipid bilayer with the helices perpendicular to the surface of the bilayer. In the HDL model an ApoA-I dimer stacks helix end on with another dimer to form a barrel with an oblong cross section. The barrel surrounds the apolar edges of two surface phospholipid monolayers and an inner cholesterol and triglyceride layer. ApoA-II dimers can fit between the ApoA-I molecules to increase the HDL barrel's perimeter.

M-PM-A4 MONTE CARLO ENERGY CALCULATIONS ON GLYCOSYLATED PEPTIDES AS CONFORMATIONAL MODELS FOR GLYCOPROTEINS. Anthony J. Duben and C. Allen Bush. Dept. of Chemistry. Illinois Institute of Technology. Chicago, IL 60616.

A conformational energy space composed of empirical interatomic energy functions using parameters of Scheraga and coworkers was constructed for model dipeptides containing N-glycosylated asparagine or alternatively O-glycosylated serine or threonine. This conformational space, which contains rather complicated undulating potential functions has a tendency to trap the Monte Carlo trajectory when searched by the Metropolis algorithm. Therefore it was not possible to carry out calculations which were completely convergent to the thermodynamic result. Nevertheless, it was possible to show that for dipeptides having the threonine - or the more flexible serine -O-glycosyl linkage to α N-Acetyl galactosamine a β turn conformation is most probable. Although it was shown that β turn conformations are possible for asparagine dipeptides linked by an N-glycoside to β N-Acetyl glucosamine, extended peptide conformations are more probable. Our results are illustrated by projections onto two dimensional population density maps analogous to Ramachandran energy maps but which show density of probability as a function of selected pairs of angles.

M-PM-A5 NEW COMPACT FOLDED STRUCTURES IN PROTEIN MOLECULES. L.S. Hibbard and G.D. Rose. The Milton S. Hershey Medical Center, The Pennsylvania State University, Hershey, PA 17033.

A new, automatic method for the identification of compact folded structural units in protein molecules based on objective geometric criteria has been devised. The results of this study are a set of compactly folded units which are observed repeatedly in protein molecules; some of these units have yet to be described in the literature. The usual α-helix:α-helix and α-helix:β sheet structures described previously (J.S. Richardson, Adv. Prot. Chem. 34, 167, 1981) turn out to be a subset of the units we find. Additionally, these compact folded structures can be used in a straightforward way to generate a hierarchical tree relating polypeptide segments distant in sequence, but close in space. (Supported in part by PHS Grants GM29458 and AG00088.)

M-PM-A6 MODELLING STRUCTURE/FUNCTION IN MEMBRANE-ACTIVE PLANT TOXINS. M.M. Teeter and M. Whitlow. Dept. of Chemistry, Boston University, Boston, MA. 02215

The crystal structure of the hydrophobic plant protein crambin which has 46 amino acids has been recently determined (Hendrickson and Teeter, Nature 290, 107-113(1981)). Comparison of the completed sequence of crambin (Teeter, Mazer and L'Italien, Biochemistry 20, 5437-5443(1981) to that of other proteins revealed that it was homologous to a class of membrane-active plant toxins which are hemolytic, cause skin and skeletal muscle contractation and kill diverse types of phytopathogenic bacteria. To date, no toxicity has been demonstrated for crambin. Although different in function, circular dichroism studies in our laboratory indicate crambin and the toxins are similar in secondary structure in solution. We have chosen to use these small, disulfide crosslinked proteins to establish the principles of a structure prediction scheme which could be applied to other series of homologous proteins such as snake venom neurotoxins or immunoglobulins. The residues conserved between crambin and the plant toxins may show which features are necessary to preserve the secondary and tertiary structure. The aspects different from crambin but common to all the toxins might define the functional site for these proteins.

Our results show a striking preservation of the amphipathic helices found in crambin for the plant toxins, despite the fact that the toxins are much more basic than crambin. The pI of the toxins are 11 versus 7 for crambin. The preserved feature may be important in the lipophilic character of the toxins.

M-PM-A7 IDENTIFICATION OF STRUCTURE-DETERMINING SEQUENCES IN RIBONUCLEASE.
R.P.Carty,F.Gerewitz,Department of Biochemistry, S.U.N.Y. Downstate Medical Center,450 Clarkson Avenue Brooklyn, N.Y. 11203 and M.R.Pincus, Laboratory of Theoretical Biology, Building 10,Rm. 4B56,National Institutes of Health,Bethesda, Md. 20205. (introduced by Mones Berman).

An approach to studying the location of structure-determining sequences in ribonuclease A has been developed. The method involves the use of ribonuclease peptide fragments(isolated from proteolytic digestions of the enzyme) as inhibitors of the refolding of the enzyme from the denatured,reduced state. Four peptide sequences, 11-31,40-61,99-104,105-124, have been found to give inhibition of the refolding process. By far the most effective peptide-inhibitor found thus far was 105-124 which contains the postulated nucleation site for Rnase A refolding [R. Matheson and H.A. Scheraga (1978) Macromolecules 11,819]. This peptide showed virtually total inhibition at a molar ratio of 1.7:1 peptide-to-protein. The least effective peptide was the sequence 40-61 which showed only 40% inhibition(at 2 hrs.) with the peptide in 7.5 M excess. Thus inhibition is highly sequence-dependent and not dependent on such factors as chain length or hydrophobicity(both peptides have the same percentage of hydrophobic residues). The other two peptide fragments 11-31 and 99-104 both cause less inhibition than that of 105-124,the former inhibiting about 88% in 10 M excess,the latter 42% in 3 M excess. The time course for the appearance of native enzyme in the presence of inhibitor peptides suggests that each peptide binds to specific critical intermediates on the folding pathway.

M-PM-A8 PREDICTION OF THE THREE DIMENSIONAL STRUCTURE OF MURINE PRE-KAPPA LIGHT CHAIN LEADER SEQUENCE WITH CONFORMATIONAL ENERGY CALCULATIONS
M.R. Pincus and R.D. Klausner. Laboratory of Theoretical Biology, Building 10,Rm. 4B56, National Institutes of Health,Bethesda, Maryland 20205. (introduced by David Foster).

The three-dimensional structure of the signal secretory peptide for murine pre-kappa light chain N-Acetyl-Glu-Thr-Asp-Thr-[(Leu)3-Trp-Val]2-Pro-Gly-NHCH3 has been calculated using conformational energy calculations.To compute the lowest energy form for this hexadecapeptide and for long peptides in general we have devised a strategy of combining all non-degenerate low energy minima of small oligopeptide blocks to "build up" longer peptide units. Application of this method to the sequence (Leu)3-Trp-Val results in structures in which (Leu)3 is alpha-helical and with Trp-Val in a variety of low energy conformations, the lowest in energy of which was alpha-helix.When the lowest energy conformations for the pentapeptides were combined and subjected to energy minimization, the lowest energy structure was one in which the first 8 residues were in an alpha-helix while the terminal Trp-Val assumed a variety of low energy conformations, the lowest still being alpha helix. Addition of the amino and carboxyl terminal peptides to the central hydrophobic core resulted in a final structure in which the first 4 residues assumed a semi-extended structure,succeeded by an alpha-helical octapeptide, (Leu)3-Trp-Val-(Leu)3,which ended in a distinct chain reversal involving the last 4 residues.All possible beta conformations with hairpin turns at the central Trp-Val sequence and the fully extended conformation are much less stable than the calculated global minimum energy structure. This final structure is in agreement with experimental data on synthetic leader sequences and with proposed models for the structure of membrane proteins.

M-PM-A9 A THEORETICAL STUDY OF THE INTERACTION OF METAL IONS AND AMINO ACIDS.
A.Gupta, G.H.Loew, J.Lawless, Molecular Research Institute, 701 Welch Road, Suite 203, Palo Alto, California 94304. Extraterrestrial Research Division, Mail Stop 239-9, NASA-Ames Research Center, Moffett Field, California 94035.

Recent experiments at NASA-Ames suggest that ion-exchanged clays could have served as primitive templates for the concentration and selection of the biological subset of amino acids from a random population of organic compounds available on primitive earth. The detailed nature of the metal-amino acid complexes presumably formed is investigated using an INDO semiempirical molecular orbital method which allows for the treatment of transition-metal complexes. Bidentate complexes of Ni^{2+} and Cu^{2+} ions with β- and γ-amino acids and a series of α-amino acids are studied to calculate the energy change in the equilibria: $n(AA) + M(H_2O)_6^{2+} \overset{\Delta E}{\rightleftharpoons} (M(AA)_n (H_2O)_{6-2n})^{+(2-n)} + 2n(H_2O)$, where AA is amino acid, M is Ni or Cu and n = 1 or 2. Calculations using the experimental of composite geometry of the molecules and complexes in the above equilibria indicate Cu^{2+} ions superior to Ni^{2+} ions in binding amino acids. The metal ion specificity (Cu^{2+} better than Ni^{2+}) is retained in the calculations using totally optimized geometries of the individual species and complexes. The order of preference for amino acids is γ > β > α. Moreover, among the various α-amino acids considered, there is little preference for the choice of -R group on Cα atom or substitution at the nitrogen atom of the amino acid. These computational results indicate that while ion-exchanged clays are capable of adsorbing amino acids from dilute solution, a preferencial selection of the biological subset of the amino acids does not occur by formation of metal-amino acid complexes.

M-PM-A10 EXCLUDED VOLUME OF COILED POLYMERS AND RIGID MACROMOLECULES (PROTEINS AND DNA).

Jan Hermans, Department of Biochemistry, University of North Carolina, Chapel Hill NC 27514.

Excluded volume effects between polymer chains and rigid particles are generally seen as the cause of: precipitation of proteins by polymers, exclusion of proteins from polymer gels and transformation of double-helical DNA to compact particles. Theories of excluded volume have represented the polymer chains as, respectively, long thin rods and impenetrable spheres; however, results of these theories do not agree well with experiment. It is much more appropriate to represent the polymer as a segmented chain having many possible conformations as a consequence of fully or partly free internal rotation about segments. This model has been used in two complementary theoretical approaches: the one by Monte Carlo simulation, the other by recourse to the well-known statistical properties of polymer chains. Results of the two theoretical methods agree perfectly. Amongst others, theory predicts that for long polymer chains: (1) excluded volume per polymer segment is independent of polymer chain length, (2) excluded volume is proportional to the radius of spherical proteins, (3) excluded volume is larger for asymmetric particles than for spheres of the same volume; all three predictions agree with experiment. Excluded volume for exclusion of long rodlike particles by polymers is proportional to rod length; theory thus predicts that volume exclusion indeed contributes a significant destabilization of the double-helical conformation of DNA in favor of a compact globular form.

M-PM-A11 KINETICS OF PROTEIN POLYMERIZATION: MODEL CALCULATIONS ON HOMOGENEOUS NUCLEATION AND GROWTH. R.de Levie, M.P.Firestone (Chem.Dept.,Georgetown University, Washington D.C. 20057) and S.K.Rangarajan (Dept.of Inorg.& Phys.Chem.,Indian Institute of Science, Bangalore, India 560012).

The kinetics of protein polymerization are described in terms of successive monomer addition. All monomer addition steps involving clusters larger than a critical nucleus are characterized by the same rate constant $\vec{k}$, and corresponding monomer dissociation steps by a rate constant $\overleftarrow{k}$. Furthermore we have assumed that the monomer concentration c_1 remains essentially unchanged. Under such conditions, a closed-form solution has been obtained which expresses all cluster concentrations in terms of the concentration c_n of the critical nucleus. The latter can be expressed subsequently in terms of c_1.

During nucleation, c_n increases, whereas it remains constant during the subsequent growth or elongation phase. During growth, the concentrations of clusters in the neighborhood of c_n are constant; the extent of this neighborhood expands toward larger cluster size. The resulting size distribution during growth is highly polydisperse, and quite different from that obtained after equilibrium has been reached. One can define a flux which is constant during growth and given simply by $(\vec{k}c_1-\overleftarrow{k})c_n$.

The observed, highly non-linear dependence of viscosity or light scattering on time is due to the non-linear relation between these physical observables and cluster size & concentration, not to failure of the model. NIH grant 5 R01 HL 12256-17.

M-PM-A12 ELECTRON MICROSCOPY versus HYDRODYNAMICS FOR DETERMINING THE SHAPE OF PROTEIN MOLECULES. Harold P. Erickson, Anatomy Department, Duke University, Durham, N. C. 27710.

For many years sedimentation data have been among the most important observations for determining the size and shape of protein molecules. The ratio f/f_{min} is corrected for the estimated water of hydration to give f/f_o, and the axial ratio of the corresponding smooth prolate ellipsoid is calculated using the Perrin equation. This standard hydrodynamic analysis can, however, greatly overestimate the axial ratio, as shown by the following two examples. In a recent study (J. Biol. Chem. 256:9724) of phosphofructokinase (PFK), a 330,000 MW tetrameric enzyme, the sedimentation coefficient of 12.2 S gave a value of f/f_{min} = 1.39. For 0.3 g/g water of hydration f/f_o = 1.24. This corresponds to a highly asymmetric prolate ellipsoid, with an axial ratio of approximately 5. Electron microscopy showed, however, that the molecules are 14 nm long by 9 nm diameter, i.e., the axial ratio is really only 1.5. A similar discrepency exists for the case of tubulin, a 110,000 MW dimeric molecule. Sedimentation data (Biochem. 14:4559) gave values of f/f_{min} and f/f_o essentially identical to those of PFK, again suggesting a highly asymmetric particle. The tubulin dimer as seen in the microtubule wall, however, measures 8 x 5 x 5 nm; these dimensions are also consistent with our recent images of individual molecules. Thus electron microscopy demonstrates that the tubulin molecule also is only slightly elongated, with an axial ratio of 1.6. The above two examples and other published data suggest that values of f/f_{min} between 1.25 and 1.4 are typical of globular proteins. For truly asymmetric molecules, such as fibrinogen, fibronectin and tropomyosin, f/f_{min} is greater than 2.0. Thus hydrodynamic data in these two extreme ranges should suggest a globular or asymmetric shape, respectively, but a more detailed calculation of axial ratio is not meaningful. For the five proteins mentioned, and in general for proteins larger than 100,000 MW, individual molecules can be imaged routinely by electron microscopy (J. Mol. Biol. 134:241; 150:399; J. Ulstr. Res. 71:95) providing much more definitive structural information.

M-PM-A13 X-RAY DIFFRACTION STUDIES OF COLLOID CRYSTALLINE TMV. Seth Fraden, D.L.D. Caspar and W. Phillips. Rosenstiel Center, Brandeis University, Waltham MA 02254.

The liquid crystalline properties of TMV have been investigated both experimentally and theoretically. Onsager's studies quantitatively explain the observed transitions from an isotropic to nematic liquid crystal phase. In 1950 Oster discovered a phase of TMV that displayed Bragg scattering of visible light. Oster suggested that the Bragg diffraction of light is caused by layers of parallel oriented TMV particles separated by water. Kreibig and Wetter (1980) recently prepared colloid crystals of TMV at concentrations of 5-10% in water and measured the repeat in the axial dimension by light scattering. The separation between the 3000 Å thick layers of rods is approximately 300 Å and they reported a small variation in the repeat between planes of TMV particles among crystals in the same sample. Our X-ray diffraction studies show that crystalline order extends in the plane of the TMV particles. The lattice constant of this hexagonal array of the rod-shaped particles in which particle surfaces are separated by about 300 Å of water shows a large variation among crystals in the same sample.

Supported by NIH grant CA 15468 to D.L.D. Caspar.

G. Oster, J. Gen. Physiol. 33, 445-473 (1950).
U. Kreibig, C. Wetter, Z. Naturforsch. 35c, 750-762 (1980).

M-PM-B1 TEMPERATURE-DEPENDENT MOLECULAR DYNAMICS OF NEAT CHOLESTEROL ESTERS James A. Hamilton, Geoffrey Ginsburg, and Donald M. Small, Biophysics Inst., Boston Univ. Schl. Med. Boston, MA 02118

In their neat forms, the biologically prevalent cholesterol esters, cholesteryl oleate (CO) and cholesteryl linoleate (CL), have two metastable liquid crystalline states, the cholesteric and the smectic mesophases. In contrast, the monounsaturated (ω 9) C_{22} and C_{24} esters, cholesteryl nervonate (CN) and cholesteryl erucate (CE), have a stable smectic phase and no cholesteric phase. Natural abundance ^{13}C NMR spectra at 50.3 MHz of the four esters were recorded, and the linewidths ($\nu_{\frac{1}{2}}$) of the cholesterol ring methine carbon resonances C6 and C3 were measured, as a function of temperature above the isotropic-liquid crystal transition (Tm) of each ester. At any temperature relative to Tm, the C6 and C3 $\nu_{\frac{1}{2}}$'s and the C3/C6 $\nu_{\frac{1}{2}}$ ratios were smaller for CE and CN compared with CL and CO; thus, the cholesterol ring reorientations are more highly anisotropic for the esters having a liquid-cholesteric transition. Furthermore, spectra of the cholesteric and smectic mesophases of CO and CL yielded no discernable peaks from cholesterol ring carbons, while spectra of the smectic mesophases of CN and CE showed weak, broad peaks for several cholesterol ring carbons, indicating greater motional freedom of the cholesterol ring in the stable smectic mesophases compared to metastable phases. Thus, compared to CL and CO, the long-chain esters CE and CN do not have as high a degree of pretransitional steroid ring ordering in the isotropic liquid and are less tightly packed in the region of the steroid moiety in the liquid crystalline state. These results emphasize the importance of intermolecular cholesteryl ring interactions in the formation of cholesteric phases of biological cholesterol esters and suggest that these interactions are weaker in systems with a stable smectic phase.

M-PM-B2 THE EFFECT OF CHOLESTEROL ON THE THERMOTROPIC PROPERTIES OF 1,2-DIELAIDOYL-sn-GLYCERO-3-PHOSPHOCHOLINE. B.Z. Chowdhry, A.W. Dalziel, G. Lipka, and J.M. Sturtevant (Intr. by P.B. Moore) Dept. of Chemistry, Yale University, New Haven, 06511.

High sensitivity differential scanning calorimetry has been used to investigate the effect of cholesterol (0-50 mole %) on the thermal properties of 1,2-dielaidoyl-sn-glycero-3-phosphocholine (DEPC). The excess specific heat curves for the main transition have been resolved into multiple components. For each component curve the temperature of maximal excess heat capacity, calorimetric enthalpy and van't Hoff enthalpy were selected to give the best fit to the observed excess heat capacity curve. The number of components and the corresponding calorimetric properties of the system were correlated with the DEPC: cholesterol ratio. The effect of cholesterol on the pretransition of DEPC was also examined.

The results indicate that the interaction of DEPC with cholesterol is significantly different from that of the sterol with 1,2-dipalmitoyl-sn-glycero-3-phosphocholine.

M-PM-B3 DIFFERENTIAL THERMAL ANALYSIS OF DIPALMITOYLPHOSPHATIDYLCHOLINE MIXTURES WITH FATTY ACIDS AND SODIUM SOAPS. Stephen E. Schullery, Thomas A. Seder, David A. Weinstein and Darrel A. Bryant. Chemistry Department, Eastern Michigan University, Ypsilanti, MI 48197.

Differential thermal analysis (DTA) was performed on binary mixtures of dipalmitoylphosphatidylcholine (DPPC) with three fatty acids and their sodium soaps, all in excess water. Myristic, palmitic and stearic acids initially raise and broaden the DPPC gel-liquid crystal transition temperature; at higher acid/DPPC compositions a sharp-melting complex forms. The stoichiometry of the complex is apparently 2/1 acid/DPPC for palmitic and stearic acids, but is uncertain for myristic acid. The DTA of myristic/DPPC mixtures was consistent with a simple, ideal-mixing model. The DTA of both palmitic and stearic acids were consistent with gel-state phase separation over the approximate composition range 5-30 mol % acid; phase diagrams of the peritectic type were fitted to the data. The sodium soaps behaved very differently than their corresponding acids and among themselves. Both sodium stearate and myristate eliminate the DPPC main transition and the pretransition at only a few mol % soap. New peaks at $\sim$ 30° C and $\sim$ 48° C are produced. The relative areas of the new peaks were unreproducible for the myristate/DPPC mixtures. Sodium palmitate had surprisingly little effect on the DTA behavior of DPPC. The pretransition is detectable up to $\sim$ 88 mol % palmitate. The temperature of the main transition gradually lowers three degrees and the transition width approximately doubles as palmitate is raised from 0 to 80 mol %. The apparent pK of palmitic acid (12 mol %) in DPPC bilayers in the presence of excess water with no added electrolyte was determined to be 10.2 by direct pH measurement of mixtures of known palmitic acid/sodium palmitate ratios. The intrinsic pK is estimated to be $\lesssim$ 8.5.

M-PM-B4 LIPID ORDER-DISORDER TRANSITIONS IN COMPLEXES OF MELITTIN WITH DITETRADECANOYL- AND DIPENTADECANOYLGLYCEROPHOSPHORYLCHOLINES. F. G. Prendergast, Dept. of Pharmacology, Mayo Foundation, Rochester, MN 55905.

The interaction of melittin, a 26 aminoacid peptide isolated from bee venom, with diacylglycerophosphorylcholines has been examined by application of light scattering and fluorescence techniques. Melittin interacts optimally with ditetradecanoylglycerophosphorylcholine (DMPC) and dipentadecanoylglycerophosphorylcholine (DPenPC) at their phase transition temperature (T_c). Light scattering data show that with DMPC at melittin:lipid molar ratios of approximately 1:150, the interaction is biphasic showing initially an increase in turbidity when melittin is added to DMPC at 25°C followed by a cooperative decrease with clearing of the solution. The kinetics of both phases is very dependent on melittin:lipid ratios. The steady state fluorescence anisotropy (r_{ss}) of diphenylhexatriene (DPH) incorporated into the vesicle shows a biphasic increase upon interaction of the lipid with melittin that coincides well with the biphasic changes noted for light scattering. Measurements of r_{ss}, and differential phase fluorometry were used to show that the MLT-DMPC or MLT-DPenPC complexes exhibit a highly cooperative minimal transition at 32° and 41° (compared with 24° and 33° for DMPC and DPenPC vesicles respectively) when melittin:lipid ratios are ca 1:100 - 1:150 but at higher ratios of peptide:lipid the transition becomes broadened. Thus, melittin appears to form a stable complex which is structurally highly ordered, but which must exhibit packing in the lipid domain that allows for cooperative phase transition at a higher transition temperature than the uncomplexed lipid. Supported in part by PCM7911492 and the Mayo Foundation. F.G.P. is an Established Investigator of the American Heart Association.

M-PM-B5 HELICAL LIPOSOMES. Ke-chun Lin*, Robert M. Weis and Harden M. McConnell, Department of Chemistry, Stanford University, Stanford, CA 94305.

Using optical microscopy we have observed that various binary mixtures of dimyristoylphosphatidylcholine and cardiolipin in Ca^{++}-free phosphate-buffered saline form long (30-300 μm), thin (0.5-5 μm) regular cylindrical liposomes (multilamellar) and vesicles (unilamellar). This result was not unanticipated in the light of earlier work suggesting compound formation and long-range order in these membranes**. Lateral diffusion of fluorescent lipid probes along the long axes of these tubular liposomes is rapid ($\sim 10^{-8}$ cm^2/sec). In the presence of Ca^{++} ion, $\gtrsim 10^{-6}$ M, individual tubular liposomes form remarkably regular, tightly packed, single and double helices, both left- and right-handed. At high Ca^{++} concentrations the helical structures appear to be kinetic intermediates in the formation of still more condensed structures including "helical ghosts", wherein helices are apparently enveloped within continuous lipid outer membranes. Helix formation from tubular liposomes is a remarkably rapid process requiring only a few minutes. A number of mechanisms have been observed, in each of which the thermodynamic driving force is increase of the area of membrane-membrane contact. The membrane-membrane binding may involve rapid Ca^{++}-mediated lateral phase separations. Torsional effects within the tubes are expected to be weak in that rotational shear viscosity of the tubes is estimated to be weak.

*Permanent address: Department of Biophysics, Beijing Medical College, Beijing, China.
**T. Berclaz and H. M. McConnell, Biochemistry, in press.
This work has been supported by the National Science Foundation Grant No. PCM 80-21993 (HMMcC).

M-PM-B6 METASTABLE PHASE BEHAVIOR OF CEREBROSIDES AND A SPHINGOLIPID ANALOGUE

W. Curatolo, MIT, Cambridge, MA; C. M. Gupta* and A. Bali*, Central Drug Res. Inst., Lucknow, India.

Bovine brain cerebrosides (BOV-CER) have been fractionated into 2-OH fatty acid cerebrosides (HFA-CER) and non-hydroxy fatty acid cerebrosides (NFA-CER). The thermal behavior of NFA-CER, HFA-CER, and BOV-CER model membranes has been studied by scanning calorimetry. When NFA-CER is cooled at rates ≥ 2.5°C/min, subsequent heating runs exhibit metastable behavior: a low enthalpy exotherm is observed at ∿50°C (ΔH = - (1 - 3) cal/gm), followed by a high enthalpy endotherm at 72°C ($\Delta H \sim 17$ cal/gm). Systematic variation of cooling/heating protocols indicates that NFA-CER possesses two low temperature states, one metastable and the other stable. Cooling from the liquid crystalline (l.c.) state results in formation of metastable low temperature Polymorph I, which must transform into stable low temperature Polymorph II before the l.c. state can be reached again. HFA-CER and BOV-CER display no metastability, and each exhibit a reversible thermal transition at ∿68°C with $\Delta H \sim 7$ cal/gm. Thus the presence of amide-linked 2-OH fatty acids in BOV-CER prevents metastability; this may be an important physiological function of 2-OH fatty acids in myelin. We have also studied the thermal behavior of the sphingolipid analogue, 1-palmitoyl-2-($C_{13}H_{27}$-NHCOO)-phosphatidylcholine (CMPC). This analogue exhibits metastable thermal behavior which is almost identical to that of NFA-CER, indicating that the sphingosine backbone and glycosyl headgroup are not prerequisites for such metastable behavior. Furthermore, the carbamyl group in CMPC is reversed in orientation compared with the amide of sphingolipids (-NH-CO- vs -CO-NH-), suggesting that the intermolecular hydrogen bonding potential, rather than some highly specific steric or conformational constraint, is responsible for the observed metastability of sphingolipids.

M-PM-B7 MICROEMULSIONS OF CHOLESTEROL ESTERS (CE) AND PHOSPHOLIPIDS (PL) : PROTEIN-FREE MODELS OF LOW DENSITY LIPOPROTEIN (LDL). Geoffrey S. Ginsburg, Donald M. Small, and David Atkinson. Biophysics Institute, Boston University School of Medicine, Boston, MA 02118

LDL are ~200Å particles composed of a surface of PL and protein and a core of CE which undergoes an order-disorder transition (Tm=30-47°C, $\Delta H \approx 0.7$ cal/g CE). We now describe 6 protein-free homogeneous microemulsions made of specific CEs and PLs. Sonicated dispersions of cholesteryl oleate (CO) Tm=42°C, or nervonate (CN) Tm=52°C, with egg yolk (EYL) dimyristoyl (DML) or dipalmitoyl (DPL) lecithin fractionated by agarose gel chromatography yield stable homogenous particles (molar ratio CE/PL = 0.9±0.1). Their size by electron microscopy is ~ 200Å, consistent with the surface/volume ratio of a microemulsion with a CE core and a PL surface monolayer. X-ray scattering is consistent with this model. Scanning calorimetry, x-ray scattering/diffraction, and ^{1}H NMR showed that microemulsions could undergo at least 2 specific transitions depending on composition - one arising from core CE ($\Delta H \approx 0.7$ cal/g CE) and the other from surface PL ($\Delta H \approx 5$ cal/g PL).

Microemulsion system:	EYL/CO	EYL/CN	DML/CO	DML/CN	DPL/CO	DPL/CN
Core Transition(s) Tm(°C)	42	51	46	54, 63	~ 41	~ 41
Surface Transition Tm(°C)	--	--	25	25	41	41

We conclude: (1) stable microemulsions with the size and organization of LDL can be made from PL and CE without protein, (2) EYL/CO and EYL/CN exhibit an order-disorder transition of the core CE with no PL transition, (3) DML/CO and DML/CN have a chain melting transition of the surface PL (2°> pure DML liposomes) and the core CE is stabilized as indicated by higher Tm's of CO and CN and the additional nematic-isotropic transition of the core of DML/CN (63°), (4) DPL microemulsions exhibit concomitant melting of surface PL and core CE indicative of coupling between the core and surface.

M-PM-B8 SOLUBILIZATION OF LOW DENSITY LIPOPROTEIN (LDL) BY SODIUM DEOXYCHOLATE (NaDC) AND RECOMBINATION OF ApoB WITH DIMYRISTOYL PHOSPHATIDYLCHOLINE (DMPC). PREPARATIVE METHODS AND PHYSICAL STUDIES. Mary T. Walsh and David Atkinson, Biophysics Institute, Boston University School of Medicine, Boston, MA 02118.

A lipid-free, soluble, mixed micellar complex of apoB has been isolated by gel filtration chromatography after NaDC-solubilization of LDL (d 1.025-1.050).

Differential scanning calorimetry (DSC) of apoB-NaDC exhibits a transition from 20-30°C which is irreversible after the sample is heated to 100°C. High temperatures result in complete protein unfolding-denaturation or disruption of protein-detergent mixed micelles. Particle disruption of intact native LDL occurs at 60-80°C, thus suggesting a greater thermal lability of apoB in the absence of its normal lipid environment. Gel filtration chromatography of detergent-free, lipid-free apoB prepared by detergent dialysis showed the protein to be highly self-aggregated, though soluble in aqueous buffers. Negative-stain electron microscopy showed such samples to be highly amorphous.

Soluble apoB-DMPC recombinants have been prepared by incubation of aqueous solutions of apoB-NaDC and DMPC-NaDC (2:1 w/w) at room temperature with detergent removal by extensive dialysis against detergent-free buffer. On varying the initial incubation ratio of apoB-to-DMPC from 1:10 to 1:1 (w/w), stable recombinants containing approximately 10,000 moles of DMPC per mole of apoB (dimer molecular weight of 500,000) (10:1 w/w) can be isolated by gel filtration chromatography or density gradient centrifugation. The apoB-DMPC 1:10 w/w complex is a 200±20A spherical particle as seen by negative stain electron microscopy and is vesicular as evidenced by carboxyfluorescein trapping. DSC of concentrated solutions show both a DMPC and a high temperature transition at a temperature comparable to that at which particle disruption of LDL occurs.

M-PM-B9 ION DISTRIBUTIONS IN INHOMOGENEOUS REGIONS. V.S.Vaidhyanathan, State Univ. New York, Buffalo. Under equilibrium conditions, inclusion of ion-ion interaction energy terms to limiting expression for chemical potentials of ionic species, leads to expression that concentration of an ion σ, with valence charge number Z_σ, at location x, in the inhomogeneous region, is related to its concentration in bulk solution, by the expression, $C_\sigma(x) = C_\sigma(d)\exp[Z_\sigma \beta(x)]$, where $\beta = (e/kT)\{\phi(d) - \phi(o) + (H/4\pi)Y(x)\}$, where $Y(x) = -4\pi e \sum_\sigma Z_\sigma C_\sigma(x)$, the charge density per unit volume. e is protonic charge, k is Boltzmann constant and T is absolute temperature. When a dielectric profile exists, it can be shown exactly that $-(4\pi/H) = \varkappa^2(d)\epsilon(d)$, (equalling approximately $42\,\Delta\epsilon/d^2$), where d is the magnitude of inhomogeneous region. $\Delta\epsilon$ is the difference in dielectric coefficients, $\varkappa^2(d)$ and $\epsilon(d)$ are respectively the Debye-Huckel parameter and dielectric coefficient of bulk solution.

For symmetrical electrolyte system, in place of Nernst expression, one has $[e\Delta\phi/kT] = \beta - \sinh\beta$, thus yielding reasonable values of surface concentration of ions, for potential difference of even 200 mV. It is shown that ion distribution in inhomogeneous regions, as expressed by $\beta(x)$, is the direct result of existance of a dielectric profile and validity of a generalized Maxwell's Osmotic balance equation. The dielectric profile imposes saturation of surface charge density.

M-PM-C1 SODIUM CURRENT FLUCTUATIONS IN THE CUT-OPEN AXON. I. Llano* and F. Bezanilla. Dept. of Physiology, UCLA, Los Angeles, CA 90024.

Sheets of axonal membrane from the giant axon of the squid Loligo pealei were voltage-clamped as previously described (Llano and Bezanilla, 1980, PNAS 77:7484). The internal side of the membrane was perfused with a solution containing 20 mM Na^+ glutamate, 200 mM CsF and 430 mM sucrose to eliminate K^+ currents. Pronase (0.5 mg/ml) was applied through a pipette on top of the internal side of the membrane in order to clean its surface. Fire polished pipettes (i.d.=0.5-1.0 μm) filled with internal solution and having resistances of 3-7MΩ were moved towards the internal side of the membrane. After contact with the membrane (as evidenced by an increase in pipette resistance to 50-200MΩ) slight negative pressure in some cases resulted in a further resistance increase to 1-10 GΩ. Development of GΩ-seals in this preparation was only possible after pronase treatment. Under these conditions, the activity recorded from the patch under the pipette was variable; we found many patches to be silent and some in which the currents were present for only a few minutes even though the seals remained high. In those cases in which activity was stable, the current recorded from the patch under the pipette while the whole sheet of membrane was stepped to depolarizing potentials, showed large fluctuations during the duration of the pulse. The size of the fluctuations was used to determine the single channel conductance (γ) using ensemble analysis of groups of records taken at the same potential. For membrane potentials in the range from -40 to -10 mV preliminary γ estimates range from 3 to 6 pS, and show no significant variation with membrane potential.

Supported by USPHS grant GM 30376 and a Grass Fellowship to I.Llano at the MBL, Woods Hole, MA.

M-PM-C2 **CARDIAC AND NERVE Na^+ CHANNEL DIFFER AT THEIR SAXITOXIN BINDING SITES**

R.B. Rogart, L. Regan, & J.B. Galper (Intr. by J.E. Megerman); Brigham & Women's Hosp & Children's Hosp, Harvard Med Sch, Boston, MA

The cardiac fast Na^+ channel (Ch) has been technically unamenable to direct electrophysiologic or pharmacologic study. Hence, cardiac impulse conduction and anti-arrhythmic drug action have been described by assuming that the cardiac Ch's properties can be inferred from the well characterized nerve Na^+ Ch. We measured uptake of labeled saxitoxin (*STX), a neurotoxin which has a high affinity in nerve (K_d=1.2 nM), to chick cardiac membrane. Measuring toxin uptake from 0-20 nM in physiologic solution, only 20% of binding was specific (i.e. could be competitively displaced by unlabeled toxin), but the uptake curve suggested a K_d in excess of 10 nM. An improved assay was developed, with specific binding of *STX to cardiac membrane accounting for >75% of total *STX uptake. With this assay, in isotonic CsCl solution we measured a K_d=10-12 nM for cardiac Na^+ Ch compared to K_d=0.4-0.6 nM for nerve Ch. This 15-30 fold difference in *STX affinity was also found in physiologic solution, with a K_d of 16-22 nM for heart vs. a K_d of 1.1-1.4 nM for nerve Na^+ Ch. The measured off-rates for *STX at 2-4°C were τ_{off}= 2.9 min and 1.6 min for nerve and heart respectively. Since these off-rates were quite similar, this suggests that the decreased affinity of *STX for heart Na^+ Ch is primarily due to a decreased on-time of toxin binding in heart as compared to nerve. One explanation of these data is that some portion of the cardiac Ch, presumably not present in nerve, blocks access of toxin to its binding site. These results show significant differences in properties between the fast Na^+ Ch in heart and nerve, indicating the need for further direct characterization of the properties of the cardiac Na^+ Ch.

M-PM-C3 PARTIAL ISOLATION AND RECONSTITUTION OF NERVE MEMBRANE SODIUM CHANNEL.

Villegas, R., Villegas, G.M., Suárez-Mata, Z. and Rodríguez, F. C.B.B., IVIC. Caracas 1010A and Instituto Internacional de Estudios Avanzados, Caracas 1015A, Venezuela.

The present work describes experiments carried out to isolate the Na channel from the nerve membrane. (I) The first part describes reconstitution experiments carried out with membrane particles, obtained by treatment of lobster nerve membrane suspended in 0.7 M sucrose, 10 mM Tris-Cl, pH 7.5, with 0.25% cholate plus 30 mM octyl glucoside for 10 min, followed by centrifugation at 150,000 x g for 20 min and fractionation of the supernatant by gel exclusion chromatography with a Sepharose 6B column. The samples collected from the column were pooled into two fractions. When the membrane material in each fraction was collected and incorporated into soybean liposomes, it was found that one of the fractions has Na channel activity. The electrophoretic patterns of the fractions revealed that only the active one has a component which does not enter the SDS-9% polyacrylamide gel and the ≃ 250,000 and ≃ 120,000 mw peptides; it was also enriched in the ≃ 50,000 mw peptide. (II) The second part describes experiments carried out with two similar fractions, obtained by treatment of the membrane suspended in 0.3 M sucrose, containing 25 mg/ml of soybean lipids, with 0.5% cholate plus 30 mM octyl glucoside for 15 min, followed by centrifugation at 100,000 x g for 60 min and subsequent gel exclusion chromatography with Sepharose 6B. The electrophoretic pattern of the active fraction gave further support to the correspondence between Na channel activity and the presence of the peptides indicated previously. Further purification is required to determine the exact composition of the channel.

M-PM-C4 DEVELOPMENT OF Na^+ CHANNELS IN NEUROBLASTOMA CELLS. Ilan Spector and Jesse Baumgold, Lab. Biochem. Genetics, NHLBI, and Lab. of Neurobiol., NIMH, Bethesda, MD 20205. (Intr. by R. FitzHugh).

The development of Na^+ channels during DMSO induced differentiation of N1E-115 neuroblastoma cells was studied using electrophysiologic, ligand binding and ion flux techniques. In untreated cells in confluent cultures or in cells grown in the presence of 2% DMSO for 3 days, Na^+ action potentials elicited from a steady hyperpolarized membrane potential of -100 mV are not fully developed (average maximum rate of rise = 52 V/s; average peak spike amplitude = 0 mV). After 7-9 days in the presence of 2% DMSO the cells acquire a differentiated morphology and can generate well developed Na^+ action potentials (average maximum rate of rise 150 V/s, average peak spike amplitude +30 mV). To further characterize these electrophysiological changes the stimulation of ^{22}Na influx by batrachotoxin and scorpion toxin and the specific binding of ^{125}I-scorpion toxin was examined in replicate plates. Specific binding of ^{125}I-scorpion toxin in untreated cells or in cells treated for 3 days with 2% DMSO was similar (~250 fmol/mg protein). Binding increased markedly by day 8 in 2% DMSO and remained constant thereafter (~725 fmol/mg protein). The dissociation constant for ^{125}I-scorpion toxin binding was identical in all culture conditions and throughout DMSO treatment (Kd = 12 nM). Similarly, the rate constants of binding and dissociation of bound ^{125}I-scorpion toxin remained constant ($T_{1/2}$ for dissociation = 25 min). The increase in the Na^+ action potential characteristics and in the specific binding of ^{125}I-scorpion toxin in cells treated for 8 days with 2% DMSO were also reflected in a 2.4-fold increased stimulation of ^{22}Na influx by batrachotoxin and scorpion toxin in these cells as compared with ^{22}Na influx in untreated cells or after 3 days in 2% DMSO. These results demonstrate that the Na channel is a developmentally regulated property in neuroblastoma cells.

M-PM-C5 KINETIC ANALYSIS OF I_{Na} AND GATING CURRENT IN CRAYFISH GIANT AXONS. M.D. Rayner and J.G. Starkus, Dept. of Physiology, University of Hawaii, Honolulu, Hawaii 96822.

Crayfish axons internally perfused with a medium containing 1mM 4AP and 20mM TEA show complete blockade of potassium currents permitting clear resolution of the slowest components of sodium and gating currents. Using 1/3 Na modified Van Harraveld's solution, following careful R_S compensation and evaluation of space-clamp effectiveness, exponential stripping of signal-averaged records reveals at least 6 separable components in ionic current transients and 4 components in gating current transients.

The small slowest component (tau 1) of the ionic currents parallels the slowest decay rate seen by conventional double-pulse protocols for investigation of "slow inactivation" and has a detectable equivalent within the gating current records (tau S1). Tau 1 and tau S1 are both about 200 msecs at -20mV but only 8 msecs at +70mV (at 6°C). The most heavily-weighted component of the I_{Na} falling phase (tau 3) also appears to have a kinetic equivalent (tau S2) within the gating currents, although both these components may be two to three fold faster than the conventionally-determined "tau h". Similarly, the major component of sodium activation (tau 5) parallels the rate of the major component of the gating currents (tau F1), while the fastest component of I_{Na} (associated with the initial delay on the rising phase) has its equivalent in the fastest component (tau F2) of gating current.

We conclude that a minimum of 7 thermodynamically-separable states is involved in the regulation of sodium currents. Supported in part by NIH Grant No. GM29263-01 and by Fellowship No. 1F32-ES05065-03.

M-PM-C6 COMPARISON OF NOISE AND ADMITTANCE DATA IN SQUID AXON INDICATES NONLINEARITY IN Na CHANNEL KINETICS. HM Fishman, HR Leuchtag, J Sanchez, LE Moore. Univ. of Texas, Galveston.

The use of linear kinetic schemes to model voltage-clamp data assumes that the underlying microscopic rate-processes are linear. To examine this assumption, Na conduction kinetic parameters were obtained directly by linear perturbation analysis (admittance) and compared with those from spectral analysis of current fluctuations. Squid axons, perfused with buffered 290mM CsF solutions and ASW externally, were space clamped with an axial-wire technique. Comparisons of both admittance, $Y(j\omega)$, and noise data were made from measurements with the same axon and clamp system, at the same potentials (-65 to 10mV) and in the same time frame (5-7 sec after a step). $Y(j\omega)$ measurements were made under low noise voltage clamp with small amplitude, synchronized pseudorandom signals and FFT computations (Fishman et al, 1979, JMB 50:43). At each voltage a set of 400 real and imaginary components of $Y(j\omega)$ at frequencies in the range 12.5-5000Hz was fitted to that of a circuit model consisting of a parallel combination of a constant-phase-angle capacitance, chord conductance, G-C branch, and G-L branch, all in series with a resistance. The Na noise data were fitted with two Lorentzians. Comparisons of the results indicated that the two corner frequencies from the noise data were significantly higher (2-4X) than the corresponding natural frequencies of the G-C and G-L branches in the $Y(j\omega)$ fits at the same potentials. This discrepancy between kinetic parameters obtained by linear analysis and noise analysis suggests that Na current noise reflects a nonlinear microscopic process. Although predictions from linear kinetic models can fit macroscopic data, nonlinear models may be necessary to describe the underlying molecular phenomena. Aided by Grants NS11764, NS13778, NS13520.

M-PM-C7 ARE GATES AND THE ION PATHWAY INDEPENDENT IN SODIUM CHANNELS OF NERVE? Peter Shrager and Mei-Ven C. Lo, Dept. of Physiology, University of Rochester Medical Center, Rochester, NY 14642.

Na^+ channel gating kinetics have been measured under conditions in which ionic current through individual channels is varied while total ionic current is held constant and small. A test is made for the location and nature of the resistance in series (R_s) with activation and inactivation gates. The speed of closing of these gates is recorded in voltage clamped, internally perfused crayfish giant axons, first in 6% $[Na^+]_o$ (94% tetramethylammonium ion) and then in 100% $[Na^+]_o$ + 3.2 nM tetrodotoxin (TTX). No electronic compensation for R_s is used. K^+ currents are reduced by 2 mM 4-aminopyridine and eliminated by subtraction of records in 100 nM TTX. Peak Na^+ currents were small (average 0.4 mA/cm^2) and differed by less than 0.2 mA/cm^2 between 6% $[Na^+]_o$ and 100% $[Na^+]_o$ + 3.2 nM TTX. Inactivation time constants (τ_h) were measured from the rate of decay of Na^+ currents. On changing from 6% $[Na^+]_o$ to 100% $[Na^+]_o$ + 3.2 nM TTX, τ_h-V_m curves were shifted by 2.7 mV in the depolarizing direction. Na^+ tail current time constants (τ_{tail}) were shifted by 3.2 mV in the opposite direction. From our best estimate for total R_s in this axon (6 Ωcm^2), and the difference in peak Na current between 100% $[Na^+]_o$ (no TTX) and 6% $[Na^+]_o$ (5 mA/cm^2) the shift expected if all the R_s were associated with individual channels is about 30 mV (hyperpolarizing). Our results suggest that almost 90% of the R_s is not of this origin, and is most likely due to the Schwann cell-connective tissue sheath. The measured shifts might reflect a weak interaction between Na^+ ions bound at a site within the open channel and voltage sensitive regions of gates. The data predict that the distance between binding site and gate is in excess of 20Å. Supported by NIH grant 5-R01-NS10500 and RCDA 5-K04-NS00133.

M-PM-C8 BLOCK OF SODIUM CHANNELS AT LOW pH IS LESS VOLTAGE DEPENDENT THAN PREVIOUSLY THOUGHT. Donald T. Campbell, Dept. of Physiology and Biophysics, University of Iowa, Iowa City, IA 52242.

Previous studies of Na channel block by protons have yielded conflicting pictures of Na channel structure. By characterizing block over a wider voltage range than in previous studies it has been possible to place greater constraints on possible models. The Vaseline gap voltage clamp technique was used to measure Na channel tail currents in single bullfrog muscle fibers at normal (7.3) and low (5.9 and 5.0) extracellular pH. To hold internal pH constant, fiber ends were cut in a solution buffered to pH 7.3 with 10 mMHEPES. Fibers were held at -120 mV to remove long-term inactivation. A prepulse to +90 mV was interrupted at the peak sodium current and followed by test pulses from -120 to +180 mV. The reduction of tail conductances in low pH solutions was well fitted by a modification of Woodhull's theory (J. Gen. Physiol. 61:687) with two important differences. First, the apparent K_d's exhibited little voltage dependence, as if the blocking site experienced only 7.8% $\pm$ 1.4 (mean $\pm$ s.d.) of the membrane voltage. Second, values of pK (0 mV) depended on pH: 4.81 $\pm$ 0.12 (pH 5.0) and 5.41 $\pm$ 0.09 (pH5.9) (mean $\pm$ s.d., n=6). These results suggest that the blocking site is closer to the outer edge of the pore than previously thought and that proton binding to the blocking site is influenced by protons bound to another nearby site. Supported by NS 15400 and MDA.

M-PM-C9 HYDROGEN ION BLOCK OF SODIUM CHANNELS OF SQUID GIANT AXONS. Ted Begenisich and Miklos Danko. Department of Physiology, University of Rochester, Rochester, N.Y. 14642 and Department of Physiology, University Medical School, Debrecen, Hungary.

Previous experiments have demonstrated a reduction of sodium channel current in nerve produced by external hydrogen ions. These results have generally been interpreted as the titration of an acid group in the open pore. An alternative explanation might be that hydrogen ions prevent the opening of the gates controlling ion flow. We have sought to distinguish between these two possibilities by measuring external hydrogen ion block with different internal solutions. These experiments were performed on voltage-clamped internally perfused squid giant axons. Internal solutions contained only Na ions, only K ions, mixed Na and K ions, or mixed Na and Cs ions. We find that the external hydrogen ion block depends upon the ionic composition of the internal solution. We take this as a demonstration that hydrogen ion block occurs within the ionic permeation pathway. We further show that the block is not necessarily a monotonic function of membrane voltage. These results are analyzed in terms of several different models for ion permeation. Supported by PHS Grants NS14138 and NS00322 (RCDA).

M-PM-C10 MOLECULAR MECHANISMS OF SODIUM CHANNEL INACTIVATION: DISCRIMINATIONS USING TEMPERATURE, OCTANOL, AND ION COMPETITION. G.S. Oxford and J.Z. Yeh, Dept. of Physiology, University of North Carolina, Chapel Hill, NC 27514 and Dept. of Pharmacology, Northwestern Univ., Chicago, IL 60611.

The qualitative similarity between sodium channel inactivation and the time-dependent block of non-inactivating channels by several internally perfused agents has prompted the suggestion that normal inactivation occurs when an intrinsic positive charge tethered to the internal membrane surface binds at a site near the channel's inner mouth and blocks ion flow. We have examined the effects of temperature, octanol, and ionic environment on the block of pronase-treated Na channels by octylguanidine (C8G) and 9-aminoacridine (9AA) in voltage clamped squid axons, and compare the results with the known modulation of normal inactivation by these perturbations. Peak Na currents are comparably temperature-dependent ($Q_{10} \sim 1.9$) in C8G and 9AA axons as well as normal axons. Steady-state I_{Na} is also temperature sensitive in 9AA axons, but is nearly independent of temperature in C8G and normal axons ($Q_{10} < 1.2$). The rates of normal inactivation and C8G block are temperature sensitive ($Q_{10} \cong 2.5$), however the rate of 9AA block is temperature independent. The addition of 0.3M octanol potentiates inactivation in normal axons (Oxford & Swenson, 1979) and enhances steady-state block of C8G, but not 9AA, in pronase-treated axons. Substitution of internal Cs^+ by TMA^+ reduces peak I_{Na} and increases steady-state I_{Na} producing "crossover"(less inactivation) in normal axons (Oxford & Yeh, 1979). Similarly, steady-state block by both C8G and 9AA is relieved by TMA substitution while peak I_{Na} is reduced. These observations provide strong support for ionic block models of Na inactivation and emphasize the importance of hydrophobic interactions in the process. (Supported by NSF grant BNS 79-21505).

M-PM-C11 CHLOROFORM SEPARATES COMPONENTS OF CHARGE MOVEMENT IN SQUID GIANT AXON. J.M. Fernández, F. Bezanilla, R.E. Taylor, Dept. of Physiology, UCLA, CA 90024; Laboratory of Biophysics, NINCDS, NIH, Bethesda, MD 20205.

The effect of the neutral general anaesthetic chloroform upon the sodium currents, gating currents and transport parameters of lipophilic ions was studied in the squid giant axon membrane under voltage clamp. Perfusion of an axon with a chloroform containing solution reversibly decreases the size of the Na^+ current. This is paralleled by a decrease in the size of the gating currents as observed in experiments without permeant ions. ON gating currents can be described by the sum of two exponentials, and the action of chloroform is to reversibly decrease the fast component of the gating currents. When the axon is perfused with a maximum concentration of 50 mM chloroform, the fast component is completely eliminated, the remaining gating current can be fitted by a single exponential corresponding to the slow component of gating. At intermediate concentrations the fast component is reduced in size only, but its time constant remains the same. The slow component remains unaffected at all concentrations. In contrast to the effect observed in the gating currents, the charge movement induced by the lipophilic ion dipicrylamine is speeded up significantly without any reduction in its size in agreement with previous experiments performed in bilayers. It is concluded that gating charges do not move in the membrane in the same manner as lipophilic ions. Therefore, gating charge movement does not occur in the bulk lipid and most likely occurs within the molecular structure of the channel where chloroform may reach via the lipid matrix to interact with specific sites to disable the movement of the gating charges. Supported by USPHS grant GM 30376 and a Grass Fellowship to J.M.F. at the MBL, Woods Hole, MA.

M-PM-C12 METHYLENE BLUE DYES AS INACTIVATION SIMULATORS. Clay M. Armstrong and Robert S. Croop. Dept. of Physiology, Univ. of Pennsylvania School of Medicine, Philadelphia, Pa. 19104.

The effects of the methylene blue family of dyes on sodium current (INa) were studied in squid giant axons. The dyes were applied internally, and in subdued light to prevent photodynamic effects. At a concentration of 0.1-0.25 mM, they speed decay of INa; i.e. they apparently speed inactivation. After removal of inactivation with pronase, the dyes restore a semblance of it. Gating current recorded during activation of channels (Ig ON) is unaffected by dyes in the absence of TTX, unless the interval between pulses is less than 10 or 15 ms, in which case Ig ON is severely reduced. The initial amplitude of Ig during channel closing (Ig OFF) is reduced almost to zero after a 10 ms pulse in dye. Ig OFF then increases to a peak about 0.3 ms after the step-back, and decays slowly. The reduction of Ig OFF parallels the time course of dye blocking of Na channels, as measured by the decay of INa. From two-pulse experiments it is clear that TTX slows dissociation of dye from the channels by a factor of 4X or more, presumably by preventing external ions from entering and displacing dye. In TTX Ig ON is reduced by dyes, and Ig OFF almost completely eliminated. Kinetic analysis indicates that 1) dyes compete with the normal inactivation mechanism; 2) dyes can block channels before the channels fully open; 3) most channels conduct transiently during recovery from dye-block; 4) normally inactivated channels do not conduct during recovery; 5) dyes prevent closing of Na activation gates and 6) thereby immobilize gating charge. The data provide strong evidence that almost all of "gating current" is in fact associated with Na channel gating: virtually all of Ig OFF is eliminated by dye-block of Na channels.

M-PM-C13 COMPARATIVE EFFECTS OF TWO BARBITURATES AND A RELATED MOLECULE ON THE SODIUM CHANNEL OF THE SQUID GIANT AXON. Robert S. Morello, Department of Physiology, University of Rochester, Rochester, New York 14642.

The modes of action of the barbiturates, phenobarbital (PhB) and pentobarbital (PB), and the related molecule, diphenylhydantoin (DPH) were compared with regard to sodium channel function of the perfused, voltage clamped squid giant axon. Tonic inhibition of sodium currents by PhB (2.5 mM), like DPH (100 μM), was reduced at more negative holding potentials. Conditioning pulses up to 2 seconds in duration however, had no significant effect on PhB action. Current inhibition in the presence of 2 mM PB was not affected by either conditioning pulses or changes in holding potential.

The effects of stimulus frequency on current inhibition were also investigated. Marked use-dependent decline in sodium currents was produced with both PhB and DPH. In each case, the degree of inhibition was greater at more depolarized potentials and at higher rates of stimulation. Unlike the local anesthetics, current inhibition was independent of the state of fast inactivation gates. Furthermore, the voltage dependence of fast inactivation was unaffected during use-dependent decline in current. Current was restored completely within 4 seconds after returning to the holding potential. Internal perfusion of the axon with papain, which removed fast inactivation, also removed use-dependence. PB exhibited little use-dependent inhibition.

By varying the pH of either the internal or external solution and applying PhB to either solution, the active form of PhB was determined. Results of these experiments indicated that the neutral molecule was responsible for both tonic and use-dependent blocks.

M-PM-D1 THE EFFECT OF IONIC STRENGTH ON EXPONENTIAL PROCESSES --- A POSSIBLE SITE OF ACTION IN A CROSS-BRIDGE CYCLE. M. Kawai, P.W. Brandt, and L.G. Cornacchia,III*. Departments of Neurology and Anatomy, Columbia University, New York, N.Y. 10032.

Lowering ionic strength is known to increase isometric tension and ATPase activity. In order to determine whether this is related to an increase in the crossbridge cycling rate or to an increase in the number of active cross-bridges, we changed the ionic strength in the range of 128-265mM and measured rate constants of three exponential processes. We employed the sinusoidal analysis technique on single fibers of chemically skinned rabbit psoas preparations; activating solution contained (mM): 6 CaEGTA, 5 MgATP, 5 free ATP, 7.5 phosphate, 9.4 CP, 80 unit/ml CPK, 0-40 Na propionate, 0-33 Na_2SO_4, 10 MOPS (pCa 4.96, pH 7.00, 20°C). The results are summarised in the phase-frequency plot (Figure). The rate constants of three processes (indicated by a, b, c) are minimally affected when isometric tension and magnitude parameters changed by a factor of 1.7. We infer from this that the kinetics of individual cross-bridges are minimally affected by ionic strength, and that the lowering ionic strength recruits more cross-bridges into the active pool. We further speculate that bridges on reserve are in the refractory state, and that the major effect of change in ionic strength is to modify the transition rate through the refractory state. Supported by grants from NIH (AM21530), NSF (PCM80-14527), and MDAA.

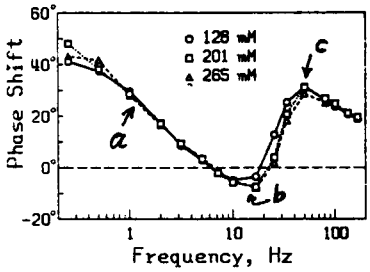

M-PM-D2 EVIDENCE FOR POSSIBLE CROSSBRIDGE ATTACHMENT IN RELAXED MUSCLE AT LOW IONIC STRENGTH. M. Schoenberg, B. Brenner*, J. Chalovich, L. Greene, and E. Eisenberg. NIH, Bethesda, MD 20205.

Biochemical studies suggest that crossbridges may be attached in relaxed muscle (Chalovich, et al., J. Biol. Chem., 256:575:1981). To test this hypothesis we compared the binding of S-1 to regulated actin with the stiffness of skinned rabbit psoas muscle fibers under identical (relaxing) conditions (in mM, 1 ATP, 3 $MgCl_2$, 1 EGTA, 10 imidazole, pH 7, 5° C, μ = 0.02 M). The experiments were performed at 5° C to avoid the appearance of active tension (Gulati, Biophys J., 33:83a:1981) which, in rabbit, occurs at higher temperatures in low ionic strength even in the presence of excess Mg^{++}. We find that, as at 25° C, troponin-tropomyosin has no effect on binding of S-1 to actin in the presence or absence of Ca^{++}, again suggesting that cross-bridges might be attached in relaxed muscle under this condition. If there is a rapid equilibrium between attached and detached states in relaxed muscle, the muscle would appear to have little stiffness on a slow time scale but would be much stiffer on a rapid time scale. Therefore we measured the stiffness using moderate (1 ms) and rapid (0.1 ms) stretches. With moderate stretches the muscle did not appear stiff but with rapid stretches the stiffness was the same order of magnitude as the rigor stiffness. In the presence of AMPPNP at μ = 0.13 M, where the binding strength of S-1-AMPPNP to actin in vitro is identical to that obtained with ATP at very low ionic strength, the muscle is stiff even with 1 ms stretches. Therefore it appears that cross-bridges can be attached to actin in relaxed muscle, at least under very low ionic strength conditions, and that the crossbridges attach and detach much more rapidly in relaxed muscle than in AMPPNP.

M-PM-D3 CHARACTERIZATION OF THE 'RAPID STIFFNESS' OF RELAXED SKINNED RABBIT PSOAS MUSCLE FIBERS. B. Brenner*, M. Schoenberg, J. Chalovich, L. Greene, and E. Eisenberg. NIH, Bethesda, MD 20205.

In order to be able to detect rapidly attaching and detaching crossbridges, we developed a technique for measuring muscle stiffness within 100 μs. A rapid length change was applied to the muscle and the stiffness was measured as the slope of the X-Y plot of the resulting force and sarcomere length changes. In order to avoid problems due to transmission time or inhomogeneities along the length of the fiber, the laser beam monitoring sarcomere length was positioned near to the tension transducer (f > 10 kHz). The incident angle of the laser beam was varied to look for artefacts related to Bragg-angle effects. At normal ionic strength, μ= 0.17 M, T = 5° C, the stiffness of the relaxed fiber (in mM, 5 EGTA, 1- 5 ATP, 3- 5 $MgCl_2$, 10 PCr, 20 imidazole, 300 Sigma U/ml CPK, + KCl, pH 7) was < 10% the stiffness of the activated fiber (5 mM CaEGTA). This stiffness increased slightly with increasing sarcomere length. At low ionic strength (1 ATP, 3 $MgCl_2$, 1 EGTA, 10 imidazole, pH 7, μ = 0.02 M) the stiffness of the relaxed fiber was much greater. It was comparable to that of the Ca-activated fiber at μ = 0.17 M and about 1/3 that of the Ca-activated fiber at μ = 0.02 M. Furthermore, under this condition, in contrast to normal ionic strength, the resting stiffness decreased with decreasing overlap. At zero overlap (SL = 4.2 μm) the remaining rapid stiffness (c. 10%) was relatively insensitive to ionic strength, as was the passive resting tension. We conclude that, at normal ionic strength, much of the observed stiffness may be due to the same passive structures that contribute to the resting tension. In contrast, at low ionic strength, the observed stiffness appears to be related to crossbridges.

M-PM-D4 ANALYSIS OF X-RAY EQUATORIAL PATTERNS FROM RESTING AND ACTIVE SKELETAL MUSCLE.
L. C. Yu, A. C. Steven, R. J. Podolsky, NIH, Bethesda, MD 20205; G.R.S. Naylor, Oxford University, Oxford, England; and R. C. Gamble, California Institiute of Technology, Pasadena, CA 91125.

Equatorial diffraction patterns from frog skeletal muscle were obtained with the radiation source at Stanford Synchrotron Radiation Laboratory. From muscles in the relaxed and the fully activated states, five reflections [1,0], [1,1], [2,0], [2,1], and [3,0], were consistently observed. The patterns were analyzed by a non-linear least squares fit method. In general, the peaks beyond [1,1] were clearly resolved in the resting state, but appeared to become weaker and broader on activation. By analyzing the line widths of the peaks within each diagram, it is concluded that (1) in the resting state myofibrils form crystalline scattering domains; (2) the systematic broadening of the peaks towards higher angles for the resting muscle is due mainly to slight variations in the lattice spacing among the myofibrils (spacings distributed with a width of about 3% of the mean value); (3) upon activation, the width of this distribution broadens to about 4%, and there is a clear increase in the unit cell to unit cell disorder. Specifically, it is estimated that the distances between centers of gravity of neighboring unit cells deviate from ideal lattice positions with a standard deviation of 25-30 Å (one unit cell contains one myosin and two actin filaments). While intensities $I_{1,0}$ and $I_{1,1}$ change substantially upon activation, $I_{2,0}$ appears to increase slightly (<20%), and $I_{2,1}$ and $I_{3,0}$ seem to decrease by 20-60%. Thus, the low signal to noise ratio of these higher orders from active muscle is due mostly to smearing of the peaks on account of perturbations within the lattice rather than loss of intensity per se. Axial projections of the myofilament density in both states have been obtained from intensities refined by this analysis.

M-PM-D5 INHIBITION OF CROSS-BRIDGE FORCE BY VANADATE ION. Alan Magid and Charles C. Goodno*, Department of Anatomy, Duke University Medical Center, Durham, NC 27710.

Vanadate ion (Vi) has been shown to be a potent inhibitor of myosin and actomyosin ATPase (Goodno, PNAS 76, 2620; 1979: Goodno and Taylor, PNAS, in press, 1981). Moreover, with ADP, it combines with myosin to form a ternary complex that interacts with actin analagously to the myosin-products complex. Therefore, we have studied the effect of Vi on force generation in skinned fibers isolated from R. piniens semitendinosus muscle. Both calcium-activated and rigor-activated contractions were studied. The rate and extent of Vi inhibition of active force (activating soln: (mM) 60 KOAc, 5 MgOAc, 4 ATP, 4 EGTA, 4 $CaCl_2$, 15 KPi, ph 7.0, 22°C) were both concentration-dependent. 5 mM Vi rapidly inhibited tension ($t_{\frac{1}{2}}$=3s) to the extent of 97%, with prompt redevelopment of tension upon Vi washout ($t_{\frac{1}{2}}$= 20s). Inhibition of active tension was half-maximal at 90 um Vi, and substitution of MOPS buffer for phosphate shifted the Vi-dependence to lower concentrations. Stiffness (estimated with a ± 0.5% length change at 10 Hz) varied roughly in parallel with tension. Identical results were obtained for mechanically- and Triton-skinned fibers. Cycling fibers between relaxing and rigor-Vi solutions (permitting calcium-free activation) caused a cycle-by-cycle tension loss. Inhibition, however produced, was not reversed by soaking the fiber in either Vi-free rigor solution (+/- Ca^{2+}) or Vi-free relaxing solution, but was fully reversed by Vi-free activating solution. Rigor cycling also restored tension, but more slowly. We interpret these results to indicate that Vi inhibition is not due to effects on the SR nor on the troponin-tropomyosin system but that Vi is a potent, active-site-directed agent for the reversible dissociation of cross-bridges, not only in actomyosin but also in muscle fibers. (Supported by NIH and MDA Research Grants).

M-PM-D6 EFFECT OF BARIUM IONS IN DEPOLARIZATION CONTRACTION COUPLING.
Caputo, C., Bolaños, P., Velaz, M.E. C.B.B., IVIC, Apt. 1827, Caracas, Venezuela.

Short muscle fibers (≃ 1.5 mm) dissected from the lumbricalis muscle of the frog were voltage clamped at -100 mV in saline solutions containing 10^{-6} g/ml TTX. Contractile responses to depolarizing pulses, could be measured with a tension transducer. In normal Ringer's solution, with 1.8 mM Ca^{++}, the time course of the response to maximal depolarizations (90 mV) shows a tension development phase and a plateau (2-3 sec), followed by a fast relaxation phase similar to that of K-contractures. In solutions prepared without calcium, tension development is not impaired, while the plateau is much shortened (< 1 sec) and the relaxation phase is faster. Equimolar substitution of barium for calcium is ineffective in restoring the normal time course of these responses, while nickel substitution is effective. Addition of barium (1.8 mM) to normal (1.8 mM Ca) saline does not affect the responses. When short (< 1 sec) depolarizing pulses are used, the maximal responses obtained in 1.8 mM Ca, 0 Ca, 0 Ca + 1.8 mM Ba, or 0 Ca + 1.8 mM Ni salines, are practically similar. It therefore appears that while barium may substitute for calcium as charge carrier for the slow inward current (Potreau and Raymond, J. Physiol. 303:91, 1980) it is ineffective in sustaining prolonged contractions. Nickel ions behave in the opposite way. Preliminary experiments indicates that fragmented Sarcoplasmic Reticulum isolated from frogs, is not effective in transporting barium ions.
Supported by CONICIT Fund S1-1148.

M-PM-D7 DOES LATENCY RELAXATION DEPEND ON THE NUMBER OF SARCOMERES IN SERIES? Louis A. Mulieri & Norman R. Alpert. Dept. Physiol. & Biophys. Univ. Of Vermont, Burlington, VT 05405

Two recent latency relaxation (LR) theories propose the underlying event to be a forceful sarcomere lengthening either by expansion of the thin filaments (Haugen and Sten-Knudsen, J. Gen. Physiol 68:247, 1976) or expansion of the T-tubules (Hoyle, Comp. Biochem. Physiol. 66A:57, 1980). In either case one expects the depth of the LR to be proportional to the number (N) of sarcomeres in series along the length of a fiber. To support previous evidence against such dependence of the LR on N (Mulieri, J. Physiol. 223:333, 1972) new experiments, free of the criticism raised by Bartels et al. (Acta Physiol. Scand. 97:476, 1976), were performed. Bundles of 10-12 fibers were dissected from the frogs anterior tibialis muscle in matched (cross sectional area and length) pairs. The LR was recorded (Mulieri, 1972) from each bundle of a pair at 3 μm sarcomere length. Then individual bundles of a pair were connected in series between the transducer levers, doubling the number of sarcomeres in series while maintaining the sarcomere length at 3μm. The depth of the LR with the two bundles in series was about equal to the value obtained from each bundle separately; however, it doubled when the bundles were hooked in parallel. This confirms that during the LR the fiber behaves as a force generator (Mulieri, 1972) rather than as a length change generator (Haugen & Sten-Knudsen, 1976) or as a volume change generator (Hoyle, 1980). Supported by NIH RO1 17592-05.

M-PM-D8 PREDICTIONS OF A MODEL OF STRIATED MUSCLE CONTRACTION. M.B. Propp, Department of Electrical Engineering and Computer Science, Massachusetts Institute of Technology, Cambridge, Mass., 02139

A model which can explain energy transduction in muscle and assimilate the structural parameters and in vitro rate constants has been developed (Propp, M.B. and T.L. Johnson, Biophys. J., 33, 25a, 1981). The positional dependence of the in vivo rate constants can be derived using few assumptions.

We present the predictions of the model for three experimental paradigms--an isometric contraction, an isovelocity contraction, and a tension transient. The model behaves rather like a muscle fibre--with varying degrees of success, it predicts the physiological properties of muscle at different temperatures (5° and 20°C) and as functions of nucleotide concentrations. The results which conform least to the properties of muscle are: the ATP flux as a function of steady-state velocity does not attain a maximum; the stiffness as a function of steady-state velocity remains relatively constant; and the values for the half-time of recovery to the T_2 level are low. As the model includes all biochemically- and structurally-distinguishable states, it provides a complete description of cross-bridge action for varied experimental conditions.

The biochemical and structural studies on the interaction of actin, myosin, and ATP thus provide sufficient information to predict "open-loop" the physiological properties of muscle when incorporated into a thermodynamic formalism based upon the theory of Markov processes and assuming the cross-bridge theory. Therefore, the parameters determining cross-bridge action can be derived from component studies and are sufficient to explain the contractile process.

M-PM-E1 INTERPRETATION OF Fe^{+2} - UQ^{-}INTERACTION IN ACCEPTOR OF BACTERIAL REACTION CENTER-INTERPRETATION OF MÖSSBAUER DATA. K.C. Mishra and T.P. Das, SUNY Albany, A. Coker, University of Port Harcourt, Nigeria, and K.J. Duff, University of Wollongong, Australia.

The primary acceptor in the reaction center of the photosynthetic apparatus of bacterial systems has been identified[1] as involving two ubiquinone (UQ) molecules linked through a Fe^{+2} ion. We have studied the electronic structure of the reduced system Fe^{+2}-$(UQ)^{-}$ using the extended Hückel procedure and analyzed the ^{57m}Fe nuclear quadrupole coupling constant (e^2qQ) and isomer shift obtained from Mössbauer measurements[2]. Our values of e^2qQ and isomer shift (with respect to iron metal) are 1.89 mm/sec and 0.92 mm/sec respectively in satisfactory agreement with the experimental values of 2.10 mm/sec and 1.10 mm/sec. For obtaining e^2qQ, we have used the recent value[3] of 0.082 barns for $Q(^{57m}Fe)$. Our theoretical results also explain the trend of the experimental data with respect to ionic ferrous compounds. The results of our analysis thus indicate that our electronic wave-functions are satisfactory and could be used for the analysis of other observed properties, among them, antiferromagnetic Fe^{+2}-$(UQ)^{-}$ exchange interaction, and the electron transfer rates associated with the acceptor system. (Supported by NIH grant GM2523003).

1. G. Feher and M.Y. Okamura in "The Photosynthetic Bacteria", R.K. Clayton and W.R. Sistrom ed., Plenum Press, New York (1978).
2. P.G. Debrunner et. al. Biophys. J. 15, 226a (1975).
3. K.J. Duff, K.C. Mishra and T.P. Das Phys. Rev. Lett. 46, 1611 (1981).

M-PM-E2 COMPLETE AMINO ACID SEQUENCE OF THE LIGHT HARVESTING PROTEIN FROM RHODOSPIRILLUM RUBRUM. G.E. Gogel, P.S. Parkes, R.A. Brunisholz*, H. Zuber* and P.A. Loach; Dept. of Biochemistry, Molecular and Cell Biology, Northwestern University, Evanston, IL 60201 USA, and *Institut für Molekularbiologie und Biophysik, ETH-Hönggerberg, CH-8093, Zürich, Switzerland.

Rhodospirillum rubrum has the smallest photosynthetic unit (psu) so far observed in photosynthetic organisms. This psu, sometimes called a photoreceptor complex (1), apparently consists of a single bacteriochlorophyll-containing light harvesting (LH) complex containing 22 to 24 bacteriochlorophyll (1). The protein component of this complex was previously isolated in pure form as a single polypeptide because of its unique solubility in organic solvents (2). Seven to eight carotenoid molecules are also present in the psu of the wild type organism but it is uncertain whether they are bound to the same protein as the bacteriochlorophyll. Similar isolation procedures were applied to prepare the LH protein from a bacteriochlorophyll-protein complex of the G-9 carotenoidless mutant of R. rubrum (3). Very recently, the complete amino acid sequence of this latter protein from the G-9 mutant was reported (4). We wish to report here that the amino acid sequence of the LH protein from wild type R. rubrum has been similarly obtained and that it appears to be identical with that of the carotenoidless mutant. Thus, the molecular weight is 6106 and the sequence is Nf-Met-Trp-Arg-Ile-Trp-Gln-Leu-Phe-Asp-Pro-Arg-Gln-Ala-Leu-Val-Gly-Leu-Ala-Thr-Phe-Leu-Phe-Val-Leu-Ala-Leu-Leu-Ile-His-Phe-Ile-Leu-Leu-Ser-Thr-Glu-Arg-Phe-Asn-Trp-Leu-Glu-Gly-Ala-Ser-Thr-Lys-Pro-Val-Gln-Thr-Ser-COOH. (1) P.A. Loach, Methods in Enzymology 69, 155-171 (1980). (2) S.J. Tonn, G.E. Gogel and P.A. Loach, Biochemistry 16, 877-885 (1977). (3) P.A. Cuendet and H. Zuber, FEBS Lett. 79, 96-100 (1977). (4) R.A. Brunisholz, P.A. Cuendet, R. Theiler and H. Zuber, FEBS Lett. 129, 150-154 (1981).

M-PM-E3 OXYGEN INTERACTION WITH THE PRIMARY ELECTRON DONOR OF RHODOSPIRILLUM RUBRUM. M.C. Woodle, K. Zebrowski-Morrison, P.L. Bustamante and P.A. Loach, Intr. by E. Margoliash; Dept. of Biochemistry, Molecular and Cell Biology, Northwestern University, Evanston, IL 60201.

A standard measurement of phototrap activity in photosynthetic material is the magnitude of the light induced electron spin resonance (ESR) signal. During the course of making such measurements, we have found that the signal magnitude measured at 77K markedly depends on the presence of oxygen. For example, compared with chromatophores frozen anaerobically, a 20 to 30% larger ESR signal was observed with chromatophores frozen in the presence of air. Interestingly, this increase in signal size was not observed when small quantities (0.1%) of organic compounds were added to the aerobic chromatophores before freezing. Among the effective compounds are ethanol, acetone and ethylamine. On the other hand, in the presence of 0.1% n-hexylamine or 0.4% triton-X-100 a 40 to 80% increase in the aerobic signal was observed. These results were obtained with saturating microwave power. Measurements at lower power showed smaller effects, indicating that the effect is most likely caused by oxygen's ability to interact with and change the power saturation properties of the signal. In our Varian E-3 spectrometer it was not possible to adjust the microwave power low enough to avoid encountering this effect. Thus, this effect is of obvious importance to consider in making quantitative measurements of phototrap activity at low temperature. The added organic molecules are presumed to alter the membrane environment, or perhaps to alter an oxygen binding site near the phototrap, such that oxygen is unable to approach the oxidized bacteriochlorophyll of the donor unit. Possible physiological roles for such oxygen interactions will be discussed.

M-PM-E4 STUDIES OF THE GEOMETRIC REQUIREMENTS FOR PHOTOSYNTHETIC CHARGE SEPARATION USING METALLOPORPHYRIN - PORPHYRIN - QUINONE TRIPLE DECKER MOLECULAR SANDWICHES. M.R. Wasielewski, M.P. Niemczyk, W.A. Svec, and D. Norbeck, Chemistry Div. Argonne National Laboratory, Argonne, IL 60439.

Work on reduced or quinone-free bacterial reaction centers points to a paradox in trying to explain the rapid forward (about 10^{12} sec^{-1}) and relatively slow (about 10^{8} sec^{-1}) return rate for electron transfer between the (BChl a)$_2$ donor and intermediary BPh acceptor. While the rapid forward rate necessitates a short distance between the donor and acceptor, subsequent slow back electron transfer yielding triplet state (BChl a)$_2$ suggests a different geometry of the donor relative to the acceptor. More recent work has suggested that an additional BChl a acts as a second intermediary acceptor preceding BPh. Thus, spatially proximate intermediary electron carriers may be crucial to promoting unidirectional charge transfer. In order to investigate this point we have developed model systems in which the final oxidized donor D^+ and reduced acceptor A_2^- molecules are separated by an intermediary electron carrier molecule A_1. The three molecules are covalently constrained such that D and A_2 cannot approach closer than ~7 Å while each is face to face with A_1. The photophysical and photochemical properties of this system will be discussed.

This work was performed under the auspices of the Division of Chemical Sciences, Office of Basic Energy Sciences, Department of Energy.

M-PM-E5 THE CHARGE RECOMBINATION PATHWAY OF THE TRANSITION $D^+Q_IQ_{II}^- \rightarrow DQ_IQ_{II}$ IN RCs FROM R. SPHAEROIDES.* David Kleinfeld, M. Y. Okamura, and G. Feher, U.C.S.D., La Jolla, CA 92093.

Purified reaction centers contain two ubiquinones, Q_I and Q_{II}, that act as the primary and secondary acceptors. The electron transfer scheme involving these acceptors and the donor D is given by:

$$DQ_IQ_{II} \underset{k_{1D}}{\overset{k_{light}}{\rightleftharpoons}} D^+Q_I^-Q_{II} \underset{k_{21}}{\overset{k_{12}}{\rightleftharpoons}} D^+Q_IQ_{II}^- \quad (D^+Q_IQ_{II}^- \xrightarrow{k_{2D}} DQ_IQ_{II})$$

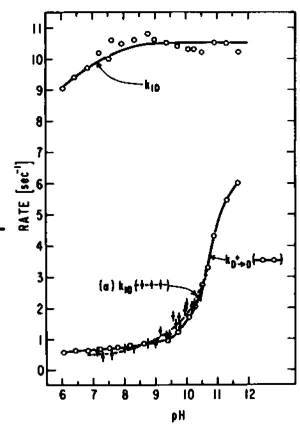

There has been a question whether $D^+Q_IQ_{II}^-$ decays by direct recombination of the electron on Q_{II} with D^+ (i.e., with rate k_{2D}) or by an indirect path via Q_I.(1) To answer this question we have measured the rates $k_{D^+\to D}$, k_{1D} and k_{12} as well as the partition coefficient $\alpha = k_{21}/(k_{12}+k_{21})$. The rates were measured by monitoring flash-induced optical absorbance changes and α was determined by using cyt c^{2+} as a probe (rather than redox agents) to obtain the relative amounts of $Q_I^-Q_{II}$ and $Q_IQ_{II}^-$. For the indirect pathway, the model predicts that $k_{D^+\to D}=(\alpha)k_{1D}$. We found this relation to hold (see Fig.) over a large pH range, thus proving that the electron from Q_{II} passes through Q_I.

* Work supported by the NSF and the NIH.

(1) See, for example, R. E. Blankenship & W. W. Parson, Biochim. Biophys. Acta 545 (1979) 429. C. A. Wraight, Photochem. Photobiol. 30 (1971) 767.

M-PM-E6 THE REDOX FREE ENERGY DIFFERENCE BETWEEN THE PRIMARY AND SECONDARY ELECTRON ACCEPTORS IN RCs FROM R. SPHAEROIDES.* David Kleinfeld, M. Y. Okamura, and G. Feher, U.C.S.D., La Jolla, CA 92093.

We utilized the methodology discussed in the previous abstract to measure the free energy difference, ΔG, between the states $Q_I^-Q_{II}$ and $Q_IQ_{II}^-$, and between the states $Q_I^-Q_{II}^-$ and $Q_IQ_{II}^{=}$. ΔG is determined from the relation (symbols defined in previous abstract):

$$\Delta G \equiv -k_BT\ell n\,\frac{k_{12}}{k_{21}} = -k_BT\ell n\,\frac{1-\alpha}{\alpha} \simeq -k_BT\ell n\,\frac{k_{1D}-k_{D^+\to D}}{k_{D^+\to D}} \quad .$$

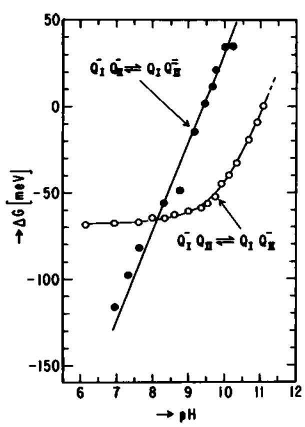

The pH dependence of ΔG at T = 295°K for both equilibria (see Fig.) shows positive slopes (~60 meV/pH) at high pH, indicating that protonation stabilizes the charge on Q_{II}. The one-electron equilibrium curve implies a pK of 9.8 for protonation of a group associated with the couple Q_I/Q_I^-, in agreement with potentiometric data.(1-3) We also measured the temperature dependence of ΔG between the states Q_I^- Q_{II} and Q_I Q_{II}^- at pH 8.0. Using the identity ΔG = ΔH - TΔS, we found ΔH = -230 meV and ΔS = -0.55 meV/°K, showing that the electron transfer between the states is enthalpy driven.

* Work supported by grants from the NSF and the NIH.

(1) R. C. Prince & P. L. Dutton, in The Photosynthetic Bacteria, 1978, R. K. Clayton & W. R. Sistrom, eds. (Plenum, N.Y.), Ch. 24.
(2) A. W. Rutherford & M. C. W. Evans, FEBS Lett. 110 (1980) 257.
(3) C. A. Wraight, Israel J. Chem. (1981), in press.

M-PM-E7 SPIN-LATTICE RELAXATION TIME OF THE REDUCED PRIMARY QUINONE IN RCs FROM R. SPHAEROIDES: DETERMINATION OF ZERO-FIELD SPLITTING OF Fe^{2+}.* R. Calvo, W. F. Butler, R. A. Isaacson, M. Y. Okamura, D. R. Fredkin, and G. Feher, Physics Dept., U.C.S.D., La Jolla, CA 92093.

The spin-lattice relaxation time of the broad EPR signal (g=1.82) ascribed to the ferroquinone complex was measured by a pulse technique at 9 GHz (see Fig.). In Fe-free RCs the line narrows and the quinone relaxation rate is reduced by ~ 5 orders of magnitude showing the dominant role of Fe^{2+} in the relaxation of the quinone spin. In analogy with the Orbach process[1] we describe the relaxation by a two-step process as indicated in the inset of the Fig. The heavy arrows (P) indicate allowed transitions between Fe levels that do not involve a quinone spin-flip. A simple theory predicts the temperature dependence

$$1/T_1 \simeq 4Qe^{-\Delta/kT}/(1-e^{-2\Delta/kT})$$

where Δ is the zero-field splitting of the lowest two energy levels of the Fe^{2+}. A theoretical fit with the data gives Δ=3.3°K in agreement with the value obtained from magnetic susceptibility measurements.[2] The relaxation rate, P, of Fe^{2+} is $\sim(\Delta/J_y)^2$ faster than Q, where J_y is the predominant component of the exchange interaction ($\Delta > J_y$).

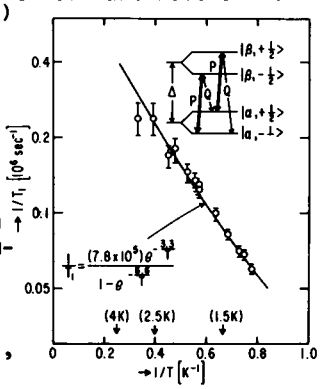

* Work supported by grants from the NSF and the NIH.

(1) R. Orbach, Proc. Roy. Soc. A264 (1961) 458.
(2) W. F. Butler, D. C. Johnston, H. B. Shore, D. R. Fredkin, M. Y. Okamura, and G. Feher, Biophys. J. 32 (1980) 967.

M-PM-E8 THE STARK EFFECT IN REACTION CENTERS FROM R. SPHAEROIDES.* D. deLeeuv, M. Malley, G. Buttermann, M. Y. Okamura, and G. Feher. S.D.S.U. and U.C.S.D., San Diego and La Jolla, CA.

The optical absorption changes (Stark effect) due to applied electric fields ($\sim 10^5$ V/cm)[1] were measured in reaction centers embedded in polyvinyl alcohol films. Three absorption minima, ΔA, in the near IR were observed (top figure); they correspond to the absorption bands at 760, 800, and 860 nm (bottom, dashed lines). For unoriented samples the absorbance change for each band is given approximately by:

$$\Delta A \sim (\Delta\mu)^2 \frac{d^2A}{d\lambda^2} E^2$$

where $\Delta\mu$ is the difference in dipole moments, between the ground and excited state, E is the local electric field, and $d^2A/d\lambda^2$ is the second derivative of the absorption spectrum. The double integral of the Stark effect spectrum $\iint \Delta A d^2\lambda$ (bottom solid line) is proportional $(\Delta\mu)^2 A E^2$. As can be seen from the Figure the Stark effect of the 865 nm band is much larger than that of the other two bands. This may be due to a mixing of the charge transfer state [$BChl^+$-$BChl^-$] with the excited state of the bacteriochlorophyll dimer that gives rise to 865 nm band. This mixing may play an important role in the primary photochemistry.

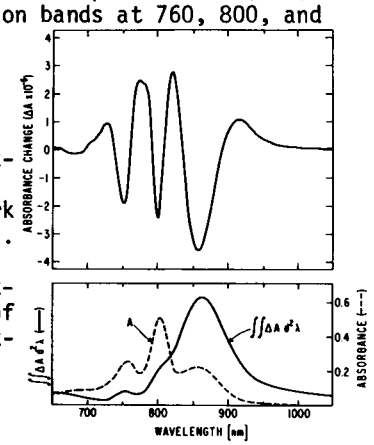

* Work supported by grants from the NSF and the NIH.

(1) M. Malley, G. Feher, & D. Mauzerall, J. Mol. Spectr. 25 (1968) 544.

M-PM-E9 ANISOTROPIC MAGNETIC INTERACTIONS IN THE PRIMARY RADICAL ION-PAIR OF PHOTOSYNTHETIC REACTION CENTERS. Steven G. Boxer, Chris E.D. Chidsey and Mark G. Roelofs, Department of Chemistry, Stanford University, Stanford, California 94305.

The quantum yield of triplets formed by ion-pair recombination in quinone-depleted photosynthetic reaction centers (RC's, R. spheroides, R-26) is found to depend on their orientation in a magnetic field. This new phenomenon is detected as follows: RC's are excited at 532nm with an 8ns pulse and the bleach of the primary donor, P, is probed with polarized light using a laser diode at 868nm. At zero-field the bleach shows a dependence of less than 1% on the polarization direction of the exciting beam. The absorbance change at some field (H) and detection polarization (η, η=0 for $\vec{E} \| \vec{H}$) divided by that at zero-field is defined as $I(H,\eta)$, and the quantum yield anisotropy is defined as:

$$a(H) = \frac{I(H,0) - I(H,\pi/2)}{I(H,0) + 2I(H,\pi/2)}$$

For RC's in a viscous solvent (>67% glycerol, room temp.), a(H) is found to be about +0.025 at 1kG, crosses zero at about 8kG, and becomes negative, and independent of field between 40 and 50kG at a value of -0.10. In the absence of glycerol (non-viscous), a(H) is 0.00 ± 0.003 at all field strengths. For intermediate viscosities, the time-dependence of a(H) is a measure of the rotational depolarization of the effect. For $0 < H < 1000$kG this effect is caused by anisotropic electron dipolar and/or nuclear hyperfine interactions, and for high fields it is dominated by the difference in the g-tensor anisotropy in the primary ion-pair. A detailed analysis of this novel effect provides structural information on the distances between and orientations of the primary reactants.

M-PM-E10 LINEAR DEPENDENCE OF EXCITON LIFETIME ON FRACTIONAL ABSORBANCE OF EXCITING LIGHT BY REACTION CENTERS IN PHOTOSYNTHETIC UNITS. R. M. Pearlstein (Intr. by N. E. Geacintov), Battelle Memorial Institute, Columbus Laboratories, Columbus, OH 43201.

Excitons, which are mobile electronic excited states, undergo random walks through the antenna chlorophyll (Chl) or bacteriochlorophyll (Bchl) arrays of photosynthetic organisms. The time interval from exciton creation, by photon absorption, until its first arrival at a reaction center (RC) is called the "first passage time", τ_{FPT}, of the random walk. Because an exciton may visit a RC more than once, measurement of the in situ Chl or Bchl fluorescence lifetime at a single excitation wavelength does not necessarily yield the value of τ_{FPT}. A theory of exciton migration and trapping presented here predicts that $\tau_{ex} = \tau_{FPT}\ (1-\rho_{RC}) + k_p^{-1}\ (1 + NI_D/I_T)$, where τ_{ex} is exciton lifetime, ρ_{RC} is the fraction of photons absorbed directly by the RC, k_p is the rate constant for photoconversion of the excited singlet to the radical pair state at the RC, and N is photosynthetic unit size. I_D and I_T are Förster overlap integrals for de-trapping and trapping, respectively; i.e., I_D is the overlap of RC fluorescence with antenna absorption, and I_T is that of antenna fluorescence with RC absorption. The theory thus predicts that a plot of τ_{ex} versus $1-\rho_{RC}$, both experimentally determinable quantities, is a straight line with τ_{FPT} as the slope. The intercept, which is also expressed solely in terms of experimentally accessible parameters, is the cumulative revisiting time of the exciton. Through its dependence on k_p it is a sensitive "fluorescence amplifier" of the state of the RC. The theory receives some support from fluorescence data taken with Rp. sphaeroides R26 chromatophores. The re-examined data call into question the usual assumption that exciton trapping in photosynthetic bacteria is trap limited.

M-PM-E11 REVERSIBLE CHARGE-SEPARATION DYNAMICS IN CHLOROPLAST PHOTOSYSTEM I REACTION CENTERS AT 25K. Mark S. Crowder and Alan Bearden, Department of Biophysics & Medical Physics, University of California, Berkeley, California, 94720.

Reaction center dynamics of dark-adapted spinach chloroplast Photosystem I have been determined by EPR spectroscopy at 25K after single laser-flash excitation. A maximum of 40% of the reaction ($P700,A:P700^+,A^-$) occurs irreversibly at 25K, independent of laser flash intensity. Back reactions, monitored by EPR detection of $P700^+$ (Signal I) after a single laser flash are biphasic: chloroplasts; 50μs (61%), 2.9ms (39%), D-144 subchloroplast particles; 90μs (67%), 170ms (33%). Fe-S cluster A is photoreduced in less than 1ms at 25K. A model for Photosystem I involving a single intermediate in the decay path between the reduced primary electron acceptor (A_1^-) and $P700^+$ and a second intermediate in the decay path between a reduced secondary electron acceptor and $P700^+$ will be presented. The use of dual flash data to determine rate constants will be discussed.

Research supported by the Biophysics Program, National Science Fd. (PCM 78-22245) and from the Department of Energy through Lawrence Berkeley Laboratory.

M-PM-E12 PROTONATED AMINO- AND IMINO-PYROCHLOROPHYLLS: MODEL COMPOUNDS FOR IN VIVO CHLOROPHYLL. R. M. Pearlstein, S. L. Ditson, R. C. Davis, and A. F. Fentiman, Battelle Memorial Institute, Columbus Laboratories, Columbus, OH 43201.

Chlorophyll (Chl) in native protein complexes has a characteristically red-shifted $S_0 \rightarrow S_1$ absorption maximum relative to monomeric Chl in a solvent. This shift is even larger for bacteriochlorophyll (Bchl) in photosynthetic bacteria. However, in at least one Bchl-protein complex, it has been demonstrated that the shift is not at all ascribable to Bchl-Bchl interactions. Thus, it is of interest to consider interactions with specific protein moieties that might produce such shifts, e.g. polarizable or charged amino acid side chains. Recently, in an attempt to model a possible Chl-(charged-amino-acid) interaction, we have shown[1] that protonation and deprotonation of an amino substituent covalently linked to the C-3 site on the Chl periphery produces a small reversible spectral shift (4 nm to the blue on protonation) of the $S_0 \rightarrow S_1$ absorption maximum. We report here results with new model Chl compounds, in which substitution has been made at the C-9 position of pyrochlorophyll (Pchl) a, i.e. the site of attachment of the keto oxygen. The compound, 9-deoxo-9-(propylamino) Pchl a, formed by reductive amination with propylamine and cyanoborohydride, displays a reversible absorbance shift of ∿6 nm to the red on protonation. We have also evidently formed the Schiff base (prior to reduction), 9-deoxo-9-(propylimino) Pchl a, which displays a reversible shift of ∿23 nm (666 to 689 nm) on protonation. We suggest that a protonated Chl Schiff base is a particularly interesting model for in vivo Chl. (Supported by the Division of Biological Energy Research, Office of Basic Energy Sciences, U.S. DOE, under contract no. W-7405-Eng-92.)

[1]R. C. Davis, S. L. Ditson, A. F. Fentiman, and R. M. Pearlstein, J. Am. Chem. Soc. (in press).

M-PM-E13 HOPFIELD CHARGE-TRANSFER OPTICAL ABSORPTION BAND IN THE PHOTOSYNTHETIC BACTERIUM CHROMATIUM. Robert F. Goldstein and Alan Bearden, Department of Biophysics & Medical Physics, University of California, Berkeley, California.

We have observed a charge-transfer absorption band, as predicted by Hopfield (1), in the cytochrome-P870 electron transfer reaction (2) in Chromatium chromatophores at 10K. First, the intermediate acceptor, I, was trapped in the reduced form by lowering the redox potential at room temperature, and then illuminating with white light at 10K for 20 min. Next, the sample was illuminated by broad-band infrared radiation (IR) (1-3 micron, 0.65 w-cm^{-2}) for 4 hrs; this decreased the I^- EPR signal by 30%. The effect of the IR (see Figure) was to promote the system from the ground vibrational state with the electron on P870 to an excited vibrational state with the electron on cytochrome c. A theoretical analysis of this effect and its relation to electron tunneling will also be presented at this meeting (3).

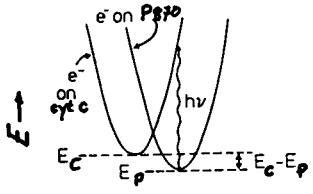

1. Hopfield, J. J., Biophys. J. 18, 311 (1977).
2. De Vault, D. & Chance, B., Biophys. J. 6, 825 (1966).
3. Bialek, W. & Goldstein, R. F., (Abstract this meeting).
(Research supported by the Biophysics Program, National Science Foundation (PCM 78-22245) and from the Department of Energy through Lawrence Berkeley Laboratory.)

M-PM-F1 STUDIES ON THE DEFECTIVE PROTON-ATPase of E. COLI uncA MUTANTS, John G. Wise, Lisa R. Latchney, Alan E. Senior, University of Rochester Medical Center, Rochester, NY 14642

The uncA gene encodes the α-subunit of the catalytic sector (F_1-ATPase) of the membrane proton ATPase of E. coli. Mutation of the uncA gene results in a loss of ATP hydrolytic and ATP synthetic activities. F_1-ATPase purified from three mutant uncA strains (uncA401, uncA447, and uncA453) is of normal size and subunit composition. These three uncA F_1-ATPases were compared to normal unc$^+$ F_1-ATPase with respect to (1) Exchangeable ATP, AMPPNP and ADP binding in the presence and absence of Mg, (2) The effects of aurovertin on ATP, AMPPNP and ADP binding, (3) Aurovertin binding, (4) ADP-induced enhancement of bound aurovertin fluorescence and (5) The reactivity of essential residues with dicyclohexylcarbodiimide (DCCD) and 4-chloro-7-nitrobenzofurazan (Nbf). uncA F_1-ATPases bound ATP, AMPPNP and ADP similarly to unc$^+$ F_1-ATPase. The maximum number of exchangeable sites was three and strong negativity cooperativity was observed. Aurovertin induced an increase in ATP, AMPPNP and ADP binding affinity in normal F_1-ATPase, but had no such effect on uncA F_1-ATPase. Both normal and uncA F_1-ATPases bound two moles of aurovertin per mole of F_1-ATPase. Aurovertin bound to uncA F_1-ATPase had 70% greater fluorescence intensity than aurovertin bound to normal F_1-ATPase. ADP induced a striking fluorescence enhancement of bound aurovertin in normal F_1-ATPase (Km ADP = 1-2μM). No such effect was observed with the uncA F_1-ATPases. The reactivity of the essential carboxyl and tyrosyl residues as judged by the respective binding of DCCD and Nbf to uncA F_1-ATPase was similar to normal F_1-ATPase. These results suggest that α↔β intersubunit conformational interaction is required for the synthesis and hydrolysis of ATP by the proton-ATPase of E. coli. This essential intersubunit interaction is lacking in three uncA F1-ATPases.

M-PM-F2 **ON THE PROTON STOICHIOMETRY OF ATP SYNTHESIS IN MITOCHONDRIA** *S. Ogawa* and *T. M. Lee*, Bell Laboratories, Murray Hill, NJ 07974.

The internal phosphorylation potential of respiring mitochondria (rat liver) was measured directly from the resonances of the phosphate compounds (P_i, ATP and ADP). The cross membrane electro-chemical potential for proton was estimated from δpH measured in NMR spectra and from the electrical potential simultaneously measured by K^+ distribution in the presence of valinomycin, monitoring the external K^+ concentration with a K^+ specific electrode in a NMR sample. At state 4, the apparent stoichiometric number n was 2.2 to 2.4. There was some dependence of the value of n on metabolic conditions of mitochondria, indicating that there were some extra processes in mitochondria other than the simple chemiosmotic theory predicts.

M-PM-F3 PROTEIN-LIPID INTERACTIONS ASSOCIATED WITH MITOCHONDRIAL PROTON TRANSLOCATION.

M.J.Pringle and D.R.Sanadi. Cell Physiology Dept., Boston Biomedical Research Institute, Boston, Mass., 02114.

The binding of oxonol VI to vesicles of bovine mitochondrial H^+-ATPase (F_1-F_o) has been used to assay the membrane potential developed by the hydrolysis of ATP and its dissipation by the proton pump blocker oligomycin or protonophoric uncouplers such as CCCP. In this spectrophotometric assay, the absorbance difference between 594 and 630nm is measured as a function of time after the rapid addition of excess ATP to 100 g/ml F_1-F_o. The method is susceptible to artefacts produced by both high concentrations of oxonol and the screening of membrane surface charges by cations, particularly magnesium. However, good results are obtained when the dye is <1μM and when a 1:1 ATP/Mg complex is added to F_1-F_o in a buffer containing 1mM $MgCl_2$.Our enzyme preparation is highly purified with ATP-Pi exchange activities of around 500nmol P_i/mg protein/min, and requires no additional phospholipids for activity. Arrhenius plots of the rates of potential generation and dissipation show discontinuities which suggest a lipid thermotropic transition and/or a conformational change in the membrane proteins. A spin label study with fatty acid nitroxide probes indicated that in the energised state the bilayer interior becomes more ordered while the surface region is unaffected. The data suggest that the membrane perturbations associated with proton translocation are more pronounced in the hydrophobic portion of the enzyme complex than in the extrinsic portion.

M-PM-F4 Functional properties of the subunits of cytochrome c oxidases.

A. Azzi, K. Bill, R. Bolli, C. Broger, R.P. Casey, R.B. Gennis and S. Salardi.
Medizinisch-chemisches Institut der Universität Bern, Bühlstrasse 28, CH-3000 Bern 9 / Switzerland

In order to establish the functional properties of the different subunits in cytochrome c oxidases from bovine heart mitochondria the following experimental approaches are being employed: 1. Use of covalent inhibitors (dicyclohexylcarbodiimides) of the redox associated H^+-translocation to locate the subunit(s) related to the proton pump. 2. Selective extraction, using covalent chromatography of a subunit (polypeptide III involved in H^+-pumping) and functional studies on the deficient enzyme. 3. Preparation of a cytochrome c oxidase depleted of the low molecular weight subunits (IV-VII) by controlled denaturation and its spectral-functional characterization. 4. Renaturation of denatured subunits and their functional reconstitution. 5. Purification by affinity chromatography (Rps. sphaeroides, B. subtilis) or by conventional techniques (B. caldolyticus) of bacterial a-type oxidases, possessing a limited number of subunits, and their spectroscopic and functional comparison. By these approaches a more detailed molecular picture of this complex enzyme has already been obtained.

M-PM-F5 IN VIVO MITOCHONDRIAL FLAVOPROTEIN REDOX MEASUREMENTS OF RABBIT CORNEAL NORMOXIC-ANOXIC TRANSITIONS.

B. R. MASTERS, S. FALK, B. CHANCE. Johnson Research Foundation, University of Pennsylvania, Philadelphia, PA. 19104.

Reversible normoxic-anoxic transitions from in vivo rabbit corneas were measured and displayed as mitochondrial flavoprotein fluorescence histograms. The flavoproteins were excited with a Helium-Cadmium laser at 442.6 nm, and the fluorescence was detected in the region of 550 nm. The excitation light was incident at the apex of the cornea perpendicular to the optic axis, and the emission fluorescence was detected along the optic axis. A brass ring was used to prevent motion of the eye. Since the laser excitation light did not illuminate the lens or the retina, the fluorescence from these tissues was not significant, and the measured signal was limited to the cornea. The laser excitation light was coupled to the cornea through a 300 μ diameter fused silica fiber optic probe. Either air or nitrogen was hydrated and then passed slowly over the corneal surface in order to induce the desired normoxic-anoxic-normoxic transitions. The fluorescence intensities are presented as histograms of the frequency of occurrence of the flavoprotein signals within a certain range of intensities. This method readily indicates if the corneal cell population is homogeneous (one peak histogram) or heterogeneous (multipeaked histogram). The normoxic flavoprotein histogram showed a single peak which was displaced reversibly to lower fluorescence intensities during a course of nitrogen to induce anoxia. The shift in the flavoprotein fluorescence was a 20% decrease during the transition from normoxia to anoxia. The anoxic histogram peak was sharper, indicating a smaller distribution of redox states in anoxia.

Grant support from N.I.H. EY-02421 (BRM).

M-PM-F6 PERMEABILITY OF INDIVIDUAL GIANT MITOCHONDRIA STUDIED WITH A FLUORESCENT TECHNIQUE.

Charles L. Bowman and Henry Tedeschi, Department of Biological Sciences and Neurobiology Research Center, State University of New York at Albany, Albany, N.Y. 12222.

We have impaled giant mitochondria using microelectrodes filled with a water soluble anionic fluorescent dye, Lucifer Yellow (CH) [Science 209, 1251 (1980)]. The results observed with television camera (Model 65, MK II; From Dage-M.T.I., Inc., Michigan City, Indiana) and recorded on video tape show that the dye can be delivered with negative current pulses and removed with positive current pulses. The results show that the fluorescent labeling is reversibly decreased if positive current is passed. These results indicate that the dye is in solution inside the mitochondria. In some experiments, the microelectrode was withdrawn and the decay of fluorescence was followed with time using either a microspectrophotometer or film (SO-115, Kodak, Rochester, N.Y.). The decay in fluorescence intensity with time was exponential and could be accounted for by a single decay constant in most cases. If the decay in fluorescence intensity is due entirely to the loss of Lucifer Yellow from the mitochondrion, a permeability coefficient can be calculated. With discontinuous illumination to reduce the possibility of bleaching, the calculated permeability coefficients range from 10^{-7} to 10^{-8} cm/sec. Since other mechanisms of fluorescent decay exist, we view the calculated permeability coefficients to represent a maximum value. The results show that mitochondria that have been subjected to a successful impalement have an intact membrane.

We thank Felix Brogna of Farrand Optical Co., Valhalla, N.Y. for loaning the microspectrophotometer and W. Stewart of NIH for supplying Lucifer Yellow (CH). Supported by NIH Grant GM27053.

M-PM-F7 ROTATIONAL MOTION OF CYTOCHROME c DERIVATIVES BOUND TO MITOCHONDRIA MEASURED BY FLUORESCENCE AND PHOSPHORESCENCE ANISOTROPY. Sudha N. Dixit, A.J.Waring, P.S. Wong, G.V. Woodrow III and J.M. Vanderkooi, Department of Biochemistry and Biophysics, School of Medicine, University of Pennsylvania, Philadelphia, PA19104.

The lifetimes of metal-free and metal-substituted cytochrome c in the singlet (10 nsec) and the triplet (9 msec) states allow us to study the molecular motions of the protein by measuring the anisotropy of emissions in the nanosecond and millisecond time regimes, respectively. The anisotropy of fluorescence in porphyrin cytochrome c in solution decays at a rate consistent with the rotation of the whole molecule. However, when the metal-free protein is bound to cytochrome c-depleted mitochondria, the anisotropy of fluorescence does not decay, indicating that there is no motion of the bound protein up to about 100 nsec. On a longer time scale, the anisotropy of phosphorescence in zinc cytochrome c bound to mitochondria displays a biphasic curve; the fast component corresponds to a rotational time of 300 usec, attributable to rotation of the protein in a cone about an axis normal to the membrane plane. The slow component with rotational time of 6 msec could be due to the rotation of whole mitochondria itself. Based on these results, it is concluded that there is rotation of cytochrome c in the membrane at a rate compatible with the turn-over time for mitochondrial electron transfer. (Supported by NSF PCM 80-3125).

M-PM-Po1 MYOSIN PHOSPHORYLATION DECREASES ATPASE IN SYSTEMS WITH ORGANIZED FILAMENT ARRAYS
K. Franks and R. Cooke, University of California, San Francisco, CA 94143 and D.K. Blumenthal and J.T. Stull, University of Texas, Dallas, TX 75235 (Intr. by R.L. Burke)

We have studied the effect of myosin light chain phosphorylation on the ATPase of actomyosin, myofibrils, and myofibrils lightly cross-linked with glutaraldehyde. Our previous work (Cooke, et al B.J. 33:235a, 1981) showed that myosin phosphorylation decreases the ATPase of fibers in isometric contractions at 35°C; however, it appeared to not affect actomyosin ATPase measured at a lower temperature, 25°C. We have now measured the ATPase of actomyosin and myofibrils at 35°C under a variety of conditions and again find that myosin phosphorylation has no effect on the activities. We have a lightly cross-linked myofibrils with glutaraldehyde (0.01%, 15', 0°C), and found that this cross-links < 1% of the myofibrillar proteins as judged by SDS gel electrophoresis. When unfixed myofibrils are contracted by ATP the organized filament array seen in the light microscope is lost, however this array is preserved in contracting fixed myofibrils. The ATPase of the myofibrils is not changed by fixation. When the myosin light chains of fixed myofibrils are phosphorylated using purified kinase and calmodulin, the ATPase is reduced by about a factor of 2. If the sarcomere structure of fixed myofibrils is destroyed by incubation in 0.6M KCl + $MgPP_i$, the ATPase is much lower and is unaffected by myosin phosphorylation. We conclude that the control of ATPase by myosin phosphorylation is evident only in systems with an ordered array of filaments and that light cross-linking can preserve this array in contracting myofibrils. (supported by HL16683, and a Career Development Award to R.C.)

M-PM-Po2 MEASURING CROSSBRIDGE ANGLES WITH PARAMAGNETIC PROBES IN RIGOR, RELAXED AND CONTRACTING MUSCLE FIBERS.
R. Cooke, University of California, Department of Biochemistry & Biophysics, San Francisco, CA 94143 and Vincent A Barnett and David D. Thomas, Department of Biochemistry, University of Minnesota Medical School, Minneapolis, MN 55455

We have used electron paramagnetic resonance spectra to measure the angular distribution of spin label probes bound specifically to sulhydral groups on the myosin heads of glycerinated rabbit skeletal muscle. As outlined by Thomas and Cooke (Biophys. J. 32: 981, 1980) the probes are highly oriented with respect to the fiber axis in rigor muscle and they display an almost random angular distribution in relaxed muscle. Preliminary results show that during isometric contractions the majority (about 80%) of the probes maintain a random angular distibution similar to relaxed muscle, while a smaller fraction (about 20%) have an angular distribution resembling rigor muscle. Lowering the temperature to 0° causes a decrease in both tension generated and the oriented fraction of probes. A decrease in the concentration of creatine kinase (40μM to 20μM) or creatine phosphate (20mM to 10mM) did not affect the fraction of oriented probes, suggesting that their presence is not due to a lack of ATP supply. The most straightforward interpretation of these data is that during isometric contractions approximately 20% of the myosin heads are attached to actin and the probes on these attached heads have the same orientation as is observed in rigor muscle. In a rigor muscle, myosin heads are thought to be attached at the end of their "power stroke" while in isometrically contracting muscle they are probably distributed throughout the "power stroke." Thus the probe appears to be located in a domain of myosin whose orientation does not change during the "power stroke" of the contractile cycle.

M-PM-Po3 LIGANDS WHICH COMPETE WITH ATP DECREASE SLIGHTLY THE VELOCITY OF MUSCLE CONTRACTION
Edward Pate and Roger Cooke, Department of Mathematics, Washington State University, Pullman, WA 99164 and Department of Biochemistry/Biophysics, University of California, San Francisco, CA 94143

One of the unsolved probelms in muscle contraction is to understand the biochemical steps that occur in the actin-myosins-nucleotide interaction in the filament array of a muscle fiber and their relationship to muscle physiology. Data allowing one to link specific steps in the actomyosin cycle with observed properties of fibers can be of use in understanding this relationship. Using glycerol-extracted, rabbit psoas fibers, we have measured force-velocity curves for contracting fibers in the presence of ligands which compete with ATP for the nucleotide site. The ligands ADP, AMPPNP and PP_i were used. When fibers were incubated in 50μM ATP, which was regenerated by creatine kinase and creatine phosphate, 5mM AMPPNP and 5mM PP_i decrease Vmax by approximately 30% and 50% respectively. At 1mM ATP and 4.75mM ATP, 5mM ADP has little effect on Vmax. Although these ligands are known to bind tightly to the nucleotide binding site on myosin, they thus cause little modification of the force velocity curves. This result is analyzed in terms of a model for the actin-myosin interaction in fibers.
(Supported by HL16683 and a Career Development Award to R.C.)

M-PM-Po4 AN ULTRASTRUCTURAL RE-EVALUATION OF DIAMETERS OF MUSCLE THICK FILAMENTS. T.F. Robinson and L. Cohen-Gould. Albert Einstein College of Medicine, Bronx, New York 10461

New ultrastructural, in situ measurements of diameters of contractile filaments in skeletal muscle differ considerably from those previously reported. Past measurements have been made in thin, transverse epoxy sections, that were non-specifically stained with uranium and lead salts to overcome background scattering of epoxy polymer. Diameters of 10-12 nm for thick filaments (plus cross bridges of 5 x 10 nm) and 5-7 nm for thin filaments have been obtained with this technique[1]. In transverse de-embedded sections the hexagonal lattice has some considerable differences from that in epoxy sections. Muscle samples from rat atrium and frog sartorius were fixed, dehydrated, embedded in polyethylene glycol, and sectioned. Sections were de-embedded in graded PEG-ethanol, mounted on coated grids, critical point dried, and viewed (EM) without staining[2]. Thick filament profiles in single myofibrils within a section thickness (0.1μm) range from circular to asymmetric[3]; diameters range from 20 to 36 nm (not corrected for shrinkage) and yield eccentricity ratios varying from 1.5 to 1.0 (circular profiles). A separate core region cannot always be discerned. Portions of thick filaments touch or partially envelope neighboring thin filaments. These results have tantalizing implications for models of cross bridge structure and lattice dynamics[3], especially in view of recent experiments in skinned muscles in which minimum diameters in osmotically compressed myofilament lattice are within this range of values[4]. 1) Huxley, In Struct. and Fn. of Muscle, 2nd ed., Acad. Press, p. 308 (1972). 2) Wolosewick and Porter, J. Cell Biol., 82, 114 (1979). 3) Robinson, Cell Tiss. Res., 211, 353 (1980). 4) Millman and Nickel, Bioph. J., 32, 49 (1980). Work supported by NIH HL-24336, NY Heart Assoc. Grant-In-Aid, and NIH RCDA HL-00568 (TFR).

M-PM-Po5 SOLUBILITY OF OXYGEN IN MUSCLE. Michael Mahler, Department of Physiology, UCLA, 90024

From the time course of tissue PO_2, the time course of its rate of O_2 consumption ($QO_2(t)$) can be calculated by solution of the diffusion equation for O_2, and depends directly on the solubility (α) of O_2 in the tissue (J. Gen. Physiol. 71:559,1978). This method has been applied to the excised frog sartorius muscle, with the tissue boundary approximated by a hemi-elliptical cylinder (Biophys. J. 33:25a,1981). The general form of the calculated time course of Q_{O_2} after a single tetanus agrees well with that deduced from measurements of recovery heat production (Dr. E. Homsher), but the absolute values of $Q_{O_2}(t)$ are subject to the same uncertainty as the value of α, which has never been measured directly. In the sartorius of R. pipiens at 20°C, measurements were made of the steady-state suprabasal Q_{O_2} when the muscle twitched every 12 sec ($\Delta Q_{O_{2ss}}$), and the total suprabasal O_2 consumption after a 0.2 sec tetanus ($\Delta[O_2]$), with both the diffusion method, with α unspecified, and the direct method of Kushmerick and Paul (J. Physiol. 254:693,1976). The direct method gave 2.93±0.26(11) μl/g·min for $\Delta Q_{O_{2ss}}$, and 6.62±0.32(11) μl/g for $\Delta[O_2]$. The diffusion method gave 0.0894±0.0079(9) atm·cm^3/g·min for $\Delta Q_{O_{2ss}}/\alpha$, and 0.195±0.013(13) atm·cm^3/g for $\Delta[O_2]/\alpha$. The values of α for which the diffusion method gave the same results as the direct method were 0.0328 and 0.0339 ml/cm^3·atm. These values exceed the solubility of O_2 in water (0.03102), and since the muscle is only about 85% water by volume, suggest that α for intrafiber water is appreciably larger than for bulk water. This is consistent with the considerable evidence that intrafiber water is in a more ordered state than bulk water, and the hypothesis that, by analogy with the effect of temperature on α in bulk water, a decrease in water mobility causes an increase in α. (Supported by American Heart Association, Greater Los Angeles Affiliate).

M-PM-Po6 SIMULTANEOUS MEASUREMENTS OF MEMBRANE POTENTIAL, SARCOPLASMIC FREE CA^{++}, AND ISOMETRIC TENSION IN SINGLE BARNACLE MUSCLE FIBERS INJECTED WITH ARSENAZO III. G.R. Dubyak and A. Scarpa, Dept. Biochem-Biophysics, University of Pennsylvania, Philadelphia, PA 19104 USA.

Single barnacle muscle fibers were injected with the Ca^{++} indicator arsenazo III (AS3); multi-wavelength spectrophotometry was used to monitor Ca^{++}-induced changes in differential absorbance (ΔA) of the dye simultaneously with changes in membrane potential (E_m) and isometric tension (P). Previous studies have demonstrated that these fibers, which are normally characterized by a passive membrane response to depolarizing current pulses, will exhibit all-or-none action potentials (AP) when injected with Ca^{++}-chelators. Consistent with the capacity of AS3 to act simultaneously as a Ca^{++} indicator and a Ca^{++} buffer, AS3-injected fibers produced AP when depolarized beyond certain levels. Depolarizing pulses longer than 25 ms elicited trains of multiple AP; the number of such repetitive ATP was proportional to stimulus duration, while their frequency was proportional to stimulus intensity. The resting E_m of these fibers was -50 ± 5 mV and the peak E_m during ATP was 0 to -10 mV. Increases in ΔA(673-713 nm), indicative of increased cytosolic Ca^{++}, were negligible during sub-AP threshold depolarization. Supra-AP threshold stimulation was accompanied by large, linear increases in ΔA(673-713 nm) which reversed direction within 5 ms of repolarization. During long depolarizing pulses which produced multiple AP, peak ΔA(673-713 nm) was proportional to both the total number and frequency of the multiple AP. Peak tension (P_{max}) invariably lagged 300-400 ms behind peak ΔA. Calibration of the optical transients showed that appreciable P was not generated until the free Ca^{++} reached 2 μM; a 3-fold increase in peak Ca^{++} from 2 to 6 μM was accompanied by a 20-fold increase in P_{max} (Supported by NIH-HL-15835 and an MDA fellowship to G.R.D.).

M-PM-Po7 SIMPLE MODEL OF SMOOTH MUSCLE MYOSIN PHOSPHORYLATION AND DEPHOSPHORYLATION AS RATE-LIMITING MECHANISM IN THE DEVELOPMENT OF ISOMETRIC TENSION. John W. Peterson, III Massachusetts General Hospital, Neurosurgical Service, Boston, Massachusetts 02114

A simple mathematical treatment of the model proposed by others in which a dynamic balance between Ca^{++}-dependent phosphorylation and Ca^{++}-independent dephosphorylation of myosin regulatory light chains controls the activation of smooth muscle contraction is presented. The parameters of the model can be computed from the experimentally observed stable isometric force-$[Ca^{++}]$ relationship, as is done for experiments with skinned guinea pig taenia coli smooth muscle. A simple extension of the model to the case of time-dependent activation yields an expression which quantitatively predicts the dependence of the rate of isometric tension development on the activating free $[Ca^{++}]$. The experimentally observed dependence of activation rate on free-$[Ca^{++}]$ in skinned guinea pig taenia coli is fit quite well by the predicted dependence of the model. The model include a parameter which reflects directly some average binding affinty of the Ca^{++}-dependent regulatory protein for Ca ions. Fitting the experimental data gives a value pK(binding) = 5.62, which is the value measured by Robertson et al. for Ca^{++}-binding to calmodulin. In the expression derived for the dependence of stable isometric force on free-$[Ca^{++}]$ however, this apparent binding constant is modified by a factor which includes the relative myosin kinase and phosphatase activities. The model goes on then to predict values for parameters which have not yet been measured experimentally in intact systems, such as the myosin kinase turnover number, the relative myosin kinase and phosphatase activities, and (unambiguously) the maximum extent of myosin phosphorylation.

M-PM-Po8 REDUCED AUXOTONIC SARCOMERE SHORTENING IN CARDIAC HYPERTROPHY: INTRACELLULAR COMPENSATION B.B. Hamrell, P.B. Hultgren & H.M. Hoffman, Dep't. of Physiol. & Biophys., Coll. of Med., Univ. of Vt., Burlington, VT Myocardial fibres are longer than normal (N) in pressure overload hypertrophy (H) and there are more sarcomeres in series. We hypothesized that for a given amount of isometric (constant muscle length (ML)) twitch tension there is less auxotonic sarcomere shortening in H as compared with N. Right ventricular free wall trabeculae ($>$2.0 mm long, $<$250 μm thick) were obtained from N (n=12) rabbits and rabbits with 67% reduction in pulmonary artery diameter for two weeks (H, n=9). Experimental conditions: Krebs-Ringer solution, 27°, ML (Lmax) where active twitch tension is maximal (Pmax) & $<$Lmax to 92% Lmax. Average sarcomere length at rest (SL_r) and at Pmax (SL_p) were determined with laser diffraction and photomicrography. SL_r and SL_p change ($\Delta SL = SL_r - SL_p$) in H were less than N ($p<0.05$). ΔSL in H was smaller than N at all ML, including 92% Lmax where resting tension (Prest) is nil. Programmed muscle stretches held SL constant; preliminary analysis of change in ML and tension in a stretch indicate series compliance is the same in H as in N. An increase in the number of sarcomeres in series in hypertrophy increases the number of potential crossbridges and decreases the amount of sarcomere shortening necessary to produce a given amount of fibre shortening and active tension during auxotonic contraction--a form of intracellular compensation.

Representative Muscles

	Lmax mm	Width mm	Pmax gm/mm²	Prest	SL_r μm	SL_p
N	2.96	0.097	7.18	0.90	2.38	2.08
H	3.45	0.215	7.11	1.18	2.27	2.10

Supported in part by NIH HL21182, AHA 77-845 and Vt.HA grants.

M-PM-Po9 HEAT PRODUCTION DURING ISOMETRIC TENSION TRANSIENTS PRODUCED BY TWO SPEEDS OF LENGTH CHANGE IN ISOLATED FROG MUSCLE. S. H. Gilbert. Anatomical Sciences, SUNY at Stony Brook, Stony Brook, NY 11794.

Previous studies (Gilbert, Biophys. Abs. 1979) have shown that small shortening ramps (≤1mm at 50mm/s or 1%ℓ_o in 8 ms) applied to whole frog muscles during isometric contractions cause a decrease in heat rate during early tension recovery to a level below that in an isometric contraction. Tension showed evidence of "recovery" during shortening ramps lasting longer than about 4 ms. In the present experiments heat production and tension were compared for 0.5mm releases complete in 3-4 ms and 10 ms. Pairs of R. pipiens sartorius muscles were stimulated tetanically at 0°C, and signals were recorded by the A/D channels of a Nova 4/s minicomputer, which also provided the driving signal for the servo-controlled length changer. Heat records were corrected for thermopile lag at 4-ms intervals. Tension showed no obvious inflections during fast releases and fell to a lower level than during slow ones, but tension recovery after 20 ms was about the same. Total heat production was greater following the faster releases, the difference being greatest during the first 10 ms but persisting for at least 160 ms. Since tension levels at 160 ms were independent of speed of release, the persistent difference in total heat cannot be accounted for by the thermoelastic effect. The results therefore suggest that tension recovery following length changes of different speeds may occur through different biochemical pathways.

Supported by grants from MDA and NSF (PCM79-11748).

M-PM-Po10 LASER RAMAN INVESTIGATION OF BARNACLE MUSCLE FIBERS. J.-P. Caillé, Dép. de Biophysique, Université de Sherbrooke, Sherbrooke, P.Q., M. Pigeon-Gosselin and M. Pézolet, Dép. de Chimie, Université Laval, Québec, P.Q.

Raman spectra in the frequency region of the protein vibrations of the barnacle muscle fibers will be presented. The objective of these experiments was to study the influence of Mg^{++} and ATP on the Raman spectra of a myoplasm sample. Muscle fibers were isolated from the depressor muscle of giant barnacle. The Raman spectra were obtained on intact single muscle fibers and on samples of myoplasm introduced in a glass capillary. On the sample of myoplasm the ionic content could be modified without changing the degree of hydration. The solution used with the sample of myoplasm contained, in mM, EGTA, 0.5; MgATP, 2.0, and KCl, 100 or Kacetate 100. The influence of the length of the muscle fiber and of the sarcomere length, on the Raman spectra was verified and taken into account in the analysis of the results. When the myoplasm sample was exposed to the ionic solution the diffusion of ATP could be followed. The Raman spectra of myoplasm were not significantly different from the spectra of the barnacle muscle fiber when the ionic solution contained Kacetate and MgATP (except for the band at 1045 cm^{-1}). When Kacetate was replaced by KCl or in absence of ATP, a reduction of a tryptophan band (760 cm^{-1}) was observed. These results indicate that the conformational modification reported previously (Pézolet et al. 1980. Biophys. J. 31, 1-8) were not induced by Mg^{++} or ATP but that they were induced by Ca^{++}.

This work was supported by the Medical Research Council of Canada, the National Research Council of Canada and the "Fondation de la Recherche en santé du Québec".

M-PM-Po11 REGULATION OF INTRACELLULAR IONS BY ISOLATED ADULT CARDIAC MYOCYTES. C.J. Frangakis, M.V. Frangakis and A.D.C. MacKnight. Depts. of Physiology, University of Alabama in Birmingham, U.S.A. and University of Otago, Dunedin, New Zealand.

Dispersed cardiac cells from the adult rat have been used by several laboratories as a model of myocardial function and metabolism. Even though both biochemical and morphological characteristics resemble that of the intact tissue, their ability to regulate cellular ionic gradients has been questioned. The present study attempts to address this problem and also to determine if the cellular ionic composition of the myocytes is subject to metabolic regulation. Intact elongated myocytes were prepared by collagenase digestion (Frangakis, et al, 1980, Life Sciences) and purify to 90-95% homogeneity. Cell aliquots were filtered on Nuclepore membranes, dried and assayed for Na^+, K^+ and Cl^-. ^{14}C-Inulin was used as the extracellular marker. Intracellular water content was 1.39±.16 Kg/Kg dry wt, Na: 47±5 mmoles/Kg, K: 138±6 mmo/Kg and Cl: 28±3 mmoles/Kg. Treatment of cells with Ouabain (10^{-3} M, 30' at 37°C) drastically altered both Na and K levels: (Na 70±6, K 83±10, Cl 29±3) Insulin (100 mU/ml) produced a 20% [.1<p>.05] reduction in the intracellular concentration of Na. A limited number of electrophysiological experiments were done on isolated cells, which corroborated our earlier results. When measured with high resistance microelectrodes, membrane potentials equilibrated at about -75 MV. A value comparable to that estimated from the results of the chemical analyses of Na, K and Cl. Our preliminary studies indicate that isolated cardiac cells are capable of regulating the concentration of cellular ions to levels, and through processes similar to those of the intact tissue. Supported by NIH AM 26791, Medical Research Council of New Zealand and the Office of Health Affairs of UAB.

M-PM-Po12 MECHANICAL RESONANCE OF SINGLE MUSCLE FIBERS STUDIED BY HIGH FREQUENCY SINUSOIDAL VIBRATIONS. G. Cecchi*, P.J. Griffiths*, and S.R. Taylor. Department of Pharmacology, Mayo Foundation, Rochester, MN 55905.

According to Ford, Huxley and Simmons (J. Physiol.,311:219,1981) the force responses of a single muscle fiber to small, rapid length changes can be modeled by a five-stage mechanical delay line composed of mass, viscosity and stiffness. In such a model the resonant frequency is inversely proportional to fiber length and directly proportional to the velocity of longitudinal transmission of mechanical impulses. We studied the mechanical behavior of single fibers at different frequencies of length vibrations (1 to 12 kHz) during isometric tetani. In order to excite the resonance frequency (f_n) of fibers directly, we used long fibers (9 to 12 mm) from iliofibularis muscles of the frog (Rana temporaria). The application of small (1 to 2 μm peak to peak) perturbations to one end of a preparation produced a sinusoidal force signal at the other. The amplitude of the force signal was frequency dependent. In the frequency range 0.1 to 0.3 f_n a small phase lead of force oscillations over length could be detected, while at frequencies between 0.3 f_n and the highest frequency used a phase lag of force with respect to length was observed. This phase lag increased with frequency and reached 90° at about the same frequency at which the force signal attained its maximum amplitude (at about 9 kHz in a fiber 12 mm long). The resonant frequency measured in this way was in good agreement with that expected from the measured transmission time. The frequency dependence of force amplitude was reasonably well accounted for up to frequencies of 0.6 f_n by a model (Shoenberg, Wells and Podolsky, J. Gen. Physiol.,64:623,1974). Beyond 0.6 f_n, the influence of viscous forces caused significant deviation from this model. (Supported by the MDA, MHA, and NS 14268).

M-PM-Po13 MICROELECTRODE MEASUREMENT OF A-BAND DONNAN POTENTIALS AS A FUNCTION OF RELATIVE VOLUME. Robert A. Aldoroty* and Ernest W. April, Department of Anatomy, Columbia University, NY, NY 10032.

A-band potentials as a function of relative fiber volume were measured from long-tonic fibers of crayfish carpodite extensors. Single fibers were dissected free, mechanically skinned in relaxing solution, treated with 1% Triton X-100 for 30 minutes, and washed three times with relaxing solution. Relaxed fiber volume was varied by applying osmotic pressure using polyvinylpyrrolidone (molecular mass = 360,000D). At an osmotic-compressive pressure of zero and a sarcomere length of 9.7um the A-band potential measured by microelectrodes filled with 3M KCl (R = 10 - 15Mohm) has a mean of 1.7±0.2mV while the I-band potential shows a bimodal distribution with means of 0.8±0.2mV and 3.4±1.0mV. These potentials increase with decreasing fiber volume. The compressability of the fibers was determined by light microscopic measurements of relative fiber volumes at sarcomere lengths of 8.0um, 9.7um and 11.0um and correlated with microelectrode measurements. The decrease in fiber volume with increasing osmotic compression reflects a decrease in A-band myosin rod spacing [R.J. Hawkins and E.W. April, Molec. Cryst. Liq. Cryst. 75:211-216, 1981]. Since the myosin rods of the A-band are polyelectrolytes in a solution of mobile ions the data can be interpreted in terms of Donnan equilibrium theory.

[Our appreciation to Gerald F. Elliott with whom we began these investigations. Supported by NIH (5RO1-AM18576), Insurance Medical Scientist Scholarship from the Equitable Life Assurance Society.]

M-PM-Po14 SHIFTS IN THE POSITION OF THE pCa/TENSION CURVE OF SKINNED RABBIT PSOAS FIBERS CORRELATED WITH THE KINETICS OF THE CROSS-BRIDGE CYCLE. Brandt, P.W., Cox, R.N., & M. Kawai. Depts. of Anatomy & Neurology, Columbia University, New York, N.Y. 10032.

Three ways of shifting the pCa/tension curve on the pCa axis have been studied. The midpoint shifts to higher pCa's when the substrate (MgATP,S) is reduced from 5 to 0.25 mM, when the phosphate concentration (Pi) is reduced from 7.5 mM to zero, and when the ionic strength ($\Gamma/2$) is reduced from 0.200 to 0.120. The Hill coefficients (n) of the curve in our standard saline (5 S, 7.5 Pi, 5 ATP, 10 EGTA, 10 MOPS, + salts to $\Gamma/2$ =0.200) are between 5.1 and 5.6 and fall to 3.0 with the left shift brought about by reducing S and/or Pi. These changes are associated with a reduction in the optimal frequency for oscillatory work. Left shifts produced by reduction in the $\Gamma/2$ do not result in a lower n, nor are they associated with change in optimal frequency for oscillatory work. Maximum tension increases with left shift brought about by reducing Pi or $\Gamma/2$. We propose a model which predicts that the shifts accompanying S & Pi change are related to an increase in the time cross-bridges spend in the attached states based on the following arguments. The half-time for Ca binding to TnC is aproximately 30 msec or less; thus the troponin regulating any given cross-bridge set will experience multiple bindings of Ca^{2+} over the period of a single cross-bridge cycle (ie, about one second). If the binding of Ca to TnC is necessary to initiate a cycle, then the concentration of Ca^{2+} required to maintain half the cross-bridges in the active cycle will be less than that required to half-saturate the TnC. Furthermore, if the time the cross-bridges spend in the attached states lengthens, the pCa/tension curve will shift to the left (higher Ca sensitivity). If this time shortens, the curve will shift to the right.

M-PM-Po15 PHOSPHORYLATION-DEPENDENT ACTIVATED TENSION IN SKINNED GIZZARD MUSCLE FIBERS IN THE ABSENCE OF Ca^{2+}. R.L. Bridenbaugh, P.M. Walsh, W.G.L. Kerrick, and D.J. Hartshorne. Univs. of Washington, Seattle, WA 98195; Miami, Miami, FL 33101; and Arizona, Tucson, AZ 85721.

In order to clarify the importance of myosin phosphorylation in the regulation of smooth muscle contraction, we prepared a Ca^{2+}-independent form of myosin light chain kinase by limited chymotryptic digestion of the native enzyme. This enzyme allowed us to dissociate the effects due to phosphorylation from other possible Ca^{2+}-dependent mechanisms. The use of this enzyme with skinned chicken gizzard fibers in the absence of Ca^{2+} showed the following results: Force development was associated with phosphorylation of the myosin light chains and addition of Ca^{2+} did not activate the fibers further. Pretreatment of the fibers with Ca^{2+}-insensitive myosin light chain kinase and ATPγS in the absence of Ca^{2+} caused thiophosphorylation of the myosin light chains and, on the addition of ATP or CTP, an activation of isometric tension was observed. The subsequent addition of Ca^{2+} did not increase force development. In contrast no force development occurs in the presence of CTP alone since CTP is not a substrate for myosin light chain kinase. This Ca^{2+}-insensitive myosin light chain kinase could also be used with ATPγS to activate skinned smooth muscle fibers from rabbit ileum and pulmonary artery. A comparison of Ca^{2+}-activated tension in the skinned gizzard muscle fibers with Ca^{2+}-insensitive myosin light chain kinase-activated tension suggests that the phosphorylation of the myosin light chains is the dominant factor in the development of tension in smooth muscle. Supported by grants from The American Heart and Muscular Dystrophy Associations and National Institutes of Health.

M-PM-Po16 EXTRACELLULAR MEASUREMENTS OF Ca^{++} IN GUINEA PIG ATRIUM DURING ACTIVITY. Chang K. Suh and W.W. Sleator, Dept. of Physiology and Biophysics, University of Illinois, Urbana, Il. 61801.

Calcium ion activities in extracellular space of guinea pig atrial muscle were measured with liquid ion-selective electrodes made from one of the neutral ligands developed by Simon and colleagues (specifically ETH 1001). The electrode tip diameters were 2 to 5 micrometers, and the time constant of the electrode-recording system as used was somewhat less than 1 second. Changes in calcium activity were measured during steady states at several frequencies and during and immediately following rest intervals of various durations, with the following results: 1) During rest intervals interposed in a steady-state at 2 contractions per second, E^e_{Ca} changed in two phases: an initial decline for a few seconds was followed by a slow increase lasting through rest intervals of up to a minute's duration. 2) When stimulation at lower frequency (0.2 cps) followed the steady-state of high frequency, decreasing contractions were accompanied by additional increases in E^e_{Ca} (ΔE^R) following the relaxation of contractions. 3) During the steady-state, the Ca^{++} cellular exchange per contraction per 100 gm cells was estimated from ΔE^R, and its value was about 1.8 μmoles per beat at 1 cps, and 1.3 at 2 cps. 4) Caffeine (2.0 mM) significantly decreased the Ca^{++} cellular exchange in the steady-state and increased Ca^{++} efflux during rest intervals. These findings support the thesis that activator calcium which disappears from releasable sites during a rest interval moves across the cell membrane into extracellular space.

M-PM-Po17 VELOCITY OF SHORTENING AND ISOMETRIC PROPERTIES DURING MYOGENESIS. P.J. Reiser*, B.T. Stokes* and J.A. Rall. Dept. Physiology, Ohio State Univ., Columbus, 43210 (Intr. by B.D. Lindley).

Numerous reports have appeared describing myosin ATPase activity and light chain composition as markers of slow and fast muscle development. In view of ambiguities, we undertook a functional description of myogenesis. The velocity of unloaded shortening (Vo) and isometric contractile properties of 24 posterior latissimus dorsi (PLD) muscles of the chicken were studied at various intervals between embryonic (E) day 15 and two weeks post-hatch (PH). Vo was determined by the slack test. Isometric properties included time to peak twitch force, t(Pt); time to one-half relaxation, t(1/2R) time to one-half peak tetanic force, t(1/2Po); normalized maximal rate of tetanic force production, (max. dP/dT)/Po; and twitch and tetanic forces normalized with blotted muscle mass, Pt/M and Po/M. The results show that Vo, normalized with muscle length (ML), changes significantly between days 15E and 20E and again between days 4PH and 15PH. The value of (max. dP/dT)/Po undergoes similar significant changes. The values of t(Pt), t(1/2R) and t(1/2Po) all change significantly between days 15E and 20E but do not during the first two weeks PH. Others have demonstrated that Vo and (max. dP/dT)/Po are well correlated with myosin ATPase activity for adult muscles from various animals and for developing mammalian muscle. It is postulated that the myosin ATPase activity of the PLD muscle does change during development. Supported in part by the Muscular Dystrophy Association.

	Vo/Lo	max dP/dT/Po	t(Pt)	t(1/2R)	t(1/2Po)	Pt/M	Po/M
	(ML/sec)	(%Po/ms)	(ms)	(ms)	(ms)	(mN/mg)	(mN/mg)
15 days E	3.43±.18	0.64±.09	225.5±42.0	343.4±13.1	103.1±14.1	0.93±.06	1.12±.05
15 days PH	7.97±.43	1.41±.16	65.0±2.4	67.7±4.1	46.8±2.7	2.80±.27	5.00±.43

M-PM-Po18 CALCIUM AND SODIUM SELECTIVE MICROELECTRODES AND INTRACELLULAR FREE $[Ca]_i$ AND a^i_{Na} IN SHEEP CARDIAC PURKINJE FIBERS. Donald M. Bers and David Ellis (Introduced by A.J. Brady). Depts. of Physiology, UCLA School of Medicine, Los Angeles, CA 90024, USA; and Edinburgh University Medical School, Edinburgh, Scotland.

Ca resin microelectrodes, Na-resin microelectrodes (made using Simon's neutral ligands, ETH001 and ETH227) and recessed tip Na-glass microelectrodes were used. Ca microelectrodes were calibrated in Ca-EGTA solutions which were also used to determine the Ca-EGTA association constant ($3.16 \pm 0.21 \times 10^6$/M) and total EGTA ($0.92 \pm 0.02$ mM) by the method of Bers (1981), (100 mM KCl, 10 mM HEPES, nominal 1 mM EGTA, 0.02-2.0 mM $CaCl_2$, pH = 7.00 at 21°C). Na resin microelectrodes were strongly affected by submicromolar [Ca], less so without the lipophilic anion tetraphenylborate and Na glass electrodes virtually unaffected by Ca. Resting free $[Ca]_i$ in sheep cardiac Purkinje fibers was found to be 75-590 nM which should be considered as an upper limit since most potential artifacts would cause overestimation. From these values, with the resting a^i_{Na} (5-7 mM) and membrane potential one can estimate the coupling ratio of Na/Ca exchange <u>if</u> the exchange is at equilibrium at rest ($n = 2(E_{Ca} - E_m)/(E_{Na} - E_m)$). This ratio is 2.4 - 2.9 Na per Ca in agreement with recent reports of electrogenic Na/Ca exchange in heart. The increase of free $[Ca]_i$ produced by 90% decrease of $[Na]_o$ expected to result from Na/Ca exchange is greatly enhanced by loading of intracellular Ca buffering systems (by 10 μM acetylstrophanthidin or K free perfusion) or by reduction of SR Ca capacity. Changes of pH_i induced by NH_4Cl are accompanied by changes of free $[Ca]_i$ suggestive of a competition or common use by Ca and H of intracellular binding sites or compartments. Supported by the American Heart Association, Greater Los Angeles Affiliate and The MRC of Great Britain.

M-PM-Po19 ENERGY BALANCE STUDIES IN SKELETAL MUSCLE SHORTENING AT $1/2V_{max}$. E. Homsher, T. Yamada, A. Wallner, and J. Tsai. Dept. Physiol. School of Medicine, UCLA, Los Angeles, Ca. 90024.

Enthalpy production (heat+work,h+w) and high energy phosphate (P) hydrolysis were measured in 3 sec tetani of R. pipiens sartorius muscles at 0 C over two time intervals: a.) a 0.35 s period, beginning after 2 sec of stimulation, during which the muscles shortened from a sarcomere length of 2.4 to 1.9 u at a velocity of $1/2V_{max}$, and b.) a 0.65 s isometric period (post-shortening) beginning at the end of shortening. Measurement of the levels of creatine, inorganic phosphate, and adenine nucleotides indicated that the only significant net measured reaction occurring was the splitting of phosphocreatine. The mean rate of P hydrolysis was 1.58±0.23 umol/g s (mean±S.E., n=25; 'g' is blotted muscle weight). The mean rate in the post-shortening period was 0.43±0.09 umol/g s, n=17) which is significantly less than that during shortening and not different from that (0.32± 0.11 umol/g s) in an isometrically contracting muscle which had not shortened. The h+w produced during (18.8±0.9 mJ/g, n=17) and after (10.8±0.5 mJ/g, n=17) shortening are accounted for by the measured changes in P; i.e., no significant unexplained enthalpy is produced during either period. The results at $1/2V_{max}$ are different from those obtained in similar studies at V_{max} (J. Physiol., 1981, 313; 60-61P) in which excess h+w is produced during shortening and excess P hydrolysis occurs during the post-shortening period. As the present study was performed under conditions similar to those at V_{max}, the difference in the two sets of results is not due to a freezing artifact, a rate limitation of ADP phosphorylation by PCr, or a rate limiting actomyosin ATP cleavage step. The data suggest that the shortening velocity alters both the rate of ATP splitting and the distribution of crossbridge states during shortening. (Supported by USPHS grant HL 11351 and the MDAA.)

M-PM-Po20 EVIDENCE FOR t-TUBULAR CONDUCTION FAILURE IN FROG MUSCLE IN THE PRESENCE OF ELEVATED EXTRACELLULAR Ca^{2+} CONCENTRATION. J.N. Howell, S.G. Howell, A. Shankar and F. Wei, Department of Zoology and College of Osteopathic Medicine, Ohio University, Athens, Ohio 45701.

Evidence from tetanus tension measurements has suggested that extracellular Ca^{2+} concentration in the range of 5-15 mM interferes with action potential conduction in the t-system (Howell and Snowdowne, Am. J. Physiol. 240:C193-200, 1981). In order to explore this suggestion further, we photographed single fibers from R. temporaria leg muscles during tetanic contraction. Wavy myofibrils in the axial core of the fibers were seen in 10 mM Ca^{2+} Ringer's at sarcomere lengths of 1.5 to 1.3 µm. Larger fibers (200 µm dia.) exhibited wavy myofibrils at longer sarcomere lengths than smaller fibers (150 µm). No wavy myofibrils were observed with sarcomere lengths greater than 1.5 µm in high Ca^{2+} or at any length in Ringer's containing 1.0 mM Ca^{2+}.

Additional evidence was obtained from after-potential measurements. The average amplitude of the late afterpotential (LAP) fell from 10.0 mV in normal Ringer's to 7.6 mV in 10 mM Ca^{2+} Ringer's, significantly different at the .01 level of confidence in a paired t-test. The time constant of the LAP was unchanged. The configuration of the early after-potential (EAP) was also changed in high Ca^{2+}. The notch and hump pattern was eliminated; action potential repolarization slowed at a less negative potential than in normal Ringer's to an intermediate rate of repolarization for about 2 msec and then decayed with a time constant slower than that of the EAP in normal Ringer's. These observations are consistent with the idea that elevated extracellular Ca^{2+} concentration causes t-tubular conduction to become decremental. (Supported by NSF Undergraduate Research Participation Award and funds from the College of Osteopathic Medicine.)

M-PM-Po21 ANALYSIS OF THE CREATINE KINASE REACTION IN THE ISOLATED PERFUSED RAT HEART USING P-31 NMR SATURATION TRANSFER. Kumpei Kobayashi, Eric Fossel and Joanne Ingwall. Departments of Physiology and Biophysics and Medicine, Harvard Medical School, Boston, MA 02115.

Unidirectional creatine kinase fluxes were measured by P-31 NMR saturation transfer techniques in the Langendorff perfused or modified working heart preparation with Krebs-Henseleit bicarbonate buffer at 37°C containing 15 mM glucose. Tissue levels of creatine phosphate and ATP were altered to different steady states by altering cardiac work, by perfusing with 10 mM pyruvate, by lowering the pH of the perfusate from 7.4 to 7.0, or by adding 25 mM KCl to the perfusate. The forward fluxes (CrP→ ATP) for each of these conditions, in µmoles/g dry weight/sec, are: 29 and 43 for glucose-perfused working hearts at peak systolic pressures 50 and 150 mmHg, respectively; 31 and 35 for working hearts supplied with pyruvate at 75 and 125 mmHg, respectively; 27 for hearts perfused at pH 7; and 29 for KCl-arrested hearts. For each condition studied, the flux for the forward reaction was larger than the corresponding reverse flux. This difference was the result of adenylate kinase activity and ATPase activity. These activities were determined for the exchange of phosphate between γ-ATP and β-ATP and between γ-ATP and intracellular inorganic phosphate. From these results, we conclude that the creatine kinase reaction is probably at equilibrium under all conditions studied and that the apparent difference between forward and backward fluxes can be accounted for by the ATPase and adenylate kinase reactions.

M-PM-Po22 HORMONE DEPENDENT CHANGES IN NMR WATER RELAXATION TIMES IN TISSUES OF AGED FEMALE RATS. Paula T. Beall, Lalit K. Misra, Carlton F. Hazlewood, and Ronald L. Young, Depts. of Physiology, and Obstetrics and Gynecology, Baylor College of Medicine, Houston, TX 77030.

Significant changes in water proton relaxation times of tissues have been found in ovarectomized mature (12 month) female rats investigated as a model for menopause. Six month old retired breeder rats were divided into three groups; controls, ovarectomized, and ovarectomized treated with the estrogen-anti-estrogen drug, Clomid*(clomiphene) at 2mg/kg/week. After 6 months, spin-lattice,T_1, relaxation times of various tissues were measured on a Bruker SXP NMR spectrometer at 30 MHz and 25°C. In normal aged females, gastrocnemius muscle had T_1 values of 693 ± 21 ms, while estrogen deprived animals had T_1 values of 651 ± 34 ms (Mean ± SD). Cardiac ventricular muscle values were elevated in ovarectomized animals (660 ± 17 ms for controls and 716 ± 64 ms for ovarectomized). Livers were similar, excet for the clomiphene treated group, where a slight elevation may indicate an effect of the drug on the liver (240 ± 35 for controls, 228 ± 18 ms for ovarectomized, and 290 ± 27 ms for drug treated). Uterine values for young (3 1/2 month) nonpregnant females were 766 ± 83 ms, while those for non-active retired breeders with ovaries were 640 ± 35 ms and for estrogen deprived animals were 575 ± 69 ms; hydration values for young uteri were 74% while old ovarectomized uteri were 79%, opposite to any explanation by water content. Treatment with Clomid prevented some of the estrogen dependent changes, and none of the changes were solely due to hydration differences. These findings have significance for NMR scanning in mature females whose bodies may have experienced age or hormone dependent relaxation time changes. Since this group may be screened for cancer, care must be taken to determine hormone status. Supported by ONR contracts N00014-76-C-0100 and N00014-K-81-0167 and private donations.

M-PM-Po23 A POSSIBLE MECHANISM FOR THE ACTION OF CAFFEINE IN HEART AND SKELETAL MUSCLE. J. Poledna, R.E. Weiss & M. Morad, Dept. of Physiology, Univ. of Penna., Phila., PA 19104

In intact cardiac or skeletal muscle fibers caffeine potentiates twitch tension. Higher concentrations cause contracture. In skinned fibers from both tissues caffeine releases Ca^{2+}-loaded intracellular stores. These effects suggest that in the intact fibers caffeine enhances the release of Ca^{2+} from the SR. We explored the mechanism by which caffeine potentiates twitch tension, by measuring its effect on the intrinsic birefringence signal. In skeletal and cardiac muscle the 2nd component of birefringence signal is thought to be related to Ca^{2+}-releasing activity of the SR, e.g. voltage changes across the SR (Baylor and Oetliker, 1975; Weiss and Morad, 1981). The 2nd component of the signal occurs prior to myofilament shortening, as measured by change in the intensity of the 0 or 1st order laser diffraction line or by scattered light or by onset of tension. In single skeletal muscle fibers (Rana pipiens) and in mammalian atrial trabeculae caffeine (1-2mM) enhanced twitch tension, but suppressed the 2nd component of the birefringence signal. In skeletal muscle fibers where developed tension is suppressed by stretch and hypertonic solutions (1.5X) caffeine also suppressed the 2nd component of the signal. The effect of caffeine is very rapid and reversible. The birefringence signal is strongly influenced by $(Ca^{2+})_o$ in cardiac, but not in skeletal muscle fibers. A possibility consistent with all of the results in cardiac and skeletal muscle is that the 2nd birefringence signal originates from synchronized conformational changes of the Ca-ATPase induced by rapid release of Ca^{2+} prior to activation of tension. Caffeine may bind to Ca-ATPase, preventing or slowing the rapid conformational changes and freeing more Ca^{2+} for contraction. Such a mechanism would increase tension, slow relaxation and suppress and delay the 2nd component of the birefringence signal.

M-PM-Po24 THE RELATIONSHIP BETWEEN CAFFEINE CONTRACTURE AND HISTOCHEMICAL FIBER TYPE. P.D. Allen, J.F. Ryan, J.L. Fernandez, F.A. Sreter. Dept. of Muscle Res., Boston biomedical Research Institute, and Department of Anesthesia, Harvard Medical School, Boston, MA 02114.

We have examined the relationship between the histochemical fiber type and the effects of caffeine and halothane in fast twitch (FT) rabbit tibialis anterior and in slow twitch (ST) semitendinosus. Caffeine increases the twitch at low doses and causes contracture at high doses. Halothane potentiates the response to caffeine. In FT specimens, no twitch potentiation was seen at any caffeine concentration and a single phase contracture response occurred at high concentrations of caffeine (16-32mM). When 1% halothane was added to the medium, a similar response was seen but at lower caffeine concentrations(4-8mM). In ST preparations, twitch potentiation was seen at low concentrations(0.5-1mM) and a biphasic contracture occurred at slightly higher concentrations(2-4 mM). Unlike FT muscle, ST muscle did not loose its ability to relax at high caffeine concentrations (32mM). As with FT, ST responses to caffeine were potentiated by halothane. The response of a FT muscle which had been transformed to 50% FT 50% ST by five weeks of 10Hz,8 hrs./day electrical stimulation was intermediate between FT and ST. ST muscle showed twitch potentiation at two concentrations of halothane(1%,3%) and contracture when exposed to 3% halothane. This response was attenuated in the transformed muscle and absent in the FT muscle. Preliminary studies in microsomal preparations from these muscles suggest that part of these differences can be explained on the basis of differences in the sensitivity to caffeine of the rate of calcium uptake and phosphoprotein formation by FT and ST microsomes. (Supported by NIH grant GM15904-14)

M-PM-Po25 MECHANISMS OF BETA-ADRENERGIC MEMBRANE HYPERPOLARIZATION IN SINGLE ISOLATED SMOOTH MUSCLES. H. Yamaguchi , T.W. Honeyman & F.S. Fay . Physiol., UMass. Med. Sch., Worcester, Mass.

Electrophysiological studies were undertaken to determine if β-adrenergic stimulation produced changes in membrane properties consistent with the hypothesis that these agents stimulated a Na^+/K^+ transport (Nature 277:32, 1979) in single smooth muscle cells enzymatically isolated from toad stomach. Membrane potentials (E_m) were recorded using micropipettes (tip diam. 0.1 μm) constructed from aluminosilicate glass. Perfusion with the β-adrenergic agent, isoproterenol (ISO;1 μM) rapidly produced a hyperpolarization of 9.5 ± 0.78 mV (mean ± SEM; n=8) from a resting E_m of -57.2 mV. Input resistance (R_{IN}) was not altered for the initial 40 sec but subsequently decreased some 20-30%. Since the resting membrane had outward-going rectifications, an increase in g_{K^+} may account for the hyperpolarization with no appreciable change in R_{IN} by ISO. However, when E_m was made more negative than E_{K^+} (-90 mV) by current injection, ISO still produced an initial hyperpolarization but this was followed by a depolarization. The initial hyperpolarization was abolished by ouabain ($\geq 5 \times 10^{-5}$ M). These results suggest that ISO produces membrane hyperpolarization both by stimulating "electrogenic ion transport" and increasing g_{K^+}. The conductance component was still apparent in the presence of ouabain and exhibited a reversal potential at ~ -90 mV. Ouabain invariably depolarized the membrane and ISO hyperpolarization was progressively reduced, suggesting a positive shift of E_{K^+}. We conclude that β-adrenergic stimulation of smooth muscle may produce separate actions to cause hyperpolarization; an increase in g_{K^+} and activation of an electrogenic Na^+/K^+ pump. Supported by a fellowship to HY from the MDA, and grants from the MDA and NIH (HL 14523.)

M-PM-Po26 THE ROLE OF THIOLS IN CAGED-ATP STUDIES AND THEIR USE IN MEASUREMENT OF THE PHOTOLYSIS KINETICS OF o-NITROBENZYL COMPOUNDS. Y.E. Goldman, H. Gutfreund,[2] M.G. Hibberd, J.A. McCray,[1] and D.R. Trentham. Depts. of Physiol. and of Biochem. and Biophys., Univ. of Penn. Phila, PA 19104, [1]Dept. of Physics and Atmospheric Science., Drexel Univ., Phila, PA 19104, and [2]Dept. of Biochem. Bristol Univ., Bristol, U.K.

Laser induced photolysis of caged-ATP, P^3-1-(2-nitro)phenylethyladenosine 5'-triphosphate is a method of rapidly introducing ATP at its site of reaction in biological systems. For kinetic studies it is of critical importance to know the rate constant of the dark reactions between the absorption of a photon by the caged-compound and release of ATP. This rate constant can be measured from the kinetics of release of the nitrosoketone byproduct (II) by coupling its release to a chromophoric reaction. This is illustrated in a study of the kinetics of photolysis of 1-(3,4-dimethoxy-6-nitro)phenylethyl phosphate (I) in the presence of thiols (equation 1).

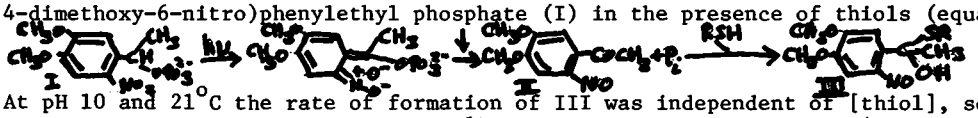

(1)

At pH 10 and 21°C the rate of formation of III was independent of [thiol], so the rate constant of the observed process (12.8 s^{-1}) equals k. From the known $[H^+]$dependence of the dark reaction (McCray et al., PNAS 77, 7237-41, 1980) the rate constant of P_i release at pH 7 is probably 12800 s^{-1}. This approach rationalizes the need for thiol reagents in biological experiments utilizing caged-ATP. Thus skinned muscle fibers in rigor failed to relax on ATP release into the fiber unless several mM reduced glutathione was present. This suggests that the glutathione protects protein thiol groups from attack by the nitrosoketone. (Supported by NIH HL 15835).

M-PM-Po27 MEASUREMENT OF DONNAN POTENTIALS IN RELAXED AND CONTRACTED MUSCLE. M. M. Dewey, S. F. Fan, P. R. Brink. Department of Anatomical Sciences, SUNY at Stony Brook, Long Island, NY 11794.

Muscle bundles were dissected from Limulus, Rana (Sartorius), Mytilus (ABRM), Homarus, giant barnacle, and honeybee and glycerinated in a 50% glycerol solution containing 100mM KCl, 5mM EGTA and 10mM buffer (pH=7.0) for two weeks. The glycerinated bundles were then rinsed in 50mM KCl, 50μm EGTA and 10mM buffer. Potentials were measured with a microelectrode filled with 3M KCl referenced to Ag-Ag chloride wire. At pH=7, all muscles produced negative potentials regardless of buffer (Tris, glycine, acetate or citrate), approximately 10mv in a relaxed state. In Limulus it was possible to measure the A- and I-band potentials. In I-band it was always less in amplitude than in the A-band. To determine the iso-electric point of the potentials in relaxed and contracted muscle, the pH was varied from 9 to 4. In Tris buffer, the iso-electric point for Limulus, ABRM, barnacle and Homarus was 5.5-6.5 in a relaxed muscle and upon shortening (fibers placed in solution containing no EGTA, 1mM ATP, 1m $CaCl_2$, 0.5 $MgCl_2$, 50mM KCl and 10mM buffer) shifted to a value of 4.5 to 5.5. Additionally, a large increase in the amplitude of the potentials was observed. Rana sartorius and honeybee muscle showed little or no change in potential amplitudes and iso-electric points when relaxed fibers were compared to shortened in any buffer used. Limulus muscle in acetate and citrate buffer showed iso-electric point shifts from 5.5-6 at rest to 6.5-7.0 when contracted and the amplitude of the potentials showed only a slight increase. While the buffers have an obvious effect on the results, the Limulus and other invertebrate muscles discussed show changes in Donnan potentials which indicate changes in the density and type of fixed change in the muscle sarcomeres. These changes may be in part responsible for thick filament shortening.

M-PM-Po28 USE OF AEQUORIN TO COMPARE THE EFFECTS OF ACETYLCHOLINE AND K^+ ON INTRACELLULAR CA^{2+} IN TONICALLY ACTIVE SMOOTH MUSCLE. Kathleen G. Morgan, Department of Pharmacology, Mayo Foundation, Rochester, MN 55905.

Aequorin, which emits light in the presence of Ca^{2+}, was injected into multiple (30-100) smooth muscle cells of strips from the dog fundus. This muscle displays purely tonic contractions and cannot not generate action potentials under normal conditions. Elevated [K] solutions (12-42 mM) were prepared by equimolar replacement of KCl for NaCl. The addition of either KCl or Acetylcholine (Ach) causes a rise in light which closely correlates in time with a rise in tone. However, when concentrations of Ach and K which produce equal increases in tone are compared, Ach produces larger increases in light. Both Ach and K decrease the resting potential of these cells but the depolarization caused by Ach is much smaller than that caused by K for the same increase in tension. This suggests that at least part of the increase in tone caused by Ach is due to a mechanism other than depolarization of the surface membrane ("pharmacomechanical coupling"). Taken together, these results suggest either that Ach decreases the sensitivity of the myofilaments of fundal smooth muscle to Ca^{2+} or that Ach releases Ca^{2+} from a pool which causes a larger aequorin signal than that which K causes. Support: AM 17238, HL 27847 and HL 12186.

M-PM-Po29 THE EFFECT OF SARCOMERE LENGTH ON THE ENERGY BALANCE IN ISOMETRIC CONTRACTION OF FROG MUSCLE. T. Yamada and E. Homsher (Intro. by W. Mommaerts). Dept. of Physiol., UCLA, Los Angeles, CA 90024

In isometric tetani 10-40 mJ/g muscle wet weight of unexplained enthalpy (the difference between the observed enthalpy and the enthalpy expected from the measured amount of high energy phosphate hydrolysis). It has been suggested that the unexplained enthalpy may be produced by process(es) associated with the redistribution of calcium within the muscle cell during the contraction. To test this idea, the heat + work production and high energy phosphate utilization were measured in a 5 sec isometric tetanus in semitendinosus muscles whose initial sarcomere length had been set at 2.3, 3.0, or 3.7 microns. The initial heat (which could be partitioned into a labile and a stable maintenance heat), isometric force, and the high energy phosphate utilization decreased with the reduction of the overlap of the thick and thin filaments. The maximal force developed at sarcomere lengths 2.3, 3.0 and 3.7 microns was 24.8 $\pm$ 1.6, 15.0 $\pm$ 1.3, and 4.2 $\pm$ 0.9 N/cm^2, respectively, while the corresponding unexplained enthalpy production was 33.6 $\pm$ 5.7 (N=25), 26.3 $\pm$ 4.5 (N=29), and 20.2 $\pm$ 3.2 (N=28) mJ/g. While the unexplained enthalpy tends to decline with initial sarcomere length, these values are not significantly different from each other. The estimated labile maintenance heat (LMH) at initial sarcomere lengths of 2.3, 3.0, and 3.7 microns was 27.7 $\pm$ 4.3, 20.5 $\pm$ 3.2, and 13.2 $\pm$ 2.1 mJ/g, respectively. These values are not significantly different from the unexplained enthalpy value at the corresponding sarcomere length. The results are consistent with the hypothesis that a) the unexplained enthalpy is produced primarily by process(es) independent of the interaction of thick and thin filaments, and b) the unexplained enthalpy and LMH are measures of the same enthalpy producing process(es). (Supported by USPHS grant HL11351 and the MDAA).

M-PM-Po30 CHANGES IN INTRACELLULAR CA^{++} LEVELS IN VASCULAR SMOOTH MUSCLE RECORDED WITH THE CA^{++} PROBE AEQUORIN. James P. Morgan* and Kathleen G. Morgan (Intr. by J. R. Blinks), Dept. of Pharmacology, Mayo Foundation, Rochester, MN 55905.

Aequorin, which emits light in the presence of Ca^{++}, was injected into multiple (40-80) cells of intact arterial smooth muscle segments from Amphiuma tridactyl. Changes in light were recorded simultaneously with changes in tension during electrical field stimulation (5-20 msec duration pulses). The preparation was continuously superfused with physiological saline solution at 19°C. The light and tension signals are both monophasic. In 5 preparations, when stimulated at 0.003 Hz, the range of time to peak and duration at half amplitude of the light signal was 2.5-21 sec and 4-37 sec while the respective values for the tension transient were 15-43 sec and 49-180 sec. These results are similar to those reported previously for mammalian gastric muscle in that light rises to a peak during tension development and that the fall of the light signal is largely over while substantial tension remains. Separate recordings of intracellular electrical activity from these cells revealed that the tissue displays spike-shaped action potentials which occur spontaneously at frequencies between 0.003,and 0.8 Hz and which are triggerable by field stimulation (5-20 msec duration pulses). The action potential amplitude ranged from 44 to 64 mV and the resting potential from -46 to -65 mV in 5 preparations. This preparation may be a valuable model system for the study of excitation-contraction coupling in vascular smooth muscle. Support: USPHS Grants HL 27847, Hl 07111, HL 12186, and NS 14268.

M-PM-Po31 TWITCH PARAMETERS AND MYOSIN LIGHT CHAIN PHOSPHORYLATION IN DENERVATED RAT SKELETAL MUSCLE
Albert C. Kirby and W.J. Brattin, Jr. Department of Physiology, Case Western Reserve University, School of Medicine, Cleveland, Ohio 44106

Post-tetanic potentiation (PTP) in mammalian fast-twitch skeletal muscle is characterized by increased contraction time (CT) and relaxation time (RT), increased twitch tension (TT), and increased phosphorylation of myosin light chain 2 (LC2). The sciatic nerve of male Sprague-Dawley rats under light ether anesthesia was severed in the flank region. Neuromuscular transmission failed within 24 hours after nerve section. Force measurements, performed on small fiber bundles prepared from the extensor digitorum longus (EDL), reveal that within 3 days after nerve section, twitch/tetanus ratio and TT per unit area increase, and CT and RT are longer; PTP does not occur. Analysis of EDL myosin light chains by the acrylamide gel technique of Manning and Stull (BBRC 90: 164, 1979) reveals that phosphorylation of LC2 in resting muscle does not change for 24 hours after nerve section, but begins to decrease by 48 hours and is essentially zero after 96 hours. Thus, the denervated EDL behaves as if it were in a state of post-tetanic potentiation with regard to TT (increased), CT and RT (increased), but these changes in force generation are associated not with an increase in LC2 phosphorylation, but a decrease. (Supported by NS-10196)

M-PM-Po32 THIN FILAMENTS ARE NOT OF UNIFORM LENGTH IN RAT SKELETAL MUSCLE. Laurel Traeger and Margaret A. Goldstein. Cardiovascular Sciences, Baylor College of Medicine, Houston, TX 77030.

Thin filament length was investigated in slow and fast muscle from adult and neonatal rats. Soleus (SOL; slow) muscle from adult and 3, 7, and 9 day old rats, and extensor digitorum longus (EDL; fast) muscle from adult rats were serially cross sectioned (60 nm sections). The number of thin filaments per 0.06 μm^2 (TF#) was counted for individual myofibrils followed from the H zone of one sarcomere, through the I-Z-I region, to the H zone of an adjacent sarcomere. TF# was pooled by distance from the Z band (Z+1, 2, 3, ... sections) or AI junction (AI+1, 2, 3, ... sections). In adult, 7, and 9 day SOL, I band TF# decreased linearly with distance from the Z band, such that TF# was 25% lower at the AI junction than at Z+1 ($p<.01$). In 3 day SOL, TF# remained constant throughout the I band. In adult EDL, I band TF# decreased 30% from Z+1 to the AI junction ($p<.01$). Although the slopes of the regression lines of TF# vs distance from the Z band were similar for adult, 7 and 9 SOL and adult EDL, in 7 and 9 SOL, TF# was 15% lower at all distances compared to adult SOL and EDL ($p<.01$). In 3 day SOL, TF# was 25% lower at Z+1 and 7% lower at the AI junction compared to adult SOL ($p<.01$). TF# was similar at all distances for adult SOL and EDL. In all muscles studied, A band TF# decreased from the AI junction to the H zone. We conclude: 1) In rat skeletal muscle thin filaments are not of uniform length, ranging in length from 0.18 to 1.1 μm. 2) There may be two stages of thin filament assembly in neonatal muscle, between 3 and 7 days when short thin filaments may be preferentially synthesized or inserted near the Z band, and between 9 days and adult when thin filaments of all lengths may be synthesized or inserted into the myofibril. Supported by Muscular Dystrophy Association and NIH Grants HL 17269, HL 17376, HL 07282 and HL 05925.

M-PM-Po33 THE INFLUENCE OF TEMPERATURE ON RESPONSES OF SKELETAL MUSCLE FROM A TROPICAL AMPHIBIAN. J.R. Lopez, C. Caputo, and S.R. Taylor. Department of Pharmacology, Mayo Foundation, Rochester, MN 55905 and Centro de Biofisica y Bioquimica, IVIC, Apartado 1827, Caracas, 101 Venezuela.

Single fibers and small bundles of cells were isolated from tibialis anterior muscles of the tropical anuran Leptodactylus insularis. Responses were recorded at temperatures in the range 0° to 30°C and compared to responses of fibers from ranid frogs (pipiens and temporaria). Isometric force in tetani, or contractures induced by caffeine or high K^+ was reversibly slowed at all stages as the temperature was lowered. Action potential kinetics were slowed too. But the influence of temperature on twitch responses was different. Differences in Ca^{2+} release and reuptake have been suggested as a reason for variable or anomalous effects of temperature on twitch force. Thus we also injected fibers with the Ca^{2+}-sensitive photoprotein aequorin to simultaneously monitor changes in free myoplasmic Ca^{2+} and twitch force. As already known, low temperatures slow the time course of Ca^{2+} transients and force, decrease the height of Ca^{2+} transients and increase the amplitude of peak force in twitches of ranid frog fibers. However, in fibers from L. insularis, the initial rates of decay of Ca^{2+} transients were not slowed and peak twitch force decreased at low temperatures. A decreased release of Ca^{2+} is apparently the cause for diminished force when it occurs at low temperatures. In twitches that are potentiated by the cold the Ca^{2+} reuptake mechanism is slowed and mechanical activation prolonged. (Supported by the CONICIT of Venezuela, AHA 77-983, MDA 32, and USPHS (NS 14268)).

M-PM-Po34 DIFFERENTIATION OF CAT MUSCLE FIBER TYPES: USE OF SKINNED FIBERS. Phyllis E. Hoar and W. Glenn L. Kerrick. Department of Physiology and Biophysics, University of Miami School of Medicine, Miami, Florida 33101.

Ca^{2+} and Sr^{2+} activation properties of functionally skinned single skeletal muscle fibers were used to distinguish between fast and slow fibers in mixed muscles of the cat. Slow fibers were activated by approximately equal concentrations of Ca^{2+} and Sr^{2+}. In contrast, fast fibers required approximately four to seven times higher concentrations of Sr^{2+} than Ca^{2+} for activation. The proteins of both fast and slow single fibers were characterized with two-dimensional polyacrylamide gels (SDS vs. isoelectric focusing dimensions). The relative proportion of fast to slow fibers in mixed muscles was determined from actual counts of randomly selected single fibers classified by Ca^{2+}/Sr^{2+}-activated tension characteristics, as well as from two-dimensional polyacrylamide gels of mixed muscle samples. The following muscles were found to contain indicated proportions of fast to slow fibers: diaphragm (costal region), 78% to 22%; medial gastrocnemias, 81% to 19%; tibialis posterior, 74% to 26%; and soleus, 4% to 96%.
Supported by The Muscular Dystrophy Association and National Aeronautics & Space Administration.

M-PM-Po35 THE EFFECT OF IONIC STRENGTH ON THE THERMAL STABILITY OF Ca-Mg-ATPase FROM SARCOPLASMIC RETICULUM (SR). Therese Wiedmer and Rodney L. Biltonen, Dept. of Pharmacology, University of Virginia, Charlottesville, Va. 22908.

The enzymatic activity of Ca-Mg-ATPase from SR of rabbit muscle increases with time upon incubation in EGTA-containing assay medium at 37°C. This increase in activity is more pronounced at low protein concentration and has been shown to result in a simultaneous loss of the ability to accumulate Ca^{2+}. These high enzyme activities correspond to those obtained after uncoupling with the Ca-ionophore A23187. It has also been reported that no such activation occurs in SR prepared in the presence of DTT (SR(+DTT)) and high salt (Johannsson, et al., Biochem. J. 196, 505-511 (1981)). We have now found that SR(+DTT) diluted into low salt buffer undergoes apparent uncoupling in the presence of EGTA or 20 mM $MgCl_2$, manifested as a severalfold increase in ATPase activity. This process is accelerated at low protein concentration and appears to be irreversible. If SR(+DTT) is stored in the presence of Ca^{2+}, ATPase does not undergo this activation. Selective modification of SR(+DTT) with N-ethylmaleimide (NEM) has also been performed. The reactivity of the SH groups essential for ATPase activity is increased after incubation at 37°C at low ionic strength in the presence of 20 mM $MgCl_2$ (uncoupled ATPase) compared to SR incubated at high ionic strength (coupled enzyme). We conclude that SR(+DTT) can readily be converted into an ATPase exhibiting characteristics of SR(-DTT) by dilution into a low salt buffer. This result suggests that low ionic strength allows the protein to overcome the constraints imposed by DTT at high ionic strength. The experiments with NEM indicate that a conformational change of the enzyme is involved in this apparent uncoupling of SR ATPase. (Supported by NIH grant GM-26894).

M-PM-Po36 PHOSPHODIESTER CHANGES ASSOCIATED WITH ELECTRICALLY STIMULATED RABBIT MUSCLE. C.T. Burt, M.G. Pluskal and F.A. Sreter. Dept. Radiology, Mass. Gen. Hosp., and Dept. Muscle Res., Boston Biomedical Research Institute, Boston, MA, 02114.

It has been shown that rabbit slow twitch muscle contains phosphodiesters (PDE) such as glycerolphosphorylcholine (GPC) to a much greater extent than fast twitch muscle. We explored the levels of PDE's like GPC in muscle undergoing fast → slow transformation. Table I demonstrates the profile from white muscles (tibialis anterior, extensor digitorum longus, or peroneus) stimulated with a specific pattern and in unstimulated controls.

Table I. Per Cent Phosphate in Various Fractions

Sample	%phosphomonoester	%GPC	All Others
Phasic Control (3)	15±5	4±3	80±2
Chronic Control (4)	13±6	2±1	86±7
Phasic Stimulated (5)	27±8	24±3	48±10
Chronic Stimulated-I (2)	24	10	66
Chronic Stimulated-II(2)	65	-	35

In phasic stimulated muscle (50 Hz, 6 weeks) there is a marked increase in levels of GPC and in the chronic stimulation pattern I (8 Hz, 8 weeks) GPC was again increased. However, GPC levels in chronic pattern II (5 Hz, 8 weeks) were below the level of detection. But phosphomonoesters were very much increased in II and one of the compounds appears to be phosphorylcholine. All stimulated muscle showed fast to slow transformation as demonstrated by gel electrophoresis under non-denaturing conditions in pyrophosphate and denaturing conditions in SDS.

GPC is certainly markedly increased in several cases of transformed muscle and hence may serve as a marker of the state of innervation. Whether case II represents an intermediate state of transformation or is unique for its particular patterns of stimulation is presently being investigated.

M-PM-Po37 CORRELATION BETWEEN INTERFILAMENT SPACING AND FORCE GENERATION IN STRIATED MUSCLE. Ernest W. April and David W. Maughan. Department of Anatomy, Columbia Univ., New York, NY 10032, and Department of Physiology, Univ. of Vermont, Burlington, VT.

Force generating capacity was measured as a function of interfilament spacing in skinned single muscle fibers from crayfish. Single fibers were dissected free, mechanically skinned in relaxing solution, and treated with 1% Brij-58 to remove internal membranous elements. Active force was induced by an activating solution containing 5.7 pCa. Light microscopic measurements of fiber diameters in relaxed and activated fibers were correlated with interfilament spacing determined by low-angle X-ray diffraction under the same experimental conditons. From the resultant fiber cross-sectional area and the unit-cell area of the control preparation, the number of unit cells (myosin rods) per fiber was obtained. From this and the measured force generated by the fiber under the various experimental conditions, the force per myosin filament was derived for the muscle fiber at the given sarcomere length (9.6 um, determined by laser diffraction). Force generating capacity is approximately 1.8×10^{-5} dynes/unit-cell at the control equilibrium interaxial spacing of 69 nm. As the A-band lattice is osmotically compressed with polyvinylpyrrolidone (40,000D) the force increases to approximately 3.0×10^{-5} dynes/unit-cell at an interaxial spacing of 48 nm which is relatively close to the *in situ* spacing of 54 nm in the intact fiber. From this point, further osmotic compression reduces force to abolition at an interaxial spacing of approximately 33 nm. Interestingly, the force elicited in the skinned control fiber is approximately 60% of the maximal force achieved by compressing the fiber to *in situ* dimensions. This suggests that the *in situ* interfilament spacing is optimal for force generation. [Supported by NIH grant 5R01-AM15876.]

M-PM-Po38 THE MUSCLE-TENDON JUNCTION OF MURINE SKELETAL MUSCLES. John. A. Trotter and Susan Eberhard. Department of Anatomy, University of New Mexico School of Medicine, Albuquerque, N.M. 87131.

The mechanical function of the muscle-tendon junction is preserved after extraction of murine skeletal muscles with Triton X-100 under the appropriate conditions (J. Trotter, Fed. Proc. 39, 2170a, 1980; Anat. Rec. *in press*). In extracted muscles the lamina densa of the external lamina is connected to a submembrane electron-dense region into which the actin filaments of the last sarcomere are seen to insert. Electron microscopy reveals that the connection is effected by fine filaments (2-6.5nm) that traverse the lamina lucida and the space formerly occupied by the plasma membrane. By varying the conditions of extraction-specifically in terms of temperature (4°-40°C), time (4hr - 48 hr), pH (6.0 - 8.0), and calcium concentrations (1.5mM $caCl_2$ or 2mM EGTA) - we have found that the submembrane electron-dense region can be separated from the myofilaments while maintaining its connections with the external lamina. It can also be separated from the external lamina while maintaining its connections with myofilaments. Therefore, this region, which appears to play an important role in the transmission of force from myofilaments to external lamina, can be independently defined in terms of its structure. We propose the term "internal lamina" for this structure. Extraction under different conditions reveals that the internal lamina is composed of a) actin filaments tightly packed together, in association with b) fine filaments arranged orthogonally to the actin filaments and c) globular structures about 30nm in diameter. Immunocytochemical experiments at the EM-level are currently under way to identify the constituents of this region. (Supported by the MDA).

M-PM-Po39 PASSIVE ELECTRICAL PROPERTIES OF EMBRYONIC SKELETAL MUSCLE OF THE CHICK. J.A. Steele, Department of Physiology, University of Alberta, Edmonton, Alberta, Canada, T6G 2H7.

The passive cable properties of posterior latissimus dorso muscle fibers (presumptive fast) from 18-21 day embryos were estimated. Intracellular microelectrode recordings were done on single isolated fibers obtained by enzymatic dissociation procedure similar to that of Bekoff and Betz (J. Physiol. 271: 25, 1977). The isolated cells were judged viable by comparison of resting membrane potentials, input resistances and membrane time constants with values obtained from fibers in intact muscle. Conventional square pulse analysis and the equations for linear, infinite cables were utilized to estimate cable properties of the isolated cells. In preliminary experiments, one microelectrode was used to pass current and a separate electrode placed nearby was used for sensing voltage. Fiber diameters were measured optically. The following values were obtained for 24 isolated fibers: diameter = 7.2 ± 1.4 μm ($\bar{x}$ ± S.D.); input resistance = 19.6 ± 6.3 mΩ; membrane time constant = 17.6 ± 5 msec; membrane resistance (Rm) = 7.7 ± 0.7 x $10^3 \Omega cm^2$; space constant = 0.89 ± 0.11 mm and membrane capacitance (Cm) = 2.3 1.2μFcm^{-2}. The Rm values are much higher and Cm values lower than values from adult p.l.d. muscles (Fedde, J. gen. Physiol. 53: 624, 1969). This difference probably reflects to some extent the relative abundance of transverse tubular membranes between embryonic and mature fibers. Application of enzymatic dissociation of muscle to obtain single fibers provides a useful technique in the study of small, embryonic muscle fibers. (Supported by MDAC grant to Dr. M. Poznansky.)

M-PM-Po40 GLUCOCORTICOID ALTERATION OF MUSCLE MEMBRANE EXCITABILITY. R. L. Ruff, D. Martyn and C. E. Stirling. Dept. Physiology & Biophysics, U. of Washington, Seattle, WA.

Excess of endogenous or exogenous glucocorticoids leads to muscle atrphy and weakness with preferential involvement of proximal muscles and Type II muscle fibers. Greuner & Stern (Arch. Neurol. 26:181-185, 1972) and Gnossie & Albuquerque (Exp. Neurol. 58:435-445, 1978) have suggested that steroids act by depolarizing Type II muscle fibers causing a decrease in action potential amplitude, thereby reducing force generation. (According to this hypothesis, the muscles should become weak before they atrophy.) To test this hypothesis, the temporal pattern of muscle wasting, in vitro twitch and tetanic tensions; and in vitro and in vivo resting membrane potentials and passive membrane properties were studied in the soleus (SOL), extensor dicitorum longus (FDL), semimembraneous (SM), and omohyoid (OMO) muscles of control and steroid intramuscular dexamethasone or cortisone acetate treated rats. One week of steriod treatment produced significant atrophy in the EDL, SM, and OMO. The soleus did not show weight loss until three week of treatment. After four weeks of steroid treatment the order of severity of muscle atrophy was OMO≥SM>EDL>>SOL. The decrease in twitch or tetanic tension always followed muscle atrophy, which argues against the tested hypothesis. In all the muscles, the twitch or tetanic force/g of muscle increased with steroid treatment. The twitch/tetanus ratio increased for the EDL and SOL, decreased in the SM and was not changed in the OMO. In vitro recorded resting membrane potentials were depolarized only in the EDL. This depolarization was seen after one day of dexamethasone treatment or one week of cortisone acetate treatment. This depolarization was not seen in vivo. Steroid treatment did not alter the in vivo measured actin potential threshold or passive membrane properties.

M-PM-Po41 PRELIMINARY EVIDENCE FOR A Mg^{2+} MODULATED, MYOSIN LIGHT CHAIN PHOSPHATASE (MLCP) REGULATORY SYSTEM IN VASCULAR SMOOTH MUSCLE. Robert S. Moreland and George D. Ford. Department of Physiology, Medical College of Virginia, Richmond, VA 23298. (RSM present address- Department of Physiology, University of Michigan Medical School, Ann Arbor, MI 48104)

In previous studies we have demonstrated a Mg^{2+} modulation of the calcium-activated actomyosin ATPase activity and also the total phosphorylation of the 20,000 M_r myosin light chain from bovine aortic actomyosin (AM). This present study was designed to examine the possible modulatory influence of Mg^{2+} on the MLCP in this preparation. The activity of the MLCP endogenous to the AM preparation was determined using both purified myosin and AM, phosphorylated with [γ-^{32}P]-ATP, as substrates. Dephosphorylation of these substrates was monitered over a 30 min. time course with varying Mg^{2+} levels from 0.1 to 15mM. MLCP activity was not seen at Mg^{2+} levels below 0.1mM under any condition studied. MLCP activity, using myosin as substrate, was slow and apparently not Mg^{2+} modulated above a 1mM Mg^{2+} requirement (apparent rate constant = $0.017s^{-1}$). However, MLCP activity, using AM as substrate, showed an initial rate of activity an order of magnitude higher than the rate with myosin as substrate, and was modulated by Mg^{2+}. Maximal activity was seen at 9mM Mg^{2+} or higher with an apparent rate constant of $0.649s^{-1}$. Following this initial fast rate, a slower rate was seen comparable to the rate using myosin as substrate. These results are suggestive evidence of two MLCP's. One MLCP shows basal unregulated activity and requires 1mM Mg^{2+}, but exhibits no further Mg^{2+} modulation. A second MLCP is apparently activated during the activation of the AM. The activity of this activated MLCP is modulated by Mg^{2+} with maximal MLCP activity at Mg^{2+} levels of 9mM and higher. Supported in part by a Grant-in-Aid (to GDF) from the American Heart Association.

M-PM-Po42 FORCE DEVELOPMENT AT VERY LONG SARCOMERE LENGTHS IN LIMULUS TELSON MUSCLE. Sandra Davidheiser and Robert E. Davies. Dept. Animal. Biol., Sch. Vet. Med., U. of Pa., Phila., Pa. 19104

The linear correlation of A-band length with sarcomere length in Limulus telson muscle has been shown to be due to staggering of long thick filaments (TF) at sarcomere lengths (SL)> 7μm (L_o), and actual shortening of TF below 7μm (Dewey et al., 1973). We have found that in telson muscle bundles stimulated electrically at a SL of 14μm, where there should have been no overlap between Z-line-linked actin thin filaments and TF, the isolated TF lengths were significantly shorter than TF isolated from unstimulated bundles at SL of 1.0 and 2.0 L_o (Davidheiser and Davies, 1981). The following experiments were done to distinguish between two possible TF arrangements at 2.0 L_o SL; 1) TF remain misaligned, 2) TF realign in the center of the sarcomere. Telson muscles were electrically stimulated at lengths of 8 and 10μm SL until the maximum isometric force (P) for each length developed. The bundle was adjusted to 10μm SL, passively released at a constant velocity ($\sim$ 76% V_{max}) to 8μm SL, and immediately stimulated to develop isometric P following the release. The procedure was repeated again but the muscle was stimulated during the entire period, i.e. 10 to 8μm sarcomere shortening, isometric P redevelopment at 8μm SL. A small but significant decrease ($\sim$ 17%) was measured in isometric P developed at 8μm SL for the two procedures {Δ(passive-active release)=+17.2 ± S.E. 4.2 N/cm^2, n=4}. The muscle was then slowly stretched to 14μm SL where no significant P was developed, and the procedure repeated with shortening to 12μm SL where $\sim$ 40% maximum isometric P developed. No significant difference was measured in isometric P at 12μm SL between a passive and active shortening (Δ=-5.5± S.E. 4.7 N/cm^2, n=4), thus indicating that, while TF might shorten at very long SL, they remain in a staggered array during stimulation. (NIH, HL 15835).

M-PM-Po43 HIGH-RESOLUTION LASER DIFFRACTION SPECTRA OF STRIATED MUSCLE FIBERS. Alfred F. Leung. Department of Physics, The Chinese University of Hong Kong, Shatin, N.T., Hong Kong.

At normal incidence, the fine structures of the left and right diffractions of the same order are not mirror images of the equatorial plane of the fiber and have different intensities. They do not interchange after the fiber has been rotated by 180^{o} around its longitudinal axis. These observations indicate that Bragg or skew planes formed by regular shifts in the intermyofibrillar registers are not necessary to account for the difference in the left and right diffraction intensities. The angular separations of diffractions on the meridional plane deviate from the predictions according to the rectilinear grating equation. This deviation implies that the basic assumption in diffraction theories where the optical path difference between any two points within the fiber is linearly proportional to the distance between these points is invalid. It also limits the accuracy of sarcomere length determination using the rectilinear grating equation. However, the average diffraction angle of the fine structures as a function of laser incident angle follows the rectilinear grating equation. The left or right intensity of a diffraction line as a function of laser incident angle shows a single peak. The peak incident angles corresponding to the left and right diffractions of the same order are symmetric to the axis of normal incidence and are Bragg angles of the A- and Z-discs of individual myofibrils. The diffraction measurements are consistent with the model in which the myofibrils are randomly packed within the fiber.
(Supported by the American Heart Association, Greater Los Angeles Affiliate)

M-PM-Po44 ATTEMPTS AT LOCALIZING THE POST-TRANSLATIONAL SITE OF ACTION OF ALDOSTERONE: THE BARNACLE MUSCLE FIBER AS A PREPARATION. E. Edward Bittar and Jude Nwoga, Department of Physiology, University of Wisconsin, Madison, Wisconsin 53706.

A principal feature of experiments with barnacle fibers preexposed *in vivo* overnight to 10^{-6}M or 10^{-10}M-aldosterone is that injection of $GTPNa_2$ or Gpp(NH)p not only leads to a marked stimulatory response of the ouabain-insensitive Na efflux that is greater in magnitude than that seen in unexposed, ouabain-poisoned fibers but also to a response that is *sustained*. Both the magnitude of the response and its sustained nature are unaffected by prior exposure of these fibers to actinomycin D, cycloheximide, colchicine and cytochalasin. However, the response is drastically reduced by injecting PKI or R_{II} subunits, and completely abolished by pre- or post-injecting Mg^{2+}. The response is also reduced by external application of verapamil, injecting EGTA or omitting Ca_e. *Importantly*, external application of trifluoperazine or imipramine (50 μM) before or after injecting GTP [or Gpp(NH)] causes a marked reduction in the response. Neither the injection of Ca^{2+} in varying concentration nor the injection of cholera toxin into preexposed fibers leads to responses that are appreciably greater than those seen in unexposed fibers. Collectively, these observations are still compatible with the view that aldosterone acts by promoting the participation of calmodulin-sensitive adenylate cyclase in the response to injected guanine nucleotides. Whether the sustained nature of the response to nucleotides is possibly due to slowing by excess ATP of the reassociation of regulatory with catalytic subunits (Rangel-Aldao and Rosen) and/or slowing of the putative Mg^{2+}-dependent protein phosphatase 1 is the subject of further investigation.

M-PM-Po45 LATERAL INTERCONNECTIONS BETWEEN THICK FILAMENTS IN THE H ZONE? M.E. Cantino, J.W. Lacktis and G.H. Pollack. Dept. of Anesthesiology and Division of Bioengineering (RN-10), University of Washington, Seattle, WA 98195.

It is generally accepted that bridges connect the thick filaments at the M line of vertebrate striated muscle. We have used serial thin sections to investigate other regions of the H zone for lateral connections. Preliminary studies of glycerinated muscle reveal some connections between thick filaments in all regions of the H zone. Frog semitendinosis muscles were removed and stretched by 25 percent of their in situ length. They were then incubated in a EGTA skinning solution for 4 hours, followed by glycerination for 24 hours at -10°C. After rinsing in skinning solution, the muscles were fixed in Karnovsky's fixative (glutaraldehyde and paraformaldehyde), and outer fiber bundles were removed and osmicated. Serial sections of 50 to 70 nm were cut and stained with uranyl acetate and lead citrate, carbon coated, and viewed at 80 kV in the TEM. Individual myofibrils were followed through 10 to 12 consecutive sections of the H zone. Unlike the bridges seen in the M region, which interconnect virtually every filament, bridges in other parts of the H zone were visible between some filaments, but not others. Lateral connections in the pseudo H zone were also observed, but may be M-bridges included in the plane of the sections.

M-PM-Po46 RYANODINE INHIBITION OF ZERO K^+ TOXICITY IN MYOCARDIAL TISSUES. J.L. Kenyon and J.L. Sutko, Dept. Internal Medicine (Cardiology Division), Univ. Texas Hlth. Sci. Ctr., Dallas, TX 75235.

Ryanodine is a putative inhibitor of myocardial SR Ca^{2+} release (Sutko & Willerson, Circ. Res. 46:332, 1980). Since exposure of myocardial tissues to zero K^+ results in a toxicity which is related to an intracellular Ca^{2+} overload, we have investigated the ability of ryanodine to alter the responses of guinea pig papillary muscles (PM) and calf Purkinje fibers (PF) to 0-K. Exposure of PM to 0-K resulted in marked hyperpolarization and a decreased action potential amplitude, overshoot and duration. Twitch tension increased and then decreased, while resting force increased. Both after-contractions and transient depolarizations were clearly evident in 0-K. Ryanodine (0.1-1.0 μM) given prior to or after 0-K prevented or abolished both the after-contractions and transient depolarizations, but none of the other changes. Exposure of PF to 0-K caused marked depolarization. Depolarizing voltage clamp steps resulted in the regular occurrence of current creep during the step and transient inward currents upon repolarization (cf. Eisner & Lederer, J. Physiol. 294:255, 1979). Ryanodine (1 nM-1 μM) prevented or abolished the transient inward current, but did not alter the current creep. In normal K^+, ryanodine concentrations which abolished 0-K toxicity neither altered PM action potential configuration nor blocked PF slow inward current suggesting an action other than Ca^{2+} channel blockade. Thus ryanodine may be experimentally useful for (1) dissociating ionic events originating at the plasma membrane from those arising from intracellular changes and (2) establishing the cellular basis of the toxicity associated with exposure of cardiac tissues to 0-K or cardiac glycosides. Supported by NIH grants HL 26528 and HL 34770.